Multiboson interactions at the LHC

D. R. Green

Particle Physics Division,
Fermi National Accelerator Laboratory,
P.O. Box 500, Batavia, Illinois 60510, USA

P. Meade

C. N. Yang Institute for Theoretical Physics,
Stony Brook University, Stony Brook,
New York 11794, USA

M.-A. Pleier

Physics Department, Omega Group,
Brookhaven National Laboratory,
P.O. Box 5000, Upton, New York 11973, USA

(published 20 September 2017)

This review covers results on the production of all possible electroweak boson pairs and 2-to-1 vector boson fusion at the CERN Large Hadron Collider (LHC) in proton-proton collisions at a center of mass energy of 7 and 8 TeV. The data were taken between 2010 and 2012. Limits on anomalous triple gauge couplings (aTGCs) then follow. In addition, data on electroweak triple gauge boson production and 2-to-2 vector boson scattering yield limits on anomalous quartic gauge boson couplings (aQGCs). The LHC hosts two general purpose experiments, ATLAS and CMS, which have both reported limits on aTGCs and aQGCs which are herein summarized. The interpretation of these limits in terms of an effective field theory is reviewed, and recommendations are made for testing other types of new physics using multigauge boson production.

DOI: 10.1103/RevModPhys.89.035008

CONTENTS

I. INTRODUCTION

The standard model (SM) of particle physics is based on the $SU(3)_C \otimes SU(2)_L \otimes U(1)_Y$ gauge symmetry group and describes the interactions among all the elementary particles. With the discovery of a light Higgs boson, the SM is a complete and self-consistent theory which can and should be tested as closely as possible.

Because the electroweak gauge bosons carry weak charge the SM predicts interaction vertices which contain three (triple gauge coupling) or four bosons (quartic gauge coupling). These interactions contribute to the inclusive production of pairs and triplets of gauge bosons as expected in the SM.

Previous experiments have studied the production of pairs of gauge bosons. The Large Electron Positron (LEP) collider experiments studied WW and WZ production as a function of center of mass (c.m.) energy. Indeed, the triple vertices were found to be critical in limiting the growth of the cross sections with energy giving strong confirmation of the correctness of the SM. Limits were set by the LEP experiments on anomalous triple gauge couplings (aTGCs) for the first time and these limits (Schael *et al.*, 2013) have remained the most stringent until the advent of the Large Hadron Collider (LHC) at CERN.

Experiments at the Tevatron (CDF and D0) also measured exclusive gauge pair production extending the data on final states to WW, WZ, ZZ, $W\gamma$, $Z\gamma$, and $\gamma\gamma$. In these final states the dynamics of the process, especially at large diboson c.m. energy, could be used to further test the predictions of the SM. For a recent review of the relevant Tevatron results, see Kotwal, Schellman, and Sekaric (2015).

The LHC experiments ATLAS and CMS have begun to exploit the increased c.m. energy of the LHC and the associated large increase in cross section to expand the gauge coupling studies. In particular, the energy at the triple and quartic vertices has been pushed into the TeV range. As the energy and luminosity of the LHC continue to increase, ever more incisive studies will open up.

This review covers the LHC proton-proton data taking up to the end of 2012, which occurred at 7 and 8 TeV and is referred to as LHC run I. The diboson states herein covered consist of all gauge boson pairs $\gamma\gamma$, $W\gamma$, $Z\gamma$, WW, WZ, and ZZ. In each case limits on aTGCs could be set and they have now surpassed the previous LEP and Tevatron limits. A unique feature of the LHC data is the first exploration of triple gauge boson production with $W\gamma\gamma$, $Z\gamma\gamma$, and WWW final states, compiled in this review. The corresponding first limits on anomalous quartic gauge boson couplings (aQGCs) which have been reported are herein summarized.

A second set of limits on aQGCs arise from the studies of exclusive final states in the vector boson scattering (VBS) topology. In that case the initial proton-proton state, due to the virtual emission of two gauge bosons, contains two remnant, forward going jets and a more centrally produced final state with the resulting VBS dibosons. In this review, aQGC limits are derived for the VBS states $W\gamma jj$, $WVjj$, $W^{\pm}W^{\pm}jj$, $WZjj$, and $\gamma\gamma \to WW$, where the symbol j refers to the remnant jet. In the particular case where the protons emit soft photons in the VBS initial state ($\gamma\gamma \to VV$), remnant jets are not part of the VBS signature.

In the presentation of experimental results the distributions of kinematic quantities which are well measured experimentally and which also serve as a proxy for the energy at a triple or quartic gauge boson vertex for a specific final state are shown. Where available, predicted deviations from the SM due to anomalous couplings are also shown in order to give an idea of the sensitivity of the measurement to deviations from the SM.

This article is organized as follows. In Sec. II the theory of multigauge boson interactions in the SM and the modern treatment of deviations being described by an effective field theory (EFT) are reviewed. Additionally, the impact of multigauge boson physics beyond simple shifts in aTGC and aQGC measurements is emphasized, and a model-independent recommendation for experiments is made. In Sec. III a brief description of the relevant experimental issues is given with references to the corresponding experimental aspects of the ATLAS and CMS experiments. In Sec. IV the published LHC diboson studies are presented while in Sec. V the triboson results are shown. In Sec. VI the vector boson fusion (VBF) data for W and Z bosons are shown as a proof of principle that this electroweak process can be extracted from the experimental backgrounds. Armed with those analyses, the data on VBS are presented in Sec. VII. The existing limits on gauge couplings are collected in Sec. VIII for aTGCs and in Sec. IX for aQGCs. Finally, Sec. X explores the prospects for gauge coupling studies with the increased luminosity planned for the LHC as set out by CERN.

II. THEORY

There are a variety of theoretical motivations for testing the structure of multiboson interactions at the LHC. Given the non-Abelian nature of the electroweak (EW) sector of the SM, this allows one to directly test non-Abelian gauge theories. While this of course had already been done in other ways with QCD, the weakly coupled nonconfining nature of the EW gauge symmetry allows for its investigation in unprecedented detail, at higher energies, and with larger data sets. Even more important is the connection between the study of multiple EW gauge bosons and the structure of electroweak symmetry breaking (EWSB).

The $W^{\pm}$, Z, and γ (through mixing) represent the SM particles most strongly coupled to EWSB other than the top quark. Since the discovery of a Higgs boson by ATLAS (Aad *et al.*, 2012h) and CMS (Chatrchyan *et al.*, 2012b), we have definitive proof that the ultimate mechanism of EWSB must look very much like the simple *ad hoc* Higgs mechanism. However, this results in many more theoretical problems than answers. In particular, the appearance of spontaneous symmetry breaking without a dynamical origin associated with a scalar field brings the hierarchy problem to the fore. Since EW gauge bosons can be cleanly identified at the LHC, they provide one of the best ways to seek any structure to EWSB beyond the Higgs.

Both the non-Abelian nature of EW gauge bosons and their connection to EWSB were used in past phenomenological studies that have spurred decades-long experimental programs at different colliders. Historically these two threads, EWSB and non-Abelian couplings, were studied independently despite their intertwined nature.

The origin of testing the non-Abelian structure using EW gauge bosons goes back to Hagiwara *et al.* (1987). There a parametrization of possible triple gauge boson couplings consistent with Lorentz invariance and charge conservation was given:

$$\mathcal{L}_{WWV} = ig_1^V(W_{\mu\nu}^\dagger W^\mu V^\nu - W_\mu^\dagger V_\nu W^{\mu\nu}) + \frac{i\lambda_V}{m_W^2} W_{\lambda\mu}^\dagger W_\nu^\mu V^{\nu\lambda} - g_4^V W_\mu^\dagger W_\nu(\partial^\mu V^\nu + \partial^\nu V^\mu) + g_5^V \epsilon^{\mu\nu\rho\sigma}(W_\mu^\dagger \overleftrightarrow{\partial} W_\nu)V_\sigma + i\tilde{\kappa}_V W_\mu^\dagger W_\nu \tilde{V}^{\mu\nu} + \frac{i\tilde{\lambda}_V}{m_W^2} W_{\lambda\mu}^\dagger W_\nu^\mu \tilde{V}^{\nu\lambda} + i\kappa_V W_\mu^\dagger W_\nu V^{\mu\nu}, \quad (1)$$

where W^μ is the W^-, V represents either the Z or γ, the two-index V or W tensors are Abelian field strengths, and $\tilde{V}$ is the result of contracting two indices with the four-index epsilon tensor. Historically, this was a very relevant parametrization since it preceded the experimental WW production studies at LEP II and large deviations from the non-Abelian structure had not yet been ruled out. Once energies sufficient to produce dibosons were achieved, the effective Lagrangian (1) could lead to deviations in processes such as those shown in Fig. 1, or constraints placed on the various couplings. This parametrization was then carried forward and has been used as the basis for experimental studies of aTGCs for approximately the last three decades.

The historical connection between multiple vector boson production and EWSB is the role of the Higgs in unitarizing VBS (Cornwall, Levin, and Tiktopoulos, 1973, 1974; Dicus and Mathur, 1973; Llewellyn Smith, 1973; Lee, Quigg, and Thacker, 1977; Chanowitz and Gaillard, 1985). Well before the discovery of the Higgs, it was known that the scattering of massive vector bosons without a Higgs-like state has amplitudes that grow as $\sim E^2$. Naively, if the SM EW gauge bosons were scattered at energies $\sim 4\pi m_W/g$, tree-level unitarity would appear to be violated. Of course this did not mean that unitarity would actually have been violated, it simply meant that the theory of EWSB and massive gauge bosons would become strongly coupled and unpredictive at these scales. If the Higgs existed, the growth with energy would be canceled by the Higgs contribution, and perturbative unitarity would have been manifest and calculable within this framework. To test VBS, the simplest process one can study experimentally is shown in Fig. 2. As in the case of aTGCs, the proposal to use VBS to test EWSB preceded the experimental observation of a Higgs boson. At that point there were promising alternatives to the *ad hoc* Higgs mechanism which could explain EWSB dynamically, such as technicolor (Farhi and Susskind, 1981) and composite Higgs models (Kaplan and Georgi, 1984). In these models unitarity was not violated either: instead of invoking the Higgs, VBS would be unitarized by massive beyond-the-SM

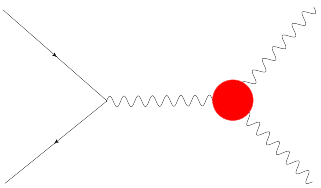

FIG. 1. Diboson production via the Drell-Yan process at a lepton or hadron collider. The red insertion represents using a term from the parametrized Lagrangian in Eq. (1).

FIG. 2. VBS in the SM with the exchange of gauge bosons on the left-hand side and the Higgs on the right-hand side needed to preserve perturbative unitarity in the SM.

(BSM) states which couple to SM gauge bosons, as shown in the right-hand side diagram of Fig. 2. If the energy of the collider is too low to directly produce the new states responsible for perturbative unitarity, an indirect way of studying this is again through anomalous couplings. For instance, if one introduces both aTGCs as in Eq. (1) and anomalous quartic gauge bosons couplings as shown in Fig. 3, both will have effects on VBS measurements. Regardless of how deviations from new sources of EWSB are parametrized, the connection between EWSB and VBS has been viewed as a window into the nature of EWSB since the early days of planning for the Superconducting Super Collider (SSC) (Chanowitz and Gaillard, 1985). Since the discovery of a Higgs-like state, the direct connection to perturbative unitarity studies has been reduced; nevertheless, it will be an important validation of the SM to show the effects of the Higgs on vector boson scattering at the LHC. Additionally, there could still be small deviations in the EWSB that would manifest themselves in VBF or VBS either as obvious deviations in the differential cross section or in searches for aTGCs or aQGCs in these channels.

These two independent threads, testing non-Abelian gauge boson couplings and unitarity in massive vector boson scattering, were both originally very well motivated to search for large deviations in the EW sector. However, with the advancement of knowledge from LEP, the Tevatron, and the LHC it is important to understand their failings in our modern understanding of the SM including the Higgs. In Sec. II.B we review the breakdown of historical methods for studying multiple production of EW gauge bosons. These methods are however still used today, including in the experimental sections of this review. We also discuss how attempts to improve on testing for deviations in coupling constants have been done through EFT methods. This is a useful tool to understand where to look for deviations in experimental results and how to parametrize them, but only if used correctly. We attempt to delineate these efforts both theoretically and experimentally, as there are failings on both sides with respect to the application of EFTs for multigauge boson production. In Sec. II.B.2 we discuss the important role of multigauge boson production in searches for BSM physics which has no connection to EFTs whatsoever. This is an important and often overlooked or factorized result given the structure of the ATLAS and CMS Collaborations, which

FIG. 3. Examples of VBS contributions from aTGCs and aQGCs.

typically relegate these processes to BSM groups that try to avoid regions of SM-like kinematics, or use them as control regions. Nevertheless, the relation that massive gauge bosons have to EWSB dictates that searches for BSM in SM EW-like kinematic regions are as important as any other topic in studying multigauge boson production in the SM. Finally, in Sec. II.B.3 we collect all conventions for anomalous couplings and effective operators used in the experimental results that are covered in this review.

Making any connection to BSM physics using multiple production of EW gauge bosons requires a precise understanding of the theoretical predictions for the SM. There has been rapid progress in this field over the past few years; notably, several new next-to-next-to-leading-order (NNLO) QCD calculations have become available. Simultaneously the LHC has entered into an era where there are sufficient statistics in multiple gauge boson production channels that NNLO and higher-order corrections are required to explain the data well. In addition, to go beyond the first implications of the Higgs and delve into possibilities for EWSB, the Higgs itself has become inextricably intertwined in current and future predictions for the LHC. Therefore, before turning to BSM possibilities, we briefly review in Sec. II.A the current theoretical understanding of SM predictions for multiple EW gauge boson production.

A. Current theoretical understanding of SM cross sections

The precision of theoretical calculations over the past decade has grown by leaps and bounds, particularly, in the last few years. Prior to the LHC, the state of the art for many calculations was next to leading order (NLO) in α_s, and even that was not fully developed. In particular, in 2005 there was an "experimentalists NLO wish list" developed at Les Houches (Buttar *et al.*, 2006) for many processes relevant for the LHC. Since then, this wish list has essentially been completed, and now Monte Carlo (MC) programs are available to calculate at NLO in QCD automatically. This amazing progress of course has been matched experimentally by the exquisite high-statistics measurements done at the LHC. This has necessitated at least three important new developments in theory.

The first is simply improving the theoretical precision of inclusive cross sections from NLO to NNLO in α_s, ultimately reaching this accuracy in fully differential cross sections as well. There has been much progress on this front that we discuss further in the next section. Increasing the order of the calculations can also introduce new production channels. At lowest order all production processes that we discuss in this review are quark initiated; however, for instance at NNLO in α_s, $pp \to VV$ includes both $q\bar{q} \to VV$ and $gg \to VV$. This implies that when reaching NNLO accuracy defined for the quark initiated process we have reached LO only in gluon initiated processes. Therefore it is also important to advance to NLO for gluon initiated processes to learn the size of the first correction. Here there is some recent progress that we will discuss for the channels where it has been calculated.

The second necessary development is the inclusion of NLO EW corrections. If we parametrize the cross section as going from LO to higher in powers of α_W and α_s (keeping in mind the caveat of new channels at higher order) as

$$d\sigma \sim d\sigma_{LO}\left(1 + \sum_i \alpha_s^i d\sigma_{N^iLO} + \sum_i \alpha_W^i d\sigma_{N^iLO_{EW}} + \text{mixed corrections}\right), \tag{2}$$

reaching NNLO QCD accuracy implies the need for NLO EW as well, since at the EW scale $\alpha_s^2 \sim \alpha_W$. This of course is just a rough estimate, as there are many factors that enter besides the coupling constant. However, EW corrections typically have the opposite sign as QCD corrections, especially in the high invariant mass and high-p_T regions, and are thus important in searching for new physics.

The third new development is due to the nature of the measurements performed at the LHC. In attempting to isolate multiboson processes, one has to deal with many QCD background processes. Reducing the QCD background by exclusively looking in the zero-jet final state of a leptonic diboson decay is experimentally advantageous. However, this introduces a new scale into the problem which is typically disparate from the hard scale. The existence of two very different scales requires one to resum the large logarithms which arise to make accurate predictions.

In Secs. II.A.1–II.A.3 we outline the current status of theoretical calculations for three distinct types of processes at the LHC. First we discuss the inclusive diboson processes, whose large cross sections and potentially clean final states can provide a standard candle for many measurements and searches at the LHC. We then discuss the exclusive VBF and VBS processes which represent a subset of those for inclusive single or diboson production. Finally we briefly discuss the theoretical status of triboson production. These new measurements go beyond those at previous colliders and will become more important with the high luminosity (HL-) LHC run, both as a signal and as a background to searches. For a more complete status of SM theoretical calculations beyond those of just multiboson production see Campanario *et al.* (2015), Andersen *et al.* (2016), and Rauch (2016). Note also that there are a number of multipurpose event generators used for the various multiboson processes, such as VBFNLO (Arnold *et al.*, 2009, 2011; Baglio *et al.*, 2014), MADGRAPH5_AMCNLO (Alwall *et al.*, 2014), POWHEG BOX (Alioli *et al.*, 2010; Frixione, Nason, and Oleari, 2007; Melia *et al.*, 2011; Nason, 2004; Nason and Zanderighi, 2014), SHERPA (Gleisberg *et al.*, 2009; Gleisberg and Höche, 2008; Höche *et al.*, 2009; Schumann and Krauss, 2008), and MCFM (Campbell and Ellis, 1999; Campbell, Ellis, and Giele, 2015; Boughezal *et al.*, 2017; Campbell, Ellis, and Williams, 2011b). In Secs. II.A.1–II.A.3 we concentrate on the current status of theoretical calculations rather than comparing the different MC capabilities.

1. Diboson production

For diboson production, the state-of-the-art QCD calculation is NNLO for W^+W^- (Gehrmann *et al.*, 2014; Grazzini, Kallweit, Pozzorini, Rathlev, and Wiesemann, 2016), $W^\pm\gamma$ (Denner *et al.*, 2015; Grazzini, Kallweit, and Rathlev, 2015a), $W^\pm Z$ (Grazzini, Kallweit, Rathlev, and Wiesemann, 2016), ZZ (Cascioli *et al.*, 2014; Grazzini, Kallweit, and Rathlev,

2015b), $Z\gamma$ (Denner *et al.*, 2016; Grazzini, Kallweit, and Rathlev, 2015a), and $\gamma\gamma$ (Campbell *et al.*, 2016). There has been recent rapid progress on this front using q_T subtraction techniques and in the near future public codes, such as MATRIX (Wiesemann *et al.*, 2016), should be available to automate event generation. To get to this accuracy, VV' with an additional jet has also been calculated to NLO accuracy in QCD. It will also be important to understand how to combine NNLO cross sections with parton showers to simulate fully differential events (Alioli *et al.*, 2014). It is important to also push $gg \to VV$ to NLO because when computing formally at NNLO, this is only the lowest order $gg \to VV$ process. Recently there has been progress in this, with $gg \to W^+W^-$ being calculated at NLO (Caola *et al.*, 2016) as well as $gg \to ZZ$ (Caola *et al.*, 2015). Finally, the matching of NLO gluon initiated processes to a parton shower must also be included and was recently done for ZZ (Alioli *et al.*, 2016).

The NLO EW corrections have also been computed for a subset of the processes for which the NNLO QCD corrections are known. The NLO EW corrections were calculated by Biedermann, Denner *et al.* (2016) for ZZ production including decay. For the case of W^+W^- this was carried out by Biedermann, Billoni *et al.* (2016). The $Z\gamma$ and $W\gamma$ processes were calculated at the NLO EW order by Denner *et al.* (2016) and Denner *et al.* (2015), respectively. In the case of $W\gamma$ and $Z\gamma$ this was done in combination with the NLO QCD corrections. First calculations of NLO EW corrections to off-shell vector boson scattering have also been performed (Biedermann, Denner, and Pellen, 2016). The next frontier is the joint calculation to NNLO in QCD and NLO in EW, as well as including the decays in the calculations.

For diboson production, once NNLO in α_s is reached, there is also the possibility to evaluate the interference between $gg \to VV$ and $gg \to H \to VV$. This was pointed out and calculated by Campbell, Ellis, and Williams (2011a) where a non-negligible effect was demonstrated.

There are also various types of resummation that have been carried out for diboson production such as threshold resummation, p_T resummation, and, in certain cases, jet-veto resummation. Threshold resummation can give a good approximation for higher-order calculations, for instance the W^+W^- cross section was approximated to NNLO using threshold resummation by Dawson, Lewis, and Zeng (2013). However, given that all diboson channels are now computed at fixed order to NNLO, these calculations would have to be pushed further to compete.

The resummation of p_T is useful for all diboson channels, given that in these colorless final states it provides a roughly universal prediction. The prediction for the p_T spectrum of dibosons can now be tested in a new regime, as done previously for single gauge boson production. It is also important to get the correct kinematic distributions since dibosons are important backgrounds for many other processes including Higgs boson production. The current state of the art is NNLO + NNLL (next-to-next-to-leading log) which for W^+W^- and ZZ is computed in Grazzini *et al.* (2015). Given that the $W^\pm Z$ final state was only recently computed at NNLO, the current state of the art for this channel is NLO + NNLL as in Wang *et al.* (2013), but this should change in the near future.

For the W^+W^- channel, a jet veto is used by the experiments to control the background coming from top quark pair production. More generally an exclusive measurement is made in different jet multiplicities. In this case jet-veto resummation is also needed since there is a large difference of scales between the jet-veto scale and the invariant mass of the diboson system. In fact, not including this effect led to early measurements of the W^+W^- cross section being significantly overestimated when experiments extrapolated from fiducial to inclusive measurements. The effect of the jet veto is also correlated with p_T resummation and its impact on extrapolating to the total cross section was first pointed out for p_T resummation by Meade, Ramani, and Zeng (2014) and for jet-veto resummation by Jaiswal and Okui (2014). These results naively disagreed, but after taking into account scale choices and adopting a uniform approach, they agreed at NLO + NNLL (Jaiswal, Meade, and Ramani, 2016). Currently the state of the art for jet-veto resummation for this channel is NNLO + NNLL as performed by Dawson *et al.* (2016). This slightly reduces the effect of the jet veto on the total cross section compared to NLO + NNLL. Additionally one must include the NLO effects of $gg \to VV$ in the calculation, as done by Caola *et al.* (2016), where it was shown to be large, but this needs to be resummed as well. Hopefully a more complete theoretical picture for this channel will be developed in the next few years and the same level of scrutiny will be applied to all diboson channels simultaneously.

2. Vector boson scattering and vector boson fusion

From the experimental point of view, the separation between VBF and VBS comes down to whether a single gauge boson is produced from two ($VV \to V$), or whether two gauge bosons come out ($VV \to VV$). They are of course related as shown in the representative VBS diagrams shown in Fig. 3, as the VBF fusion process can also contribute to VBS. However, experimentally VBF, where only one gauge boson is produced, can be tagged separately from VBS allowing the TGC and QGC vertices to be tested separately in principle. The current theoretical state of the art is NLO in QCD corrections, and this is implemented in the MC generator VBFNLO. Additionally, the NLO EW corrections are also known for these processes (Andersen *et al.*, 2016). It is important to combine all effects at this order in the future.

3. Triple boson production and beyond

The process $pp \to VV'V''$ is interesting for a variety of reasons. Leptonic V decays represent some of the most relevant multilepton backgrounds to new physics. Additionally, they represent a new and independent avenue for testing TGCs and QGCs beyond those from diboson production and offer consistency conditions that must be satisfied once these processes are observed with sufficient statistics. The process $W^\pm\gamma\gamma$ was calculated at leading order by Baur *et al.* (1997) and can be used as a test of the QGC. This process was then calculated at NLO in QCD (Lazopoulos, Melnikov, and Petriello, 2007). By now, general triboson processes are available at NLO in QCD, for example, implemented in the generator VBFNLO. The effects of EW corrections have also been calculated at NLO accuracy for

instance by Yong-Bai *et al.* (2016) for WWW and by Yong-Bai *et al.* (2015) for WZZ. Higher multiplicity EW gauge boson production will also be observable in the future and can be computed with existing MC generators at NLO in QCD.

B. Beyond the standard model interplay

As discussed earlier, the study of multiple gauge boson production is an important avenue for searching for new physics at the LHC due to its connection to non-Abelian gauge theories and EWSB. In particular, before the EW sector was tested at high precision by LEP or the evidence of the Higgs mechanism was directly found, large deviations were possible. However, we are now in an era where the EW structure $SU(2) \times U(1)_Y$ of the SM is established, and the measured Higgs boson mass and couplings closely resemble those of the SM Higgs. This in turn has led to a modernization of our theoretical and experimental understanding of how to use multigauge boson production to probe new physics.

For instance, the parametrization of aTGCs given in Eq. (1) manifestly breaks the gauge invariance that we know to be true and was reformulated in a "gauge-invariant" manner to fully incorporate LEP results [see Gounaris *et al.* (1996) for a review]. This reduced the general parametrization of Eq. (1) to a subset of related couplings and better formulated the search for aTGCs as deviations from the SM values $g_1^Z = g_1^\gamma = \kappa_Z = \kappa_\gamma = 1$ [appropriately rescaled by the coupling constants g of $SU(2)$ and g' of $U(1)_Y$] while all other terms are nonexistent at tree level. We discuss this further in Sec. II.B.3. However, to truly make Eq. (1) gauge invariant requires the introduction of new fields that transform under $SU(2) \times U(1)$ which requires a *model-dependent* choice.

Up until the discovery of a Higgs boson, there were many competing models for EWSB. The reason for this proliferation of models was that the Higgs mechanism in the SM has EWSB put in by hand and cannot explain why the symmetry is broken. Additionally the Higgs mechanism on its own suffers from extreme fine-tuning unless new physics occurs around the TeV scale. Models such as technicolor (Weinberg, 1976; Susskind, 1979), where EWSB occurs dynamically, and similarly to other examples of spontaneous symmetry breaking in nature, offered an attractive alternative. In the extreme case of strongly coupled EWSB such as technicolor, or other incarnations of Higgsless models (Csaki *et al.*, 2004a, 2004b), there is no Higgs field and the extra modes required for gauge invariance come from the "pions" of a larger broken symmetry. There are also models of strongly coupled EWSB which include a mode that resembles the SM Higgs, but the Higgs is also a pseudo-Goldstone boson of a larger symmetry, for instance in composite Higgs (Georgi and Kaplan, 1984) or little Higgs models (Arkani-Hamed *et al.*, 2002; Arkani-Hamed, Cohen, and Georgi, 2001). In both of these cases, gauge invariance is parametrized through a nonlinear representation of the modes, similar to the one used for chiral Lagrangians that describe the breaking of global symmetries in QCD. In weakly coupled models with fundamental scalar fields, e.g., the minimal supersymmetric SM (MSSM), there is a Higgs field that can be used directly to make gauge-invariant contributions to aTGCs and is often described in the literature as a linear representation. Regardless of the choice of "new physics" parametrization (or even simply the Higgs itself) that restores gauge invariance for aTGCs, accounting for deviations such as those parametrized in Eq. (1) requires the introduction of new physics beyond the SM. However, the parametrization does have implications for the size of deviations expected and the interpretation of experimental results. Once a Higgs boson was discovered (and there were many hints for this from prior EW precision tests that this would be true), a linear representation is highly favored and makes any other starting point almost as contrived as assuming $SU(2) \times U(1)$ is not a good symmetry. This of course does not preclude the fact that the Higgs could be a composite from dynamical symmetry breaking, but it does restrict the form of corrections as we will see.

A useful method for looking at the effects of new physics that incorporates all the previous ideas in a "model-independent" framework is to use an EFT description of the SM. This is in fact what all quantum field theories are in our modern understanding of Wilsonian renormalization. In practice, this means defining a scale Λ of new physics higher than the energy scale being probed in the experiment and using the fields of the SM to write higher dimension operators in addition to the dimension $\Delta \leq 4$ operators of the SM

$$\mathcal{L}_{\mathrm{EFT}} = \mathcal{L}_{\mathrm{SM}} + \sum_i \frac{g_i \mathcal{O}_i}{\Lambda^{\Delta_i - 4}}, \tag{3}$$

where g_i are called Wilson coefficients. Given that Λ is much higher than all the scales involved, the contributions to observables are well described by a perturbative series in momenta and energy $(E/\Lambda)^{\Delta_i - 4}$ provided that the dimensionless Wilson coefficients are $\mathcal{O}(1)$. This series then allows experiments to search for the effects of the lowest dimension operators which contribute the most to observables. At a given dimension Δ there are always a finite number of operators that can contribute to any observable. In fact through $\Delta = 6$ all operators are known and have been reduced from a general set (Buchmuller and Wyler, 1986) to an irreducible basis (Grzadkowski *et al.*, 2010). Given that there is only one gauge-invariant operator at dimension 5, the SM neutrino mass operator, the dominant effects of new physics describable by an EFT occur at $\Delta = 6$ unless they are forbidden by an additional symmetry assumption. Given that the EFT includes within it all the symmetries of the SM, this serves as the best starting point for describing small deviations to the SM from physics occurring at higher mass scales. We describe these EFT methods in more detail in Sec. II.B.1, their relation to previous aTGC studies, and where they should and should not be used. It is important to note though that an EFT manifestly does not describe physics at a scale Λ accessible to the LHC. Given that one of the most important reasons for studying multiple EW gauge boson production is its strong coupling to the EWSB sector, the possibility that there may be new physics at the EW scale that affects these measurements is a logical possibility. In fact in almost any model of new physics that explains EWSB naturally, there are new particles near the EW scale with EW quantum numbers that would contaminate the same final states used for the measurements of cross sections. The EFT formalism cannot be used for this

possibility, and currently there is almost no experimental effort in this direction where the kinematics are very SM like. In Sec. II.B.2 we discuss some possible uses of multigauge bosons to search for new physics in this region and to test the SM in ways other than what is utilized by EFT, aTGC, aQGC, and vector boson scattering measurements.

1. EFT interpretation of SM measurements

Given our current experimental and theoretical understanding, treating the SM as an EFT is an incredibly well-motivated starting point. It incorporates all the symmetries and fields we know and by definition matches the current data in the limit $\Lambda \to \infty$, since we have no current evidence of BSM physics. As mentioned earlier, this is not a truly model-independent description of all new physics—for instance those with a scale directly accessible at an experiment cannot be analyzed effectively in this manner. However, it is a useful description for those models which are well described through an EFT. Given a model that is well described through an EFT one can then perform a matching calculation of Wilson coefficients in the full model and EFT to set bounds on all such applicable models. In particular, this formalism can describe both "linear" representations for BSM and nonlinear representations that are still viable when the compositeness scale is large. For example, in the strongly interacting light Higgs (SILH) model (Giudice *et al.*, 2007) if the scale of composite resonances m_* is well above the scale we have currently probed, the standard nonlinear representation can be expanded and matched onto the EFT description. In Sec. II.B.3 a list of all EFT operators and conventions typically used will be given, as well as their relation to anomalous couplings [a more extensive discussion can be found in Degrande *et al.* (2013b)]. Before going into the conventions, it is important to understand that despite EFTs being a well-motivated framework that can apply to many different models, there are also drawbacks depending on how they are used experimentally and theoretically. The drawbacks arise for two "different" reasons, unitarity and model dependence; however, they are both related to the range of validity of the EFT formalism.

The power of EFTs to describe new physics in a model-independent manner comes explicitly from the expansion $(E/\Lambda)^{\Delta_i-4} \ll 1$. However, this means that the effects on SM observables are also small. If one introduces an operator into an effective Lagrangian and naively calculates the experimental limits, the most discriminating power comes from the opposite regime $(E/\Lambda)^{\Delta_i-4} \sim 1$, where the EFT is not valid and an infinite set of operators would be needed to describe the physics. Beyond invalidating the nature of the EFT expansion, naively calculating with a given operator, with a contribution $(E/\Lambda)^{\Delta_i-4}$ to a matrix element, will also give an apparent unitarity violation at some energy. This is different from the motivations based on tree-level unitarity violation in vector boson scattering studies back when the nature of EWSB was unknown (although the concept of unitarity violation is just as meaningless there once understood properly as strong coupling). Unitarity violation from the SM EFT is *completely unphysical* and simply reflects an incorrect use of an EFT. Apparent unitarity violation is simply just another guise for the EFT becoming strongly coupled and unable to make predictions. This point is theoretically well understood; however, experiments still refer to unitarization methods when they use an EFT framework for multigauge boson measurements [due to these inconsistent limits $(E/\Lambda)^{\Delta_i-4} \ll 1$ and $(E/\Lambda)^{\Delta_i-4} \sim 1$ for setting the most powerful bounds]. This is understandable given that the implementation of a higher dimension operator at the MC level is always just included as an extra interaction term and thus can be used outside of the physically sensible region if additional constraints are not imposed. In practice an additional form factor is included to avoid apparent unitary violations in the MC predictions [this is also the case for the use of anomalous gauge couplings as in Eq. (1)]. This typically takes the form

$$F(\hat{s}) \sim \frac{1}{(1+\hat{s}/\Lambda_{FF}^2)^n}, \tag{4}$$

where $\hat{s}$ is the invariant mass of the system, Λ_{FF} is an arbitrary scale unrelated to Λ in practice, and n is some positive power. The n used depends on the type of EFT operator or anomalous coupling of interest. This is due to the fact that as the operator dimension Δ_i grows there is naively a larger growth in energy that would have to be dampened by an insertion of a form factor with a sufficiently large n to make the amplitude convergent in this setup. There are also other methods used for unitarization such as K-matrix unitarization [see for instance Kilian *et al.* (2015)] which directly deforms the S matrix of the theory to enforce unitarity, instead of putting a form factor into the action.

The form factor approach used for unitarization can be related to the physical intuition from matching a UV theory onto an IR EFT. For instance in the case of Fermi's theory of weak interactions, the dimension-6 charged-current (CC) four-fermion operator arises as an expansion from integrating out the W at tree level. This corresponds to an expansion of the W propagator in a geometric series of p^2/m_W^2 and keeping the lowest order term. The expansion is given by

$$\frac{g^2}{p^2-m_W^2} = \frac{g^2}{m_W^2}\frac{-1}{1-p^2/m_W^2} = \frac{-g^2}{m_W^2}\sum_{k=0}^{\infty}\left(\frac{p^2}{m_W^2}\right)^k, \tag{5}$$

for $|p^2/m_W^2| < 1$. If only the $k=0$ term is kept, this gives the usual relation that the amplitudes for SM CC interactions are well reproduced by a dimension-6 four-fermion operator when $p^2/m_W^2 \ll 1$:

$$\mathcal{A}_{\mathrm{SM}} \sim \mathcal{A}_{\bar{\psi}\psi\bar{\psi}\psi}. \tag{6}$$

However, $\mathcal{A}_{\bar{\psi}\psi\bar{\psi}\psi} \sim E^2$ which would make it appear that unitarity was violated by CC interactions in Fermi theory, which of course is not the case in the full SM. There is no actual violation of unitarity; the Fermi theory with only $\Delta_i = 6$ operators is simply incomplete when $E \sim m_W$. Moreover, to even give an approximately correct answer as E approaches m_W would require keeping more and more terms in the infinite sum, i.e., many more higher dimension operators. Furthermore, above the mass of the W it is simply impossible to capture the correct scaling of the amplitude even with an

infinite number of terms, since it is outside the domain of convergence of the series. This leads to the usual overstatement that unitarity is violated in the EFT above a scale that can be predicted. This is incorrect. To make a prediction for this scale implies that we can trust perturbation theory at this scale with a finite number of terms, and this is simply not true. While unitarity is normally treated as a separate problem for EFTs compared to strong coupling, in reality they are one and the same. To go further, a particular UV completion of the EFT is needed and one is then no longer using the EFT formalism as at the start. In this particular case where the UV completion is the inclusion of the W gauge boson and its propagator, it can motivate a form for the choice of Λ and n in Eq. (4). If larger Δ_i operators are included then n would have to be increased. In the case of K-matrix unitarization there is not a good physical model since it corresponds to an infinitely heavy resonance of infinite width (Degrande *et al.*, 2013b). However, it cannot be stressed strongly enough, if one "unitarizes" an EFT one defeats the model-independent purpose of using an EFT description. Once a unitarization method is chosen, there is an explicit UV model dependence introduced, and different UV models make different predictions for the region $(E/\Lambda)^{\Delta_i-4} \sim 1$ or for lower energies as we will see.

The second drawback to using EFTs is again related to their use in an invalid region and comes from the careful application of matching Wilson coefficients to underlying theories. Naively LEP, LHC, or other experiments can set bounds on the dimensionful Wilson coefficients $c_i \sim g_i/\Lambda^{\Delta_i-4}$, and these can be compared between experiments. In fact this is often done to show the increased sensitivity of the LHC relative to previous experiments, including in this review. However, it is important to keep in mind that the dimensionful Wilson coefficient c always arises from some matching calculation where new physics at a scale M is integrated out. For example, G_F is the Wilson coefficient of the four-fermion operator that arises from integrating out the massive W and Z. In a general case there can be a new state with coupling g to SM particles and a mass M which, if integrated out at tree level to form a $\Delta = 6$ operator, gives a Wilson coefficient

$$c \sim \frac{g^2}{M^2}. \tag{7}$$

While naively one could use this EFT up to energy scales $c^{-1/2}$, if $g < 1$ one would reach the scale of the mass of the new physics M much earlier, thereby invalidating the EFT description of this model at such an energy scale. This is the case with our familiar four-fermion operator where $G_F^{-1/2} > m_W$. If one attempted to use the operator up to the scale $G_F^{-1/2}$, the predictions would be completely wrong. The resonance behavior would be missed and one would continue to wrongly assume that the operator's importance was still growing with E rather than decreasing after passing through the resonance. Furthermore, the on-shell production of W bosons in the final state would be unaccounted for if the EFT was still the description being used. Alternatively though if $g > 1$, this implies the true mass scale $M > c^{-1/2}$. This illustrates why an underlying understanding of how power counting the couplings of new physics and matching to Wilson coefficients can vastly affect whether a "bound" on an EFT operator has any meaning, or in what class of theories it has relevance. In particular, in weakly coupled theories, the range of validity can be much reduced, and by definition the underlying effects should be small. Furthermore, it is quite possible that new physics does not generate SM EFT operators at tree level as in Eq. (7), and the leading order contributions to Wilson coefficients arise at loop level (this can easily be the case if, for instance, there is a symmetry forbidding interactions between certain SM and BSM states, such as R parity or T parity). In this case

$$c \sim \frac{g^2}{16\pi^2 M^2}, \tag{8}$$

and even if $g \sim \mathcal{O}(1)$, the scale where the EFT becomes invalid is now order $c^{-1/2}/4\pi$. In such a theory, the conclusions drawn from using a bottom up EFT description would be even more misleading than the usual tree-level caveats. In strongly coupled theories, these numerical factors can naively be overcome, but of course at strong coupling there is no theoretical control. Therefore using experimental bounds on EFT operators to match to these strongly coupled theories and constrain them is an empty step unless augmented by an additional nongeneric argument that provides theoretical control. In addition, now that a Higgs boson has been discovered, we know that there cannot be a parametrically large shift in the physics of EWSB implying that new physics must appear weakly coupled at the scales we are probing at the LHC. Therefore we must be careful about the power counting of Wilson coefficients when comparing experimental results; otherwise, we are led to possibly misleading conclusions as we now illustrate.

If one takes the bounds set by different experiments on the same SM EFT operators, naively one could conclude that one experiment has increased sensitivity over another. For instance in the recent theoretical analysis of Butter *et al.* (2016) it was concluded that diboson measurements at the LHC set better bounds on operators that contribute to aTGCs than LEP. The analysis of Butter *et al.* (2016) is not incorrect. The LHC can indeed measure VBF and diboson production at high p_T enormously better than LEP. Additionally, in the aforementioned analysis they also check the first caveat discussed in this section about unitarity. However, a question still remains when using the EFT framework to set bounds: based on the scales involved and operators analyzed, are there generic statements that can come from the EFT description? Or are the results useful only to a small subset of strongly coupled models which lack predictive power? Typically these questions are not investigated in as much detail as the unitarity questions, but as we will show they can be just as important. We use the TGC as an example of how one can be misled (Contino, 2016). In Sec. II.B.3 we go into more detail about our full set of EFT operators, but for TGCs the comparison between LEP and the LHC is straightforward because there are only three operators at $\Delta = 6$ that contribute to aTGC measurements:

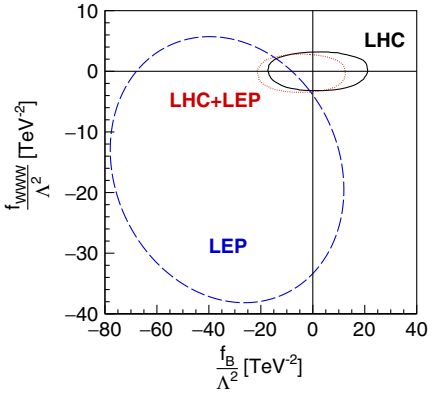

FIG. 4. A demonstration of increased sensitivity of LHC over LEP. The naming conventions are such that our c_{WWW} is their f_{WWW}/Λ^2 and our c_B is their f_B/Λ^2, the Wilson coefficients of the operators given in Eq. (9). From Butter *et al.*, 2016.

$$\mathcal{O}_W = D_\mu h^\dagger W^{\mu\nu} D_\nu h,$$
$$\mathcal{O}_B = D_\mu h^\dagger B^{\mu\nu} D_\nu h,$$
$$\mathcal{O}_{WWW} = \mathrm{Tr}(W_{\mu\nu} W^{\nu\rho} W^{\mu}_{\rho}). \tag{9}$$

Butter *et al.* (2016) performed a fit demonstrating the increased sensitivity that the LHC had from run I compared to LEP, with an example shown in Fig. 4. However, this increased sensitivity as described by Butter *et al.* (2016) comes from the high-p_T regions available at the LHC. Therefore, one must ask whether the operators used in Eq. (9) correspond to theories in which the EFT description is valid, or whether the increased sensitivity is an artifact of the high-p_T tail of the EFT. For example, one potentially viable model with alternative EWSB is the SILH model. In this model there are two parameters which describe the new physics, a coupling g_* and a mass scale m_*. As with any model, a matching calculation to a SM EFT can be performed, leading to specific predictions for the Wilson coefficients. In this case there are different power countings of couplings and masses for the different operators of Eq. (9), and when the one-dimensional bounds on the operators in Butter *et al.* (2016) are recast in terms of the m_* and g_* one reaches a contradiction. For the case of $c_{HW,HB}$ this leads to

$$c_{W,B} \sim \frac{g}{m_*^2}\left(\frac{g_*^2}{16\pi^2}\right) \rightarrow m_* \gtrsim 300\ \mathrm{GeV}\left(\frac{g_*}{4\pi}\right), \tag{10}$$

where at strong coupling the mass scale needs to be $m_* \gtrsim 300$ GeV, but the LHC has already probed this territory. In the case of c_{3W}, in Fig. 4, we naively see large gains compared to LEP, while with the SILH power counting we have

$$c_{WWW} \sim \frac{g}{m_*^2}\left(\frac{g^2}{16\pi^2}\right) \rightarrow m_* \gtrsim 20\ \mathrm{GeV}, \tag{11}$$

which shows that it is invalid to bound this type of new physics through EFTs with current data. While this is only for the SILH power counting, it is part of a more generic set of consequences for aTGCs noted by Arzt, Einhorn, and Wudka (1995). Arzt, Einhorn, and Wudka (1995) showed that the operators which lead to aTGCs must be generated at loop level, and therefore one will always be fighting the loop factor just as in the SILH power counting. Now this example of course does not invalidate the use of EFTs at the LHC. However, it illustrates the limitations in an EFT operator analysis, i.e., there could be large swaths of motivated models that cannot always be described or tested consistently in an EFT framework at the LHC. Does this mean that all channels and interpretations suffer this difficulty when using EFTs to parametrize new physics at the LHC? No, it simply reflects that for aTGCs, given that the Wilson coefficients of operators are typically suppressed, until a higher precision is reached by the LHC the EFT analysis may not be self-consistent. Once a sufficiently high precision has been reached, these bounds will be generic and useful.

EFTs have been pursued by experimentalists because of their generic character, but using them to compare to different experimental data has to be done with caution and theory prejudices in mind. For instance, if one takes the correct LEP bounds on dimension-6 operators, they are quite constrained, and there may not be increased sensitivity at the LHC as of yet unless the high-p_T behavior is exploited. As a way around this, ATLAS and CMS moved forward with a program that looked at the effects on aQGCs by ignoring all dimension-6 operators and including only dimension-8 operators in their analysis (the operators in question are listed in Sec. II.B.3). This defeats the original motivation for using EFTs, as it is focusing solely on extremely nongeneric models where dimension-6 Wilson coefficients vanish or are highly suppressed and the new physics generates leading dimension-8 operators. While not impossible (Arzt, Einhorn, and Wudka, 1995; Liu *et al.*, 2016), it is not model independent at all and requires specific mechanisms to override the standard power counting. Using the dimension-6 operators may not show improvement compared to LEP for aTGCs for instance yet, but nevertheless the bounds will apply to a much larger set of models.

EFTs are a robust theoretical tool and a welcome addition to the experimentalists arsenal. When used with the SM, they account for the Higgs and known symmetries which helps greatly when organizing search strategies for multiboson physics. However, as discussed there are many potential drawbacks as well, and they are not a panacea for model-dependent statements in experimental measurements. It simply is a fact that at this point, for many channels, the LHC is not better suited to bounding models where an EFT description is applicable. To realize this, it is not as simple as using a MC and setting a bound on the dimensionful Wilson coefficient and then comparing different colliders. One must also check whether it is consistent with unitarity and strong coupling and whether there is a self-consistent description of the coefficients of the operators and the scales being probed. While this is taught in graduate lectures [e.g., TASI (Skiba, 2011): "If one cannot reliably estimate coefficients of operators then the effective theory is useless as it cannot be made systematic."], this point has not been sufficiently stressed in the recent years where EFTs have become more and more used in the experimental communities. This does not mean that the LHC does not have

enormous capabilities for searching for new physics and constraining a wide variety of models that LEP could never dream of constraining. It is simply a question of how the experimentalists choose to parametrize the constraints. In the next section we make a recommendation of a generic procedure that applies to situations where EFTs are both applicable or not applicable.

2. Fiducial cross sections and BSM recommendations

As discussed in Sec. II.B.1, EFTs provide useful ways to search for new physics, but they also have inherent disadvantages at hadron colliders. On top of the drawbacks associated with EFTs, they are by definition useless for describing physics at scales directly accessible to the LHC. However, multiboson processes still are one of, if not the most important channels to search for new physics due to their connection to EWSB. In principle, new physics accessible at LHC energies could be discovered or constrained by direct searches in groups other than the SM groups. However, in many scenarios of BSM physics there are difficult kinematic regions which direct searches in other groups have trouble accessing. In this section we demonstrate examples where SM measurements can provide powerful discriminating power for BSM physics even when the EFT description is invalid. Most importantly, the measurements we propose are equally powerful in searching for BSM physics as EFTs, but avoid all the issues of EFT searches associated with unitarization, strong coupling, power counting, and spurious symmetry arguments.

Before discussing generalities it is useful to look at an interesting example from run I that came about, not originally from a theoretical effort but from a series of measurements by ATLAS and CMS. The W^+W^- cross section as measured by ATLAS and CMS was systematically higher than the predicted NLO cross section at both 7 and 8 TeV. This eventually led to the theoretical developments involving higher fixed order calculations as well as higher-order resummed calculations that brought theory into good agreement with the measurements [see Dawson *et al.* (2016) for the state of the art which still is slightly low compared to the measured value when jet-veto resummation effects are theoretically included]. However, an intriguing possibility before the higher-order SM calculations were available was that this could have also been caused by a new BSM contribution to the W^+W^- cross-section measurement. An example of this was provided by Curtin, Jaiswal, and Meade (2013) where the supersymmetric (SUSY) pair production of charginos would lead to a final state $pp \to \chi^+\chi^- \to W^+W^-\chi^0\chi^0$, with the same l^+l^-+ missing transverse energy (MET) final state. Typically such a process is sought in direct SUSY searches, but if the spectrum is such that the kinematics is similar to that of the SM background it is very difficult to disentangle and could be missed. Kinematics in a SUSY process similar to multiboson final states naturally arises if EW BSM states are similar to the EW scale. However, this also holds true if the mass splittings between the initially produced states and their decay products are similar to the EW scale. Curtin *et al.* (2013) realized that the W^+W^- cross-section measurement itself could be used to bound a number of these scenarios. In particular, by using this measurement the first bounds on right-handed sleptons that exceeded LEP limits were found. This was applied to other SM channels as well, for instance the $t\bar{t}$ final state in Czakon *et al.* (2014).

Having BSM physics which mimics SM final states is a very generic phenomenon. For example, many different types of models were written to attempt to explain the W^+W^- cross-section excess (Curtin, Jaiswal, and Meade, 2013; Curtin *et al.*, 2013; Curtin, Meade, and Tien, 2014; Rolbiecki and Sakurai, 2013; Jaiswal, Kopp, and Okui, 2013). Some of these did not even directly rely on partners of EW gauge bosons for production, but nevertheless led to final states that potentially contaminated the SM measurement. Almost all exotic or SUSY searches have gaps when a SM background and BSM signals become kinematically similar. Dedicated search strategies can be set up to try to close these gaps, but it is very model dependent and takes much effort to understand the SM background. Naturally, as demonstrated by Curtin *et al.* (2013), a SM measurement is already an incredibly powerful place to search for this type of generic BSM physics. However, this has been carried out only by theorists and the methods could be pushed further by those making the measurements. Unfortunately, as discussed so far, multigauge boson cross-section measurements are only used by the experiments to search for EFTs, aTGCs, and aQGCs, none of which are relevant for the processes described here. Fortunately, there is a way out already adopted by BSM groups within ATLAS and CMS, which recently has also been adopted by the SM groups and should be extended to all channels.

We recommend that for all multigauge boson measurements, the experiments place bounds via upper limits on fiducial cross sections as an alternative to EFT and anomalous coupling interpretations. The ATLAS SUSY group began giving limits like this. In addition to interpreting their signal regions through models, they included 95% confidence level (C.L.) upper cross-section limits on signal regions (Aad *et al.*, 2012k) independent of interpretation. ATLAS and CMS have given fiducial cross sections in multigauge boson production measurements, and in a few cases 95% C.L. upper limits on signal regions as well, which we strongly endorse. By giving upper limits on cross sections in different fiducial regions, any model can be interpreted whether or not an EFT approach is valid or a model must be used. There is no loss in discriminating power compared to previous studies of SM cross sections. For instance signal regions used for aTGCs or aQGCs based on high p_T or invariant mass can be kept, and theorists can easily recast the bounds. However, it avoids the interpretation issues for the experiments on the validity of EFTs, aTGCs, or aQGCs. In particular, the theoretical statement of when a certain model or approach is theoretically valid resides with the theorists. Additionally, it allows for the direct comparison with models that are not describable in the theoretical approaches implemented by the experimental groups, for instance the W^+W^- example given earlier. Furthermore, by reducing the time spent on theoretical interpretation, it allows for more "signal" regions to be investigated. We emphasize that this is not what has been done at the LHC when moving from EFTs of dark matter (DM) (Fox *et al.*, 2012) to simplified models (Abdallah *et al.*,

2015) because of concerns with the EFT approach. In the case of DM at the LHC, it was realized that having an EFT description of DM was often not valid due to the unitary or strong coupling or Wilson coefficient and power counting arguments and another approach was needed. To couple DM to SM charged particles generically requires new physics that is charged under the SM gauge symmetry which we call messenger particles (there are notable exceptions but this is quite common). Therefore it is typically more straightforward and theoretically consistent to search for these messenger particles directly, rather than searching for EFT operators via radiative processes such as monojets that may not be self-consistent. For example, this is why SUSY bounds on neutralinos were never set via *direct* production of neutralinos tagged from an initial state radiation jet. In principle one could attempt to identify simplified models for EW processes relevant for multiboson physics as an alternative to EFTs. However, there are always drawbacks to simplified models as well, and searches in BSM experimental groups typically are not nearly as sophisticated in the SM theory prediction as for a SM measurement. Rather than duplicate effort that may exist elsewhere and run into issues of theoretical interpretations such as whether or not simplified models provide sufficient coverage, it is much more useful and direct to have the SM groups of ATLAS and CMS provide upper limits on fiducial cross sections. This does not have to be motivated solely from the BSM perspective. Having more differential distributions in fiducial regions that are well understood by the experiments can point to where more SM theoretical effort is needed, e.g., NNLO QCD, NLO EW, or various resummations.

3. Theoretical conventions used in experimental results

Despite the caveats presented in the previous sections, it is useful to understand what the current measurements are based on and therefore we review the common conventions used for EFT operators that are pertinent for multiboson processes as well as the anomalous coupling parametrizations. In addition we give the dictionary that translates between these approaches, although this does not mean they are equivalent. The EFT parametrization is theoretically sound when used correctly, while anomalous couplings as in Eq. (1) are not relevant nor sensible post-Higgs. Most of the conventions used here are explicitly given in the excellent Snowmass white papers (Degrande *et al.*, 2013b, 2013c), but we give a succinct version here for completeness.

We begin with our description of the EFT operators that will be used in the experimental sections. As discussed, the operators of interest are those that include gauge fields and are of dimension $\Delta_i = 6$ or possibly $\Delta_i = 8$. The $\Delta_i = 6$ are the most important operators when the EFT is valid unless there is a systematic power counting due to a particular UV interpretation that would suppress the dimensionless Wilson coefficients (Arzt, Einhorn, and Wudka, 1995; Liu *et al.*, 2016). At $\Delta_i = 6$ there are already 59 operators in the SM (Buchmuller and Wyler, 1986; Grzadkowski *et al.*, 2010), while for $\Delta_i = 8$ an exhaustive list of 535 operators was finally classified by Lehman and Martin (2016). While there are slight differences in the number of operators at a fixed dimension in the literature depending on what assumptions are chosen, the operator basis has now been extended through $\Delta_i = 12$ in the SM using more sophisticated mathematical techniques (Henning *et al.*, 2015). However, the important and simple to understand point is that as Δ_i increases the number of operators greatly proliferates. Therefore even though in this review we are only interested in operators which can modify multiple vector boson production, there will be a much larger number of operators than can contribute at larger Δ_i. One final point to keep in mind, when using an EFT of a particular set of fields (in this case the SM fields): there is inherently a basis choice that one must make as operators can be related to one another through various identities, integration by parts, or equations of motion. In this review we focus on operators that affect multigauge boson production, but one must keep the basis choice in mind when comparing to bounds on other operators involving the gauge boson and Higgs fields not surveyed here.

At $\Delta_i = 6$ there are three independent operators, given in Eq. (9) and reproduced below, which affect diboson production by giving new contributions to triple gauge boson and quartic gauge boson couplings,

$$\begin{aligned} \mathcal{O}_W &= D_\mu h^\dagger W^{\mu\nu} D_\nu h, \\ \mathcal{O}_B &= D_\mu h^\dagger B^{\mu\nu} D_\nu h, \\ \mathcal{O}_{WWW} &= \mathrm{Tr}(W_{\mu\nu} W^{\nu\rho} W^{\mu}_{\rho}). \end{aligned} \tag{12}$$

The Wilson coefficients for the operators in Eq. (12) are given by c_W/Λ^2, c_B/Λ^2, and c_{WWW}/Λ^2. While there are only three operators that contribute at this dimension to diboson production, there are many other operators at $\Delta_i = 6$ that involve the Higgs and gauge fields. These can be shown to affect the propagators, as for instance in the case of the Peskin-Takeuchi S, T, U parameters (Peskin and Takeuchi, 1992) which all have $\Delta_i = 6$ operator definitions. While these operators do not contribute to diboson production, their Wilson coefficients are already highly constrained. Therefore it is important to keep in mind that when studying the operators in Eq. (12), a generic UV completion may already be strongly constrained leading to suppressed Wilson coefficients for these operators as well.

At $\Delta_i = 8$ there are 18 operators divided into three classes that can modify multiple vector boson production by generating additional contributions to quartic gauge boson couplings. Gauge fields, in a gauge covariant setup, can appear in the operators either in covariant derivatives or field strengths and therefore the operators are classified by their contributions from these basic building blocks. We use the naming conventions found in Éboli, Gonzalez-Garcia, and Mizukoshi (2006) that have become standard in this community (Degrande *et al.*, 2013b): S-type operators involve only covariant derivatives of the Higgs (listed in Table I), M-type operators include a mix of field strengths and covariant derivatives of the Higgs (listed in Table II), and T-type operators include only field strengths (listed in Table III). Note that not all operators in Éboli, Gonzalez-Garcia, and Mizukoshi (2006) are listed here. Some of the original operators in this notation vanish identically or can be related to others. For a more detailed discussion see Rauch (2016).

TABLE I. Each operator $\mathcal{O}_i$ is parametrized by a Wilson coefficient f_i/Λ^4. $\mathcal{O}_{S,2}$ was introduced by Éboli and Gonzalez-Garcia (2016).

S-type operators	
Operator name	Operator
$\mathcal{O}_{S,0}$	$[(D_\mu\Phi)^\dagger D_\nu\Phi] \times [(D^\mu\Phi)^\dagger D^\nu\Phi]$
$\mathcal{O}_{S,1}$	$[(D_\mu\Phi)^\dagger D^\mu\Phi] \times [(D_\nu\Phi)^\dagger D^\nu\Phi]$
$\mathcal{O}_{S,2}$	$[(D_\mu\Phi)^\dagger D_\nu\Phi] \times [(D^\nu\Phi)^\dagger D^\mu\Phi]$

The parametrization of the higher dimension operators in Eq. (12) and Tables I–III are the most relevant and sensible for the LHC and for searching for physics beyond the SM because they are inherently gauge invariant under $SU(2) \times U(1)$ and incorporate EWSB by a SM-like Higgs. There are also the analogs that are CP-violating operators at $\Delta_i = 6$ obtained by inserting a dual field strength in the place of one of the field strengths listed. In this review experimental limits on S-, T-, and M-type operators are presented, although limits using older conventions are also given.

While the operators listed are the recommended best choice for future studies, anomalous coupling measurements existed long before this modern EFT point of view and therefore there are many legacy parametrizations still used by experiments. For instance, before the Higgs was confirmed experimentally there were many other possibilities for EWSB as reviewed in earlier sections. Because of this there were other parametrizations of "higher-dimensional operators" (Alboteanu, Kilian, and Reuter, 2008; Reuter, Kilian, and Sekulla, 2013), where an effective chiral Lagrangian was used to describe EWSB and the interactions of the longitudinal modes of gauge bosons. While this parametrization is not as good a starting point post-Higgs there are still some experimental results that use it. In particular, the α_4 and α_5 parameters are used that provide new contributions to quartic gauge boson couplings and can be mapped to a Higgs-like theory straightforwardly. Assuming a Σ field describing the longitudinal degrees of freedom, one can define the longitudinal vector field as $\mathbf{V} = \Sigma(D\Sigma)^\dagger$. The α_4 and α_5 parameters are given as the coefficients of the operators

$$\mathcal{O}_4 = \mathrm{Tr}[\mathbf{V}_\mu\mathbf{V}_\nu]\mathrm{Tr}[\mathbf{V}^\mu\mathbf{V}^\nu], \tag{13}$$

$$\mathcal{O}_5 = \mathrm{Tr}[\mathbf{V}_\mu\mathbf{V}^\mu]\mathrm{Tr}[\mathbf{V}_\nu\mathbf{V}^\nu]. \tag{14}$$

TABLE II. Each operator $\mathcal{O}_i$ is parametrized by a Wilson coefficient f_i/Λ^4.

M-type operators	
Operator name	Operator
$\mathcal{O}_{M,0}$	$\mathrm{Tr}[W_{\mu\nu}W^{\mu\nu}] \times [(D_\beta\Phi)^\dagger D^\beta\Phi]$
$\mathcal{O}_{M,1}$	$\mathrm{Tr}[W_{\mu\nu}W^{\nu\beta}] \times [(D_\beta\Phi)^\dagger D^\mu\Phi]$
$\mathcal{O}_{M,2}$	$[B_{\mu\nu}B^{\mu\nu}] \times [(D_\beta\Phi)^\dagger D^\beta\Phi]$
$\mathcal{O}_{M,3}$	$[B_{\mu\nu}B^{\nu\beta}] \times [(D_\beta\Phi)^\dagger D^\mu\Phi]$
$\mathcal{O}_{M,4}$	$[(D_\mu\Phi)^\dagger W_{\beta\nu}D^\mu\Phi] \times B^{\beta\nu}$
$\mathcal{O}_{M,5}$	$[(D_\mu\Phi)^\dagger W_{\beta\nu}D^\nu\Phi] \times B^{\beta\mu}$
$\mathcal{O}_{M,7}$	$[(D_\mu\Phi)^\dagger W_{\beta\nu}W^{\beta\nu}D^\mu\Phi]$

TABLE III. Each operator $\mathcal{O}_i$ is parametrized by a Wilson coefficient f_i/Λ^4.

T-type operators	
Operator name	Operator
$\mathcal{O}_{T,0}$	$\mathrm{Tr}[W_{\mu\nu}W^{\mu\nu}] \times \mathrm{Tr}[W_{\alpha\beta}W^{\alpha\beta}]$
$\mathcal{O}_{T,1}$	$\mathrm{Tr}[W_{\alpha\nu}W^{\mu\beta}] \times \mathrm{Tr}[W_{\mu\beta}W^{\alpha\nu}]$
$\mathcal{O}_{T,2}$	$\mathrm{Tr}[W_{\alpha\mu}W^{\mu\beta}] \times \mathrm{Tr}[W_{\beta\nu}W^{\nu\alpha}]$
$\mathcal{O}_{T,5}$	$\mathrm{Tr}[W_{\mu\nu}W^{\mu\nu}] \times B_{\alpha\beta}B^{\alpha\beta}$
$\mathcal{O}_{T,6}$	$\mathrm{Tr}[W_{\alpha\nu}W^{\mu\beta}] \times B_{\mu\beta}B^{\alpha\nu}$
$\mathcal{O}_{T,7}$	$\mathrm{Tr}[W_{\alpha\mu}W^{\mu\beta}] \times B_{\beta\nu}B^{\nu\alpha}$
$\mathcal{O}_{T,8}$	$B_{\mu\nu}B^{\mu\nu}B_{\alpha\beta}B^{\alpha\beta}$
$\mathcal{O}_{T,9}$	$B_{\alpha\mu}B^{\mu\beta}B_{\beta\nu}B^{\nu\alpha}$

We strongly recommend using the parametrizations of the $\Delta_i = 6$ and 8 operators previously given instead of α_4 and α_5. If necessary one could translate results in a model of weakly coupled EWSB, i.e., a Higgs-like theory, to this parametrization and the α's would be of order v^2/Λ^2 up to a dimensionless coefficient.

Another example of pre-Higgs higher dimension operators are the quartic gauge boson coupling operators in the Lagrangian given by Stirling and Werthenbach (2000):

$$\mathcal{L} = -\frac{e^2 a_0^W}{16\pi\Lambda^2} F_{\mu\nu}F^{\mu\nu}\vec{W}^\alpha\vec{W}_\alpha - \frac{e^2 a_c^W}{16\pi\Lambda^2} F_{\mu\alpha}F^{\mu\beta}\vec{W}^\alpha\vec{W}_\beta, \tag{15}$$

where $\vec{W}_\beta$ is a three-dimensional vector of the W and Z gauge bosons. Again the gauge symmetry of the SM is not manifest, but such an operator could be generated at $\Delta_i = 8$ in a gauge-invariant way and then mapped to this operator when the Higgs acquires a VEV. In particular, one can map from all the M-type operators in Table II to these a's as

$$\frac{f_{M,j}v^2}{\Lambda^4} \sim \frac{a_{0,c}^W}{\Lambda^2}. \tag{16}$$

The exact numerical mapping depends on the normalizations and can be found in Degrande *et al.* (2013b).

There are also higher dimension operators in the outdated anomalous gauge boson coupling Lagrangian as in Eq. (1). For example, the λ_V and $\tilde{\lambda}_V$ terms are dimension-6 operators. However, this is not a consistent EFT expansion given the symmetries we know, but they are gauge invariant and can be mapped directly as

$$\frac{c_{WWW}}{\Lambda^2} \sim \frac{\lambda_V}{m_W^2}, \tag{17}$$

or its CP-violating analog, which then allows for a consistent power counting in the EFT.

Finally we must review the "modern" anomalous coupling parametrizations as given for instance in Eq. (1) reduced to the LEP scenario (Gounaris *et al.*, 1996) discussed earlier. As stressed many times, this parametrization should not be used and we recommend that the EFT basis from Eq. (12) and Tables I–III be used if one insists on a theory interpretation rather than fiducial cross sections. Nevertheless, anomalous

coupling searches existed long before the modern EFT point of view and therefore they have remained as a legacy that still remains in the experimental community. The original parametrization of anomalous triple gauge boson couplings and quartic gauge boson couplings is given in Eq. (1). As mentioned earlier, in an attempt to make Eq. (1) more relevant in the LEP era the general parametrization was reformulated in a gauge-invariant manner where $g_1^Z = g_1^\gamma = \kappa_Z = \kappa_\gamma = 1$ [appropriately rescaled by the coupling constants g of $SU(2)$ and g' of $U(1)_Y$] while all other terms do not exist at tree level in the SM. Deviations from this limit are parametrized as $\Delta g_1^V \equiv g_1^V - 1$, $\Delta\kappa_V \equiv \kappa_V - 1$, and λ_V, which are the experimentally bounded quantities in a search for BSM contributions to anomalous couplings (Gounaris *et al.*, 1996). This standard aTGC parametrization has long been used; however, it manifestly violates unitarity and lacks a systematic program for renormalization unlike an EFT (Degrande *et al.*, 2013c). As a kludge, form factors were introduced to parametrize vertex functions for triple gauge boson couplings in momentum space. This is not sensible nor gauge invariant, but has nevertheless propagated into modern measurements. The choice of parametrization (Gaemers and Gounaris, 1979; Hagiwara *et al.*, 1987) used is

$$\begin{aligned}\Gamma_V^{\alpha\beta\mu} = {} & f_1^V(q-\bar{q})^\mu g^{\alpha\beta} - \frac{f_2^V}{M_W^2}(q-\bar{q})^\mu P^\alpha P^\beta \\ & + f_3^V(P^\alpha g^{\mu\beta} - P^\beta g^{\mu\alpha}) + i f_4^V(P^\alpha g^{\mu\beta} + P^\beta g^{\mu\alpha}) \\ & + i f_5^V \epsilon^{\mu\alpha\beta\rho}(q-\bar{q})_\rho - f_6^V \epsilon^{\mu\alpha\beta\rho} P_\rho \\ & - \frac{f_7^V}{m_W^2}(q-\bar{q})^\mu \epsilon^{\alpha\beta\rho\sigma} P_\rho (q-\bar{q})_\sigma, \end{aligned} \tag{18}$$

where two of the gauge bosons are W's and V is a Z or γ, while q, $\bar{q}$, and P are the respective four-momenta. A similar approach was undertaken by Baur and Berger (1993) for a triple neutral vertex

$$\begin{aligned}\Gamma_{Z\gamma V}^{\alpha\beta\mu}(q_1, q_2, P) = {} & \frac{P^2 - q_1^2}{m_z^2}\left[h_1^V(q_2^\mu g^{\alpha\beta} - q_2^\alpha g^{\mu\beta})\right. \\ & + \frac{h_2^V}{m_z^2} P^\alpha[(P\cdot q_2) g^{\mu\beta} - q_2^\mu P^\beta] \\ & \left. + h_3^V \epsilon^{\mu\alpha\beta\rho} q_{2\rho} + \frac{h_4^V}{m_z^2} P^\alpha \epsilon^{\mu\beta\rho\sigma} P_\rho q_{2\sigma}\right]. \end{aligned} \tag{19}$$

The vertex function approach is particularly opaque compared to the EFT operator treatment and because there is not a straightforward mapping, given that the form factors are undetermined functions (although they could be taken to have a fixed value if one wanted to treat this as a Fourier transform of some position space operators). Again, this manifestly does not include gauge invariance and does not deal with strong coupling and unitarity in a systematic way. This parametrization should not be used in the future. Given the systematic gauge-invariant parametrization of the EFT, once the Higgs acquires a VEV, the Wilson coefficients can be mapped to the anomalous couplings approach. For example,

$$\Delta g_1^Z = c_W \frac{m_z^2}{2\Lambda^2}, \tag{20}$$

but this is only a one-way mapping and does not mean these two approaches are equivalent. The EFT can be extended systematically and with a full mapping of Wilson coefficients to anomalous couplings, it enforces certain correlations that would otherwise not exist in an anomalous couplings approach. While we maintain our recommendation to simply measure fiducial cross sections, if a theory interpretation must be made, use the EFT approach. However, the self-consistency of the EFT approach must also be verified as explained in previous sections or the interpretations can be misleading or wrong. For further relations between parameters or connections to MC generator parameters see Degrande *et al.* (2013b).

III. EXPERIMENTAL SETUP

Detailed descriptions of the Large Hadron Collider, the ATLAS, and the CMS detectors are available elsewhere (Aad *et al.*, 2008; Chatrchyan *et al.*, 2008; Evans and Bryant, 2008). The definitions of the physics objects used in the described analyses vary in both efficiency and purity and are selected based on the needs of the specific physics process under study. CMS makes extensive use of particle flow algorithms which use all the CMS subsystems (Chatrchyan *et al.*, 2011a; Beaudette, 2013).

The triggers selecting the final states of interest to be recorded for off-line analysis are generally based on the selection of energetic electrons or muons if present in the final state, with thresholds depending on the data taking period under study and its instantaneous luminosity. The trigger thresholds for electrons and muons are efficient for W and Z boson leptonic decays, and reconstruction thresholds also maintain high efficiency. In the absence of charged leptons in the signature, other characteristics such as the presence of energetic photons or large MET are utilized. The hadronic decay products of W or Z bosons are not required to satisfy a trigger. The performance of the ATLAS trigger system is described in more detail elsewhere (Aad *et al.*, 2012j, 2012n, 2015d), and a detailed description of the CMS system is given in Adam *et al.* (2006), Chatrchyan *et al.* (2010), and Khachatryan *et al.* (2016f).

The performance of ATLAS and CMS for photons (Aad *et al.*, 2011c, 2012m, 2014a; Khachatryan *et al.*, 2015e; Aaboud *et al.*, 2016c), electrons (Aad *et al.*, 2014b; Khachatryan *et al.*, 2015d; Aaboud *et al.*, 2016a), muons (Chatrchyan *et al.*, 2013d; Aad *et al.*, 2014d, 2014e), MET (Aad *et al.*, 2012i; 2013i, 2014g; 2016f; Khachatryan *et al.*, 2015f), and jets (Lampl *et al.*, 2008; Chatrchyan *et al.*, 2011a; Aad *et al.*, 2013a, 2013b, 2015c; 2015f; Khachatryan *et al.*, 2016a) is well documented.

The sensitivity to anomalous gauge couplings is greatest at high mass, when the hadronic decay products of the gauge bosons are merged into a single unresolved jet. Nevertheless, the mass of such jets is cleanly measured (Aad *et al.*, 2016c; Khachatryan *et al.*, 2014b) and they are key tools for such studies. In Fig. 5 the jet mass for a sample of lepton plus MET plus jets with top pair enhancements illustrates the cleanliness of the merged hadronic W boson decays.

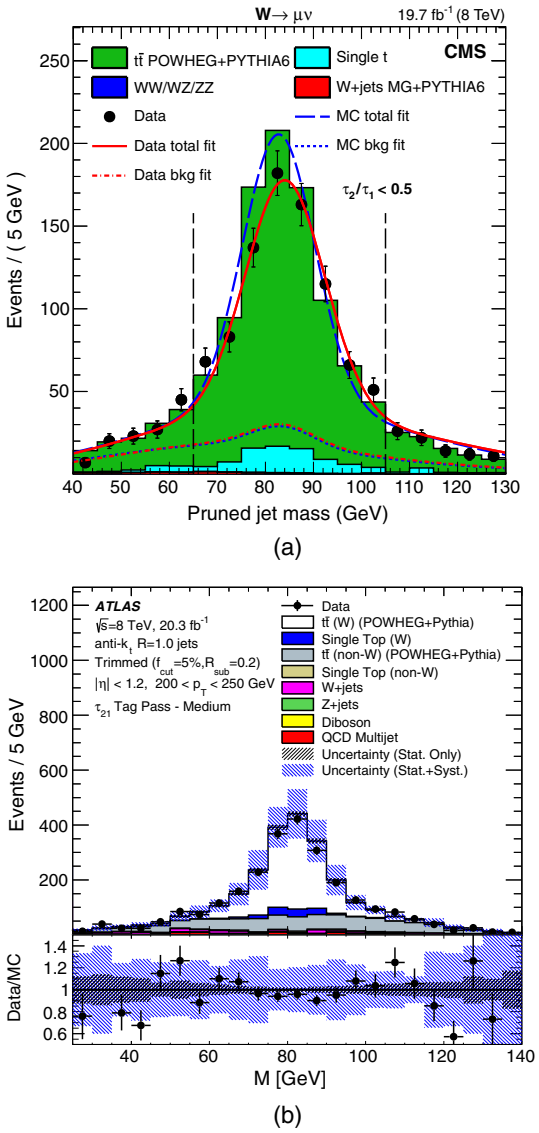

FIG. 5. Jet mass distributions in events with a leptonic W boson decay and jets with cuts appropriate for boosted top jets: (a) CMS (Khachatryan *et al.*, 2014a) for the muon channel and (b) ATLAS (Aad *et al.*, 2016c) for the combined electron and muon channels. A wide variety of MC generators is used to model SM signal and background processes in the figures of this review. We give an overview of the commonly used generators in Sec. II.A, but for the specific details of each analysis see the provided analysis references.

For the gauge bosons, the studies of photons are already listed above. For W bosons, the leptonic decays are studied using the lepton (electron or muon) plus MET signature. Hadronic decays are captured as a mass peak in the resolved dijet case at low transverse momentum and in the boosted monojet case at high transverse momentum. For Z bosons dilepton pairs are used, both electrons and muons (Aad *et al.*, 2012a; Chatrchyan *et al.*, 2014b); τ leptons are not included with one exception detailed in Sec. IV.H. In addition, the larger branching fraction neutrino pair decay mode is tagged using a MET signature. Hadronic Z boson decays are not fully resolved in the (di)jet mass from W boson decays.

The results described in this review combine the boson signatures at 7 and 8 TeV center of mass energy in a variety of final states detailed in Secs. IV–VII. Limits on anomalies in the gauge couplings appear in Secs. VIII and IX, derived by exploring the high-mass spectrum of the (multi)bosons themselves or by use of the transverse momentum of one of the bosons or one of the boson decay products depending on the specific analysis. Background processes are evaluated by using Monte Carlo models, by extrapolating from background dominated control regions, or by data-driven methods, depending on the importance of the background source and reliability of the available MC modeling.

IV. DIBOSON PRODUCTION

A. $\gamma\gamma$ production

Measurement of diphoton production represents a stringent test of higher-order perturbative QCD corrections, since beyond the LO quark-antiquark annihilation the quark-gluon channel contributes at NLO and the gluon-gluon channel box diagram at NNLO. This process is also sensitive to soft fragmentation contributions where photons arise from the fragmentation of colored partons. With the discovery of a Higgs boson (Aad *et al.*, 2012h; Chatrchyan *et al.*, 2012b) a resonant production mode has become available to which diphoton production constitutes an irreducible background that needs to be well characterized for detailed Higgs boson studies as well as for searches for new resonances.

Both ATLAS (Aad *et al.*, 2012b, 2013e) and CMS (Chatrchyan *et al.*, 2012a, 2014a) studied diphoton production at 7 TeV in data samples with integrated luminosities of up to 5 fb^{-1}. The measured total cross sections are most compatible with the theoretical predictions at NNLO, and partial N^{3}LO results including the NLO corrections to the gluon-gluon channel box diagram lead to a further 7% increase of the total cross-section prediction (Campbell *et al.*, 2016).

Both experiments provide in addition differential cross-section measurements as a function of, for example, the invariant mass, transverse momentum, and azimuthal separation of the diphoton system. As illustrated in Fig. 6, these measurements show better agreement with NNLO predictions compared to NLO ones, albeit the fixed order NNLO calculation fails to describe data in regions where fragmentation contributions (not included in the calculation) are relevant, such as low mass or intermediate transverse momentum of the diphoton system. Mass scales slightly below 1 TeV are probed already with these 7 TeV data sets.

B. $W\gamma$ production

Studies of the $W\gamma$ final state have been published by ATLAS (Aad *et al.*, 2011b, 2012f, 2013d) and CMS (Chatrchyan *et al.*, 2011c, 2014c) at 7 TeV using data samples with integrated luminosities of up to 5 fb^{-1}, where the W boson was observed in the leptonic final state with the charged lepton being either an electron or a muon and the photon was required to be isolated. Both experiments provide inclusive

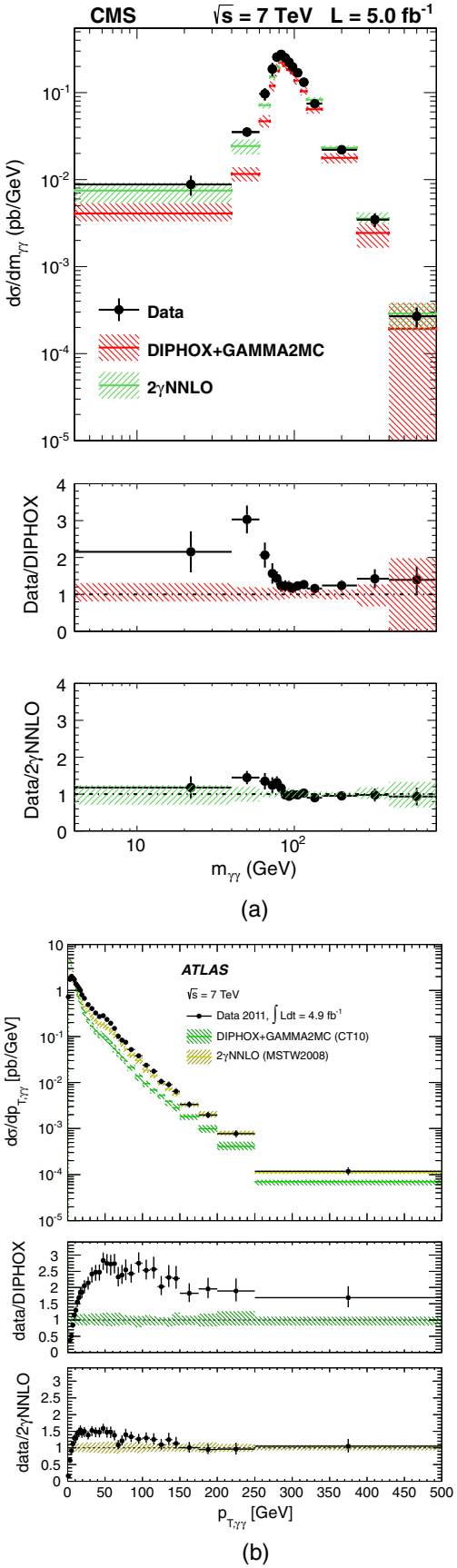

FIG. 6. Comparison of $\gamma\gamma$ differential cross-section measurements as a function of (a) the invariant mass (Chatrchyan *et al.*, 2014a) and (b) transverse momentum (Aad *et al.*, 2013e) of the diphoton system with NLO and NNLO predictions.

diboson cross sections, and ATLAS additionally provides exclusive cross sections where central jet activity has been vetoed. As illustrated in Fig. 7, CMS finds the cross section to be compatible with the MCFM prediction at NLO in QCD as a function of the photon E_{T} out to 100 GeV, while ATLAS measures inclusive cross sections higher than the NLO prediction in the inclusive process for high-E_{T} photons. NNLO corrections are found to increase the NLO prediction by ≈20%, hence improving the agreement with the measured cross sections (Grazzini, Kallweit, and Rathlev, 2015a).

The SM TGC of $WW\gamma$ contributes to $W\gamma$ production. Limits on the aTGCs $\Delta\kappa_\gamma$ and λ_γ are set by comparing their effect on the photon E_{T} spectrum with the observed spectrum as shown in Fig. 8. ATLAS uses exclusive events (vetoing central jets) to set limits on anomalous couplings in order to increase the expected sensitivity in high-E_{T} photon events,

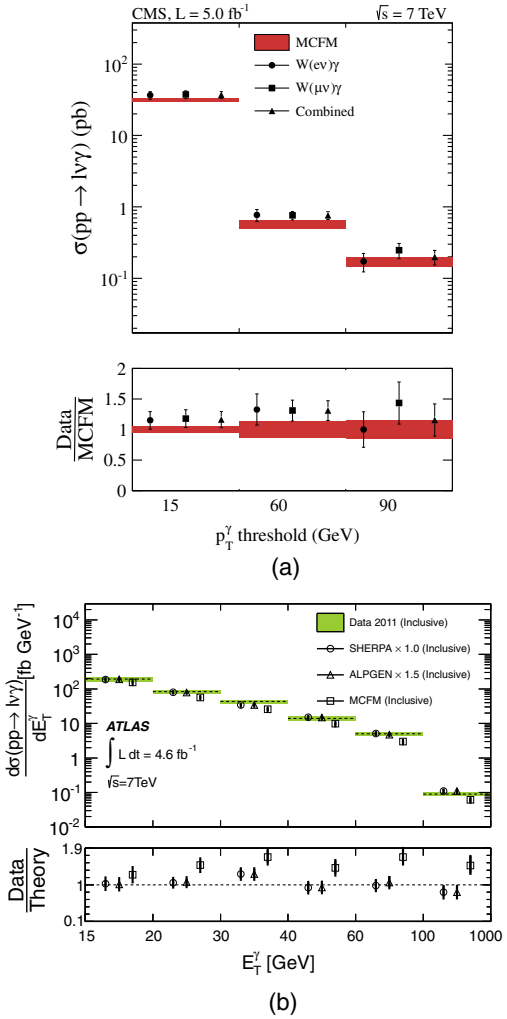

FIG. 7. 7 TeV $W\gamma$ inclusive cross section as a function of photon E_{T}: (a) comparison of the CMS measurements with MCFM predictions (Chatrchyan *et al.*, 2014c) and (b) comparison of the ATLAS measurements with MCFM, SHERPA, and ALPGEN (Mangano *et al.*, 2003) predictions, where the latter two have been scaled to match the total number of observed events in data (Aad *et al.*, 2013d). Note that MCFM gives an NLO prediction, which is known to increase by ≈20% when taking NNLO corrections into account.

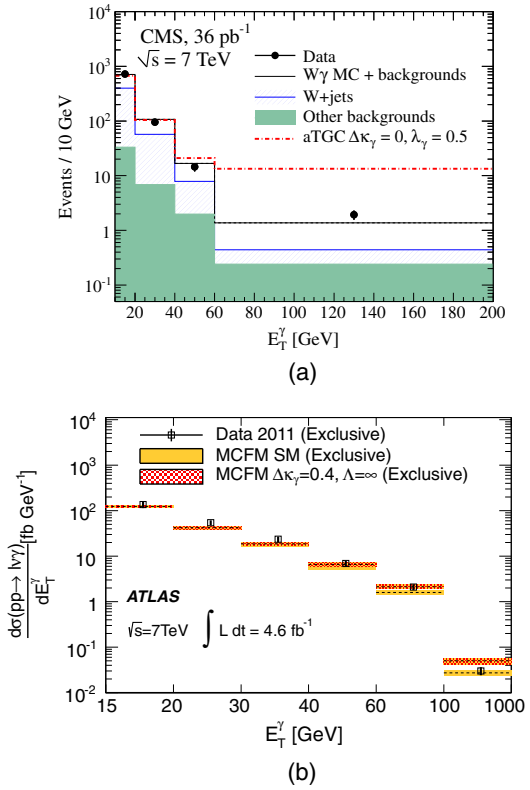

FIG. 8. Effect of aTGCs in the $W\gamma$ final state at 7 TeV: (a) photon E_T spectrum measured by CMS with an inclusive selection (Chatrchyan *et al.*, 2011c) and (b) $W\gamma$ cross section measured by ATLAS as a function of photon E_T with an exclusive selection vetoing central jets (Aad *et al.*, 2013d).

which otherwise also tend to exhibit more jet activity in the SM. For CMS, no constraints are placed on additional objects in the event due to issues of possible systematic bias in Monte Carlo modeling of those additional objects.

C. $Z\gamma$ production

The production of $Z\gamma$ pairs in final states with an oppositely charged electron or muon pair and an isolated photon has been studied by ATLAS (Aad *et al.*, 2011b, 2012f, 2013d) and CMS (Chatrchyan *et al.*, 2011c, 2014c) at 7 TeV using data samples with integrated luminosities of up to 5 fb^{-1}. Both experiments provide inclusive diboson cross sections, and ATLAS additionally provides exclusive cross sections where central jet activity has been vetoed. As illustrated in Fig. 9, both ATLAS and CMS find the cross section to be compatible with the MCFM prediction at NLO in QCD as a function of the photon E_T. NNLO corrections are found to be much smaller compared to $W\gamma$ and increase the NLO prediction by ≈8% (Grazzini, Kallweit, and Rathlev, 2015a). The same final state was studied by ATLAS (Aad *et al.*, 2016e) and CMS (Khachatryan *et al.*, 2015i) in 8 TeV data samples with integrated luminosities of up to 20 fb^{-1}. Both inclusive and exclusive production cross sections are extracted and found to be in agreement with MCFM and NNLO predictions. Figure 10 shows the inclusive differential cross-section measurements as a function of photon E_T from both experiments.

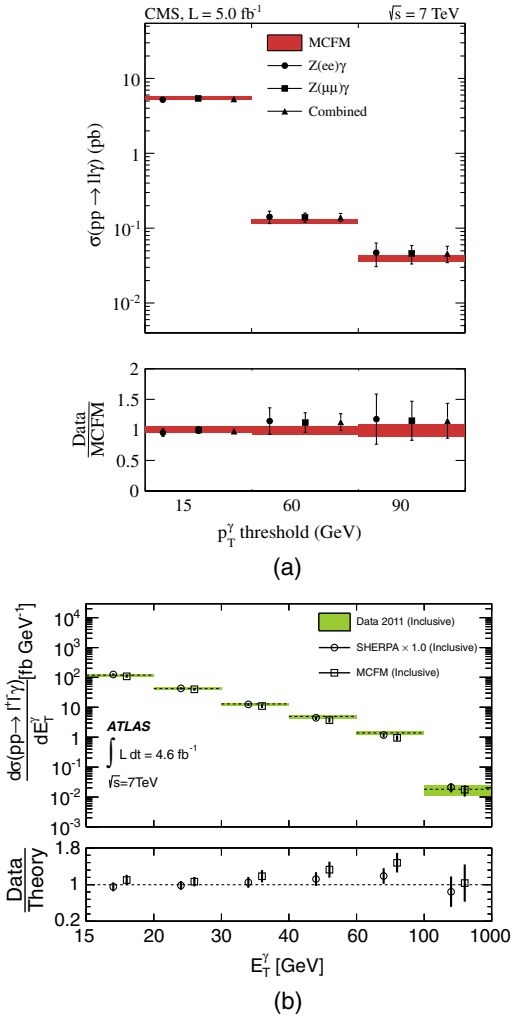

FIG. 9. 7 TeV $Z\gamma$ inclusive cross section as a function of photon E_T: (a) comparison of the CMS measurements with MCFM predictions (Chatrchyan *et al.*, 2014c) and (b) comparison of the ATLAS measurements with MCFM and SHERPA predictions, where the latter has been scaled to match the total number of observed events in data (Aad *et al.*, 2013d). Note that MCFM gives an NLO prediction, which is known to increase by ≈8% when taking NNLO corrections into account.

SM $Z\gamma$ production arises from photons radiated from initial state quarks or radiative Z boson decays to charged leptons as well as fragmentation of final state quarks and gluons into photons. $ZZ\gamma$ and $Z\gamma\gamma$ anomalous triple gauge couplings h_3^V, h_4^V ($V = Z, \gamma$) are constrained by comparing their effect on the photon E_T spectrum with the observed spectrum. The sensitivity to these aTGCs can be significantly enhanced by studying the $Z \to \nu\bar{\nu}$ decay mode due to the 6 times larger branching fraction compared to the charged lepton decay modes and the increased detector acceptance. Both ATLAS (Aad *et al.*, 2013d, 2016e) and CMS (Chatrchyan *et al.*, 2013f; Khachatryan *et al.*, 2016c) have studied the resulting final state of large missing transverse energy and an energetic isolated photon in the 7 and 8 TeV data sets and observe production rates in agreement with theoretical predictions. The photon E_T spectra extend to about 1 TeV and are utilized to constrain aTGC contributions as illustrated in Fig. 11,

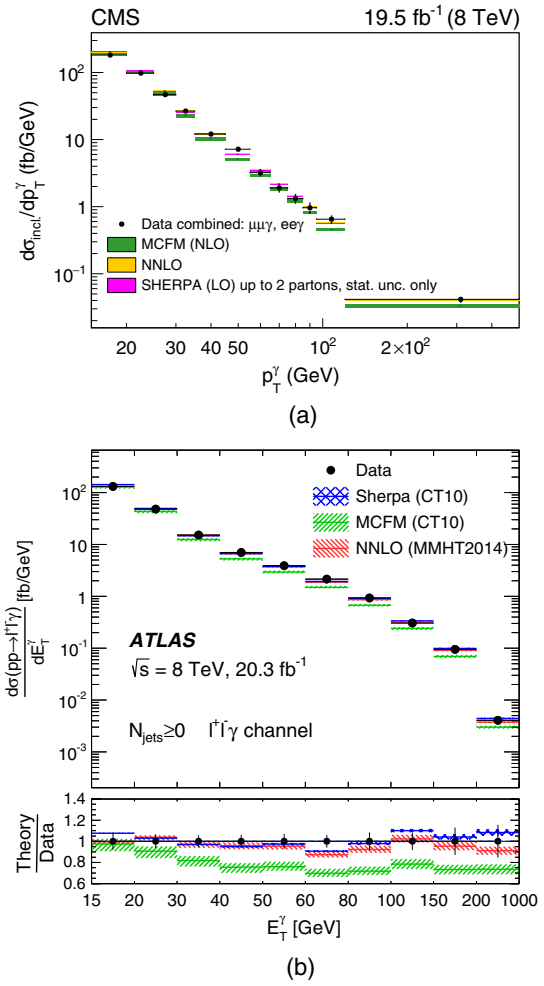

FIG. 10. 8 TeV $Z\gamma$ inclusive cross section as a function of photon E_T in comparison with MCFM, SHERPA, and NNLO predictions: (a) CMS (Khachatryan *et al.*, 2015i), where SHERPA is normalized to the NNLO cross section, and (b) ATLAS (Aad *et al.*, 2016e).

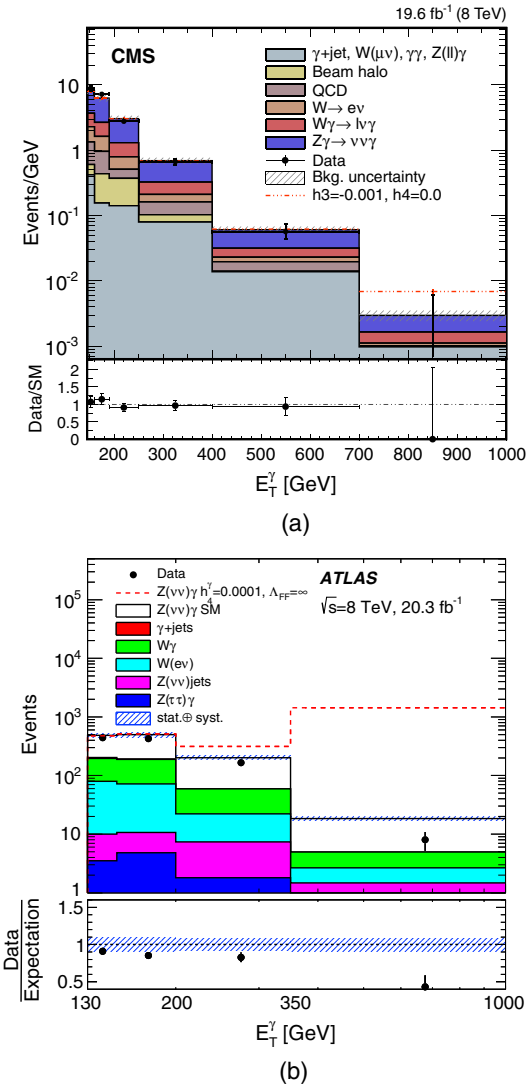

FIG. 11. Photon E_T spectrum at 8 TeV for the $Z\gamma \to \nu\bar{\nu}\gamma$ final state and effect of a representative aTGC on the spectrum for (a) CMS (Khachatryan *et al.*, 2016c) and (b) ATLAS (Aad *et al.*, 2016e) with an exclusive selection vetoing central jets.

which also serves to set the scale for the sensitivity of the data to non-SM couplings. Again, ATLAS uses exclusive events to set limits on anomalous couplings in order to increase the expected sensitivity in high-E_T photon events, which otherwise also tend to exhibit more jet activity in the SM.

D. W^+W^- production

For the case of W^+W^- production, two decay modes have been studied. In the leptonic mode, both W bosons decay into a charged lepton and a neutrino (MET). In the semileptonic case, one W boson decays leptonically while the other decays hadronically. The leptonic mode has less background but the branching fraction of the W pair is about 6 times smaller than in the semileptonic case when considering the decay modes involving electrons and muons. In addition, the WW pair mass in a semileptonic decay can be fully reconstructed up to a quadratic ambiguity, so that the energy at the TGC vertex is directly measurable in contrast to the leptonic decay case. However, in the semileptonic decay mode hadronic W boson decays cannot be fully distinguished from hadronic Z boson decays due to limited dijet mass resolution. The semileptonic WW decay is hence studied together with the semileptonic WZ decay in Sec. IV.E. Both the $WW\gamma$ and the WWZ SM TGCs contribute to WW production in distinction to $W\gamma$ production. Deviations from the SM TGC are labeled by parameters λ_V, $\Delta\kappa_V$ ($V = Z, \gamma$) following the nomenclature already introduced for $W\gamma$ production and Δg_1^Z.

The production of WW pairs in the fully leptonic decay mode with an oppositely charged lepton (electron or muon) pair and missing transverse energy in the final state has been studied by ATLAS (Aad *et al.*, 2011a, 2012d, 2013c) and CMS (Chatrchyan *et al.*, 2011b, 2013b) at 7 TeV using data samples with integrated luminosities of up to 5 fb^{-1}. Figure 12 shows the spectra of the highest p_T lepton of the final state pair as observed by ATLAS and CMS. Also shown are the modifications to the spectrum caused by aTGCs for which no evidence was found. Both experiments do not include resonant production via the Higgs boson in their signal model and observe WW production cross sections larger than (then state-of-the-art) NLO predictions, consistent with the significant

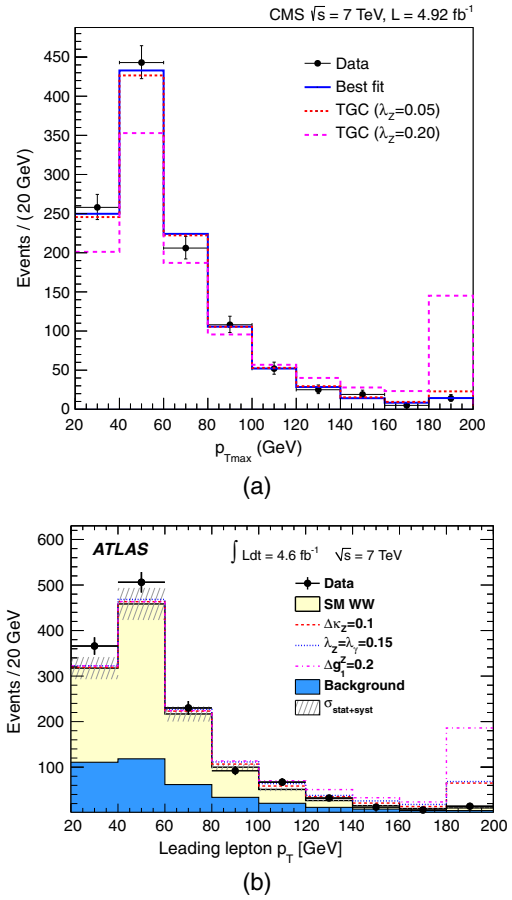

FIG. 12. Leading lepton p_T spectra in 7 TeV fully leptonic WW candidate events and the impact of different anomalous TGC predictions for (a) CMS (Chatrchyan *et al.*, 2013b) and (b) ATLAS (Aad *et al.*, 2013c). The last bin includes the overflow.

cross-section enhancements predicted by NNLO calculations (Gehrmann *et al.*, 2014). Additional measurements such as the ratio of the inclusive WW cross section to the Z boson cross section (Chatrchyan *et al.*, 2013b) and normalized fiducial cross section as function of the leading lepton p_T (Aad *et al.*, 2013c) are provided as well and are found to be in agreement with theory predictions.

WW production in the fully leptonic decay mode has been studied by ATLAS (Aad *et al.*, 2016g) and CMS (Chatrchyan *et al.*, 2013c; Khachatryan *et al.*, 2016d) as well in 8 TeV data samples with integrated luminosities of up to 20 fb^{-1}. While ATLAS includes Higgs-mediated WW production as signal, CMS subtracts the small corresponding expected contribution. The measured fiducial and total production cross sections are found to be consistent with NNLO predictions (Grazzini, Kallweit, Pozzorini, Rathlev, and Wiesemann, 2016), and (normalized) differential cross sections are measured as a function of kinematic event variables. CMS includes a measurement of the total WW production cross section in events with exactly one jet, while ATLAS vetoes events with reconstructed jets. No evidence for anomalous $WW\gamma$ and WWZ TGCs is observed and hence limits on the corresponding parameters are set. An alternative EFT formulation of aTGC with dimension-6 operators is introduced (Degrande *et al.*, 2013c) with corresponding coefficients c_W, c_{WWW}, and

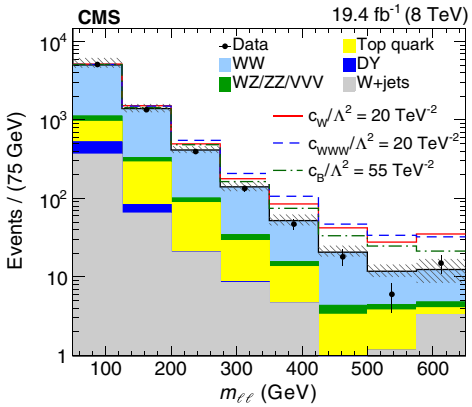

FIG. 13. Dilepton mass spectrum in 8 TeV fully leptonic WW candidate events and impact of different anomalous TGC predictions. The last bin includes the overflow. From Khachatryan *et al.*, 2016d.

c_B that can be mapped to the LEP formulation which allows comparisons with earlier data. Figure 13 shows the dilepton mass spectrum as measured by CMS (Khachatryan *et al.*, 2016d) together with the distorted spectral shape that would result from aTGC contributions. Figure 14 gives an overview of the total WW production cross sections measured at hadron colliders at different center of mass energies in comparison with the expectations of theory.

ATLAS studied WWj production in the $e\mu$, MET, and exactly one jet final state (Aaboud *et al.*, 2016g) in the full 8 TeV data set, where the largest background from top quark production is suppressed with a b-jet veto. Both $WW+1$ jet and $WW+\leq 1$ jets [the latter in combination with the 0-jet analysis (Aad *et al.*, 2016g)] fiducial cross sections are provided and in good agreement with state-of-the-art theoretical predictions. Extrapolating the $WW+\leq 1$ jets fiducial measurement to the total cross section, better agreement with the theoretical prediction is observed than in the 0-jet analysis, and the overall uncertainty improves by 12%. The ratio of $WW+1$ jet to $WW+0$ jets fiducial cross sections is found to be consistent with theoretical predictions.

E. $W^{\pm}V$ production

Semileptonic WV decays ($V=W$, Z) with one charged lepton (electron or muon) missing transverse energy and

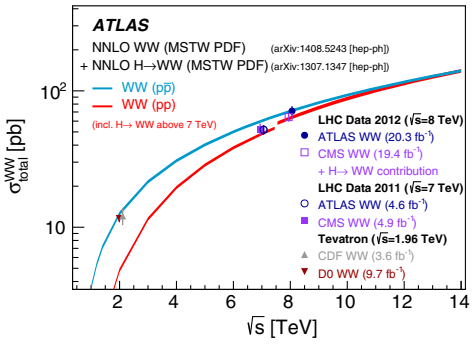

FIG. 14. Comparison of measured total WW production cross sections at hadron colliders and NNLO theory predictions as a function of $\sqrt{s}$. From Aad *et al.*, 2016g.

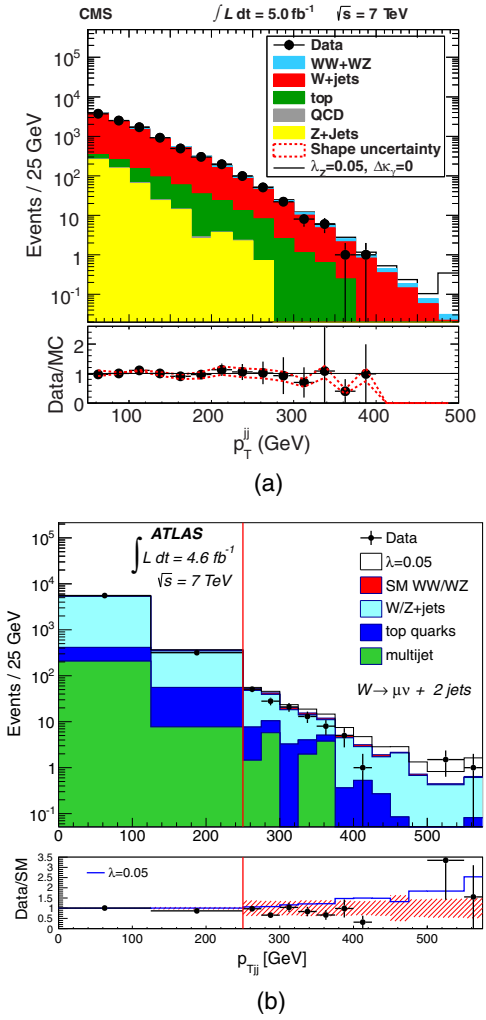

FIG. 15. Dijet-p_T spectra in the muon channel of 7 TeV semileptonic WV candidate events and the impact of different anomalous TGC predictions for (a) CMS (Chatrchyan *et al.*, 2013a) and (b) ATLAS (Aad *et al.*, 2015e). The last bin includes the overflow.

exactly two jets in the final state have been studied by ATLAS (Aad *et al.*, 2015e) and CMS (Chatrchyan *et al.*, 2013a) at 7 TeV using data samples with integrated luminosities of up to 5 fb^{-1}. The background (dominated by W + jets production)

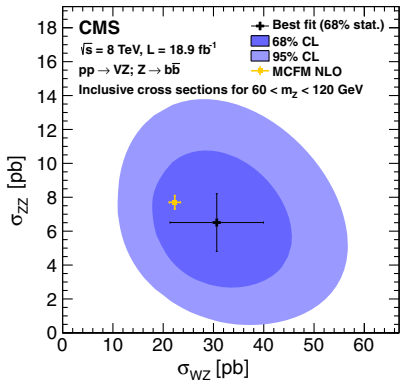

FIG. 16. 68% and 95% C.L. cross-section contours for WZ and ZZ production as observed in $ZV \to b\bar{b}V$ events in comparison with NLO theory predictions. From Chatrchyan *et al.*, 2014d.

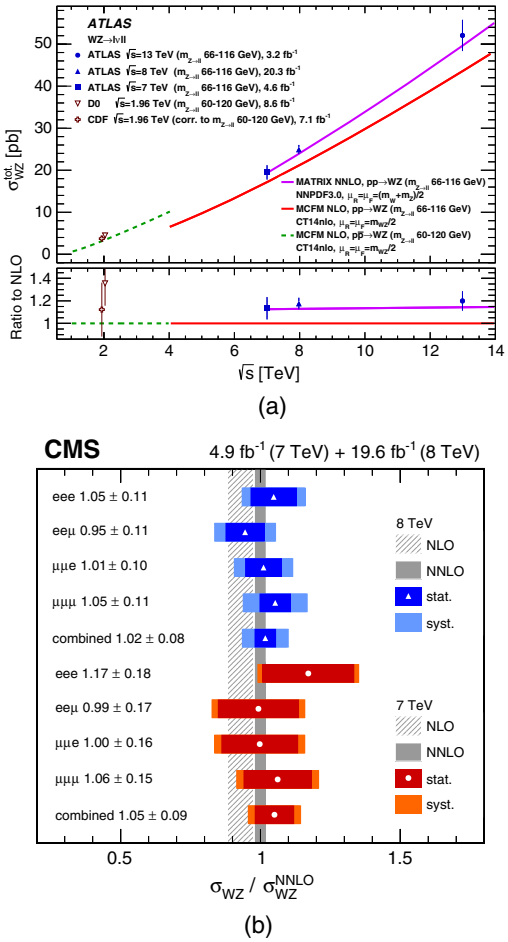

FIG. 17. Comparison of $W^{\pm}Z$ production cross-section measurements with NLO and NNLO predictions (a) at various center of mass energies (Aaboud *et al.*, 2016d) and (b) in the individual and combined channels at 7 and 8 TeV (Khachatryan *et al.*, 2016e).

is much more important in this case compared to the leptonic decay modes and care is needed to accurately assess the level of background. The measured sums of the inclusive WW and WZ cross sections are found to be in good agreement with the NLO SM prediction. Both experiments constrain anomalous WWZ and $WW\gamma$ couplings utilizing the p_T distribution of the hadronically decaying V in a narrow mass window $75 < m_{jj} < 95$ GeV that improves the signal-to-background ratio and enhances the expected contribution of WW over WZ. Figure 15 shows the observed dijet-p_T spectra measured by both experiments in the muon channel together with the potential impact of aTGCs.

F. ZV production

CMS has studied semileptonic ZV decays ($V = W$, Z), where the Z boson decays into a pair of b-tagged jets in 18.9 fb^{-1} pp data at 8 TeV (Chatrchyan *et al.*, 2014d). The second V boson is detected through leptonic final states giving rise to MET (mainly due to $Z \to \nu\bar{\nu}$), one charged lepton (electron or muon) and MET ($W \to \ell\nu$), or a same-flavor, oppositely charged lepton pair (electrons or muons, $Z \to \ell\ell$).

A significant $ZV \to b\bar{b}V$ signal is observed, and the simultaneously measured WZ and ZZ cross sections are found to be in agreement with their NLO predictions, as illustrated in Fig. 16. The fiducial cross sections for high-p_T (V) events are as well found to be in good agreement with NLO theory predictions and hence give no indication of anomalous TGC contributions.

G. $W^{\pm}Z$ production

The production of $W^{\pm}Z$ boson pairs in the three lepton plus MET final state where the Z boson decays into an electron or muon pair while the W boson decays leptonically has been studied by ATLAS (Aad *et al.*, 2012c, 2012g, 2016d) and CMS (Khachatryan *et al.*, 2016e) at both 7 and 8 TeV using data samples with integrated luminosities of up to 5 and 20 fb^{-1}, respectively.

The selected data sets are quite cleanly dominated by the signal process. The measured WZ cross sections are found to be consistent with NLO SM predictions, and differential cross sections for a variety of kinematic variables such as the transverse momentum of the Z and W boson (Aad *et al.*, 2016d) or leading jet p_T and jet multiplicity (Khachatryan *et al.*, 2016e) are provided. The cross-section ratios of inclusive W^+Z and W^-Z production are measured as well by ATLAS and found to be in agreement with NLO theory predictions. A first calculation of the SM cross section at NNLO (Grazzini, Kallweit, Rathlev, and Wiesemann, 2016) that became available only after the ATLAS analyses were published significantly improves the agreement between prediction and measurements as illustrated in Fig. 17.

WZ production includes only the TGC of WWZ as opposed to WW production which has both WWZ and $WW\gamma$ SM vertices. The variables chosen to search for aTGC are the p_T of the Z boson and the transverse mass of the $W^{\pm}Z$ system, shown in Fig. 18. As the observed spectra agree with the SM prediction, stringent limits on aTGC contributions are derived.

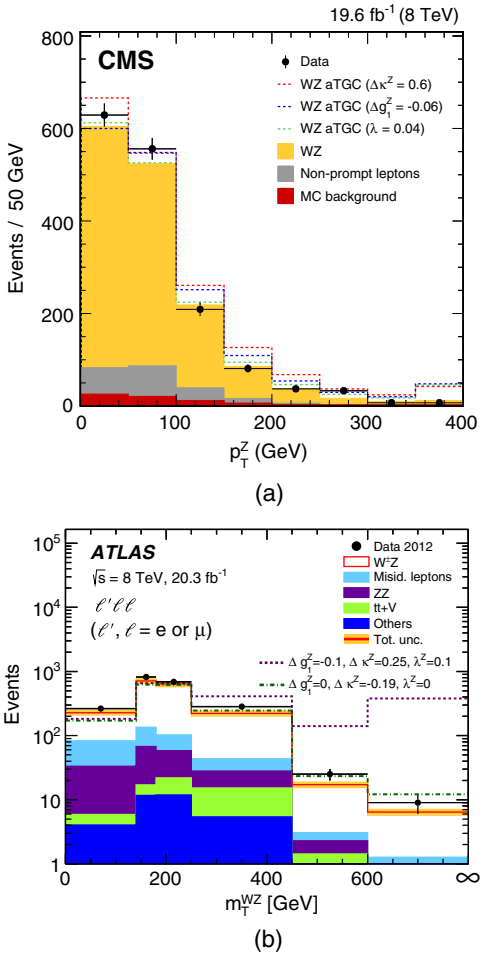

FIG. 18. Observed (a) p_T distribution of the Z boson (Khachatryan *et al.*, 2016e) and (b) transverse mass spectrum of the $W^{\pm}Z$ system (Aad *et al.*, 2016d) in $W^{\pm}Z$ candidate events at 8 TeV and the impact of different anomalous TGC predictions.

H. ZZ production

Pairs of Z bosons cannot be created at a single vertex in the SM because there is no SM TGC available; only WWZ and $WW\gamma$ exist in the SM. The HZZ vertex is not considered here to be a TGC vertex. Anomalous $ZZ\gamma$ and ZZZ couplings can be added with an effective Lagrangian approach and parametrized using two CP-violating (f_4^V) and two CP-conserving

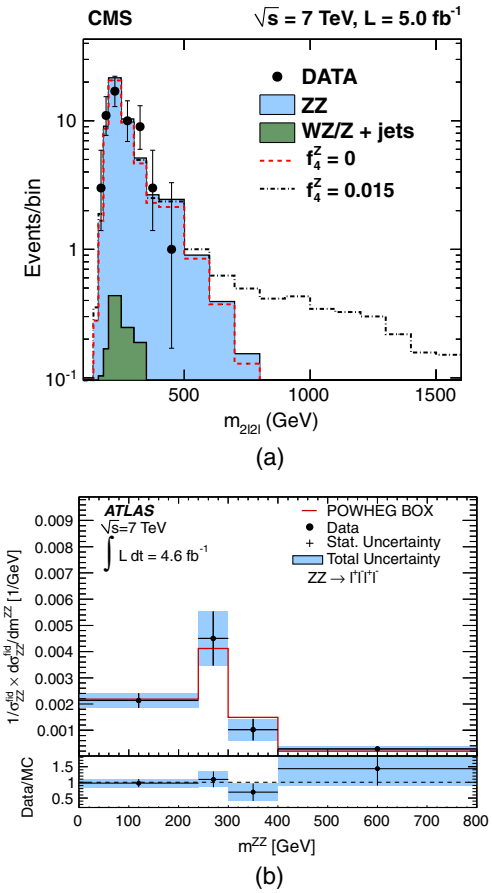

FIG. 19. (a) ZZ mass spectrum in the 4ℓ decay channel ($\ell = e$, μ) and the impact of anomalous TGCs (Chatrchyan *et al.*, 2013g). (b) Unfolded ZZ fiducial cross sections in the 4ℓ decay channel in bins of ZZ mass (Aad *et al.*, 2013f).

(f_5^V) parameters ($V = \gamma$, Z) in direct analogy to the $Z\gamma$ case, where there is also no SM TGC.

The production of ZZ boson pairs has been studied in two decay modes. In the "4ℓ" mode, both Z bosons decay into same-flavor, oppositely charged lepton pairs, resulting in a very low-background, kinematically fully reconstructable final state that however suffers from low statistics due to the branching fractions involved. In the "$2\ell 2\nu$" mode, one Z boson decays into a same-flavor, oppositely charged lepton pair, while the other one decays to neutrinos, giving rise to large missing transverse energy in the final state. While this decay mode suffers from larger background contributions and is not kinematically fully reconstructable, it benefits from better signal statistics due to the increased branching fraction and detector acceptance.

Both ZZ decay modes have been studied by ATLAS [4ℓ (Aad *et al.*, 2012e, 2013f; Aaboud *et al.*, 2016e); $2\ell 2\nu$ (Aaboud *et al.*, 2016e; Aad *et al.*, 2013f)] and CMS [4ℓ (Chatrchyan *et al.*, 2013g; Khachatryan *et al.*, 2015b); $2\ell 2\nu$ (Khachatryan *et al.*, 2015c)] at both 7 and 8 TeV using data samples with integrated luminosities of up to 5 and 20 fb^{-1}, respectively. CMS includes the decay of one Z boson into τ leptons in the 4ℓ decay mode. The measured ZZ cross sections are found to be consistent with NLO SM predictions,

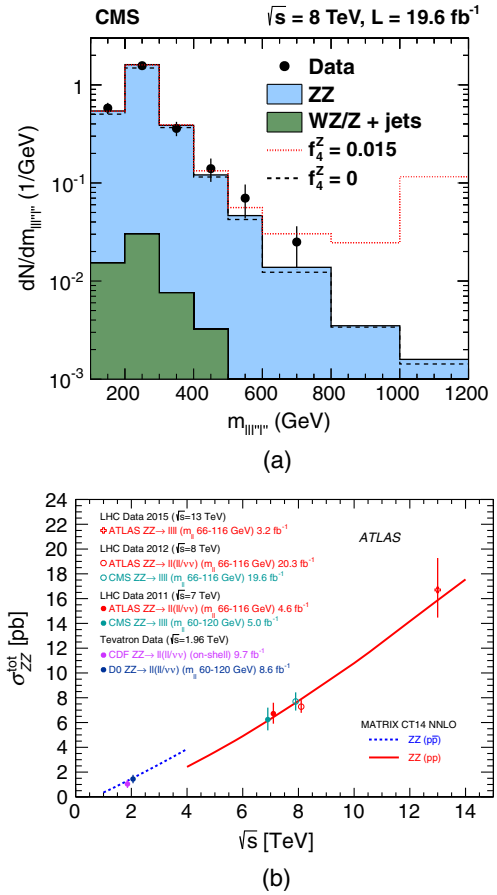

FIG. 20. (a) ZZ mass spectrum in the 4ℓ decay channel ($\ell = e$, μ) and the impact of anomalous TGCs. From Khachatryan *et al.*, 2015b. (b) Comparison of ZZ production cross sections measured at hadron colliders and NNLO predictions as a function of center of mass energy. From Aaboud *et al.*, 2016e.

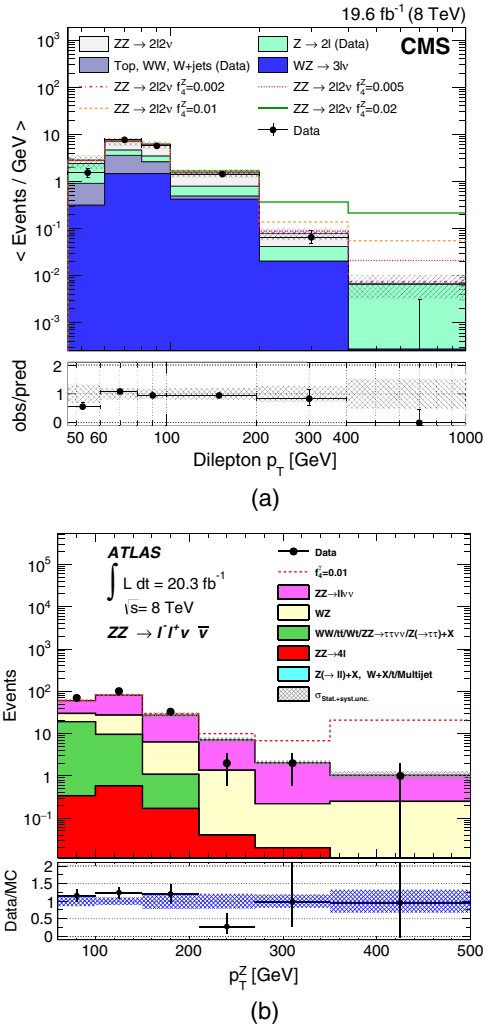

FIG. 21. Dilepton (Z) p_T distributions in ZZ candidate events at 8 TeV in the $2\ell 2\nu$ decay channel ($\ell = e$, μ) and the impact of anomalous TGCs: (a) From Khachatryan *et al.*, 2015c. (b) From Aaboud *et al.*, 2016e.

as illustrated in Figs. 19–21. NNLO corrections (Grazzini, Kallweit, and Rathlev, 2015b) increase the expected fiducial cross sections by about 15% with respect to NLO predictions.

Figures 19 and 20 show that in the 4ℓ final state masses of the ZZ pair up to about 0.5 TeV at 7 TeV and 0.8 TeV at 8 TeV are explored in a situation where the ZZ signal dominates. The dilepton, or Z, p_T in the $2\ell 2\nu$ final state at 8 TeV extends out to about 0.5 TeV as presented in Fig. 21; however, here the ZZ signal has large backgrounds compared to the 4ℓ final state.

Limits on aTGCs arise when the spectra shown are confronted with models having deviations from the SM. As is customary, 95% C.L. limits are derived for aTGCs as limits either in one dimension or in two dimensions allowing two couplings to vary freely from their SM values as will be shown later.

V. TRIBOSON PRODUCTION

The inclusive production of three gauge bosons has a much lower cross section compared to that for the production of two

gauge bosons. Large aQGC are searched for in an EFT formulation with dimension-6 or -8 operators. The lowest dimension operators that introduce only aQGC are of dimension eight.

A. $W\gamma\gamma$ production

The largest inclusive triple gauge boson cross section is that for $W\gamma\gamma$ production. The best signal-to-background ratio is achieved when studying the leptonic W boson decay modes into a charged lepton (e or μ) and a neutrino (MET), leading to a final state with one isolated lepton, MET, and two isolated photons.

ATLAS (Aad *et al.*, 2015b) has studied this final state in an 8 TeV data sample with an integrated luminosity of 20 fb^{-1} and observes first evidence for the $W\gamma\gamma$ process at the level of $> 3\sigma$, with the production rate in agreement with theoretical NLO predictions. ATLAS additionally provides exclusive cross sections where additional jet activity has been vetoed.

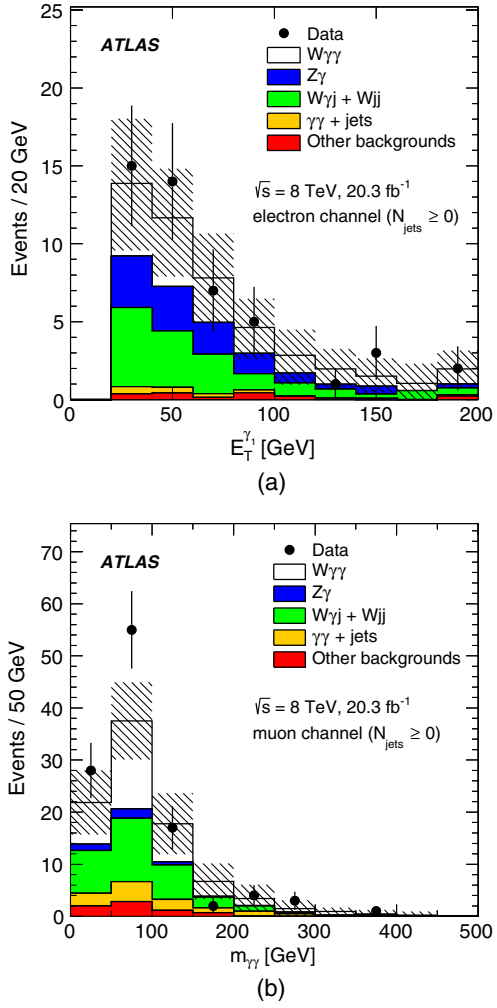

FIG. 22. $W\gamma\gamma$ candidate events at 8 TeV in the $\ell\nu\gamma\gamma$ final state: (a) E_{T} spectrum of the leading photon in the electron channel and (b) diphoton invariant mass distribution in the muon channel. From Aad *et al.*, 2015b.

Figure 22 shows leading photon E_{T} and diphoton invariant mass distributions in $W\gamma\gamma$ candidate events which extend out to about 0.2 and 0.4 TeV, respectively. There is no evidence for a large non-SM contribution to the production process. Limits on anomalous $WW\gamma\gamma$ couplings are placed using the tail of the diphoton invariant mass distribution and vetoing additional jet activity to constrain dimension-8 operators with couplings f_{T0}, f_{M2}, and f_{M3}.

B. $Z\gamma\gamma$ production

SM $Z\gamma\gamma$ triboson production arises from Z boson production with photons radiated off from initial state quarks or radiative Z boson decays to charged leptons as well as fragmentation of final state quarks and gluons into photons and cannot occur in a single vertex due to the lack of neutral $ZZ\gamma\gamma$ and $Z\gamma\gamma\gamma$ QGCs in the SM. Such anomalous QGCs can be introduced with EFT dimension-8 operators with couplings f_{T0}, f_{T5}, f_{T9}, f_{M2}, and f_{M3}.

The production of $Z\gamma\gamma$ tribosons has been studied in two decay modes, each of which requires two isolated photons in the final state. In the "2ℓ" mode, the Z boson decays into a same-flavor, oppositely charged lepton (electron or muon) pair, resulting in a low-background, kinematically fully reconstructable final state. In the "2ν" mode, the Z boson decays into neutrinos, giving rise to large missing transverse energy in the final state. While this decay mode suffers from larger background contributions and is not kinematically fully reconstructable, it benefits from an increased branching fraction and detector acceptance in order to constrain anomalous QGCs.

ATLAS (Aad *et al.*, 2016e) studied the 2ℓ and 2ν decay modes in an 8 TeV data sample with an integrated luminosity of 20 fb^{-1} and provided the first cross-section measurement for $Z\gamma\gamma$ production with $> 5\sigma$ significance. The observed production rate is found to be consistent with theoretical NLO predictions. ATLAS also provided exclusive cross sections where additional jet activity was vetoed.

Figure 23 shows the four-body $ee\gamma\gamma$ and diphoton invariant mass distributions in $Z\gamma\gamma$ candidate events which extend out to about 1.1 and 0.5 TeV, respectively. With no evidence found for a large non-SM contribution to the production process, ATLAS placed limits on anomalous QGCs using exclusive fiducial cross sections with high diphoton invariant mass requirements in the 2ℓ and 2ν decay modes.

C. $WV\gamma$ production

Semileptonic $WV\gamma$ decays ($V = W$, Z) with one charged lepton (electron or muon), missing transverse energy, at least two jets and an energetic photon in the final state represent an extension of the study of WV production described in Sec. IV.E. While the large hadronic branching fraction of the W or Z boson makes this triboson production mode more accessible, W and Z bosons cannot be fully distinguished since the dijet mass resolution is comparable to their mass difference. However, the $WW\gamma$ mode dominates because the $WZ\gamma$ cross section is smaller and the dijet mass resolution provides some discrimination. The expected SM QGC contributions to $WV\gamma$ production are $WWZ\gamma$ and $WW\gamma\gamma$.

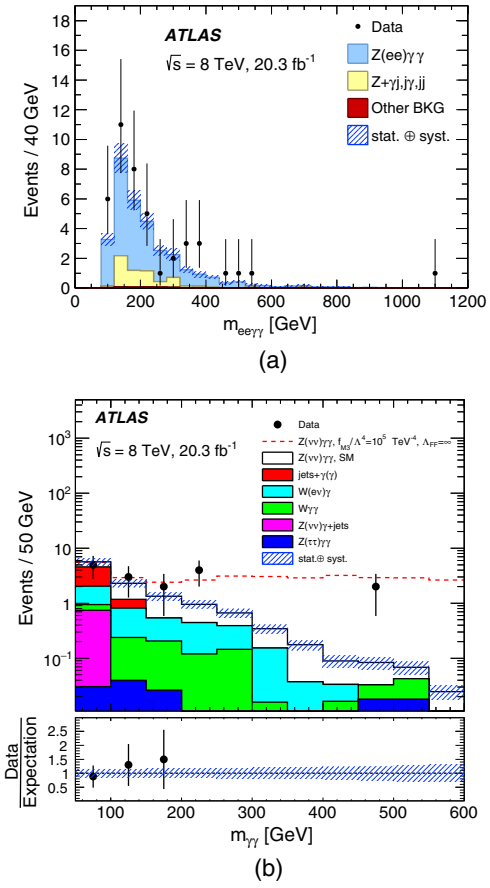

FIG. 23. $Z\gamma\gamma$ candidate events at 8 TeV. (a) Spectrum of the four-body invariant mass $m_{ee\gamma\gamma}$ in the electron channel of the $\ell\ell\gamma\gamma$ final state. (b) Diphoton invariant mass distribution in the exclusive $\nu\nu\gamma\gamma$ final state and potential impact of aQGCs. From Aad *et al.*, 2016e.

The production of $WV\gamma$ has been searched for by CMS (Chatrchyan *et al.*, 2014e) at 8 TeV using a data sample with integrated luminosity of 19 fb^{-1}. The $W\gamma$ plus jet background dominates the signal. An upper limit on $WV\gamma$ production is placed based on the observed data yields corresponding to about 3.4 times the SM NLO QCD theoretical expectation. Nevertheless useful limits can be placed on large contributions of aQGCs using the photon p_{T} spectrum as shown in Fig. 24. Constraints are provided on the dimension-8 operator with coupling f_{T0} and alternatively on the dimension-6 operators with couplings a_0^W, a_C^W for $WW\gamma\gamma$ and κ_0^W, κ_C^W for $WWZ\gamma$ vertices, respectively.

D. $W^{\pm}W^{\pm}W^{\mp}$ production

The production of $W^{\pm}W^{\pm}W^{\mp}$ constitutes the largest inclusive triple gauge boson cross section with three massive bosons and includes contributions from TGCs, Higgs production, and the SM $WWWW$ QGC. The possible decay modes include the very clean fully leptonic final state $\ell^{\pm}\nu\ell^{\pm}\nu\ell^{\mp}\nu$ exhibiting three charged leptons (e or μ) and MET as well as a semileptonic final state $\ell^{\pm}\nu\ell^{\pm}\nu jj$ with two leptons of the same sign (e or μ), MET and two jets that—while suffering from larger background contributions—benefit from a larger branching fraction.

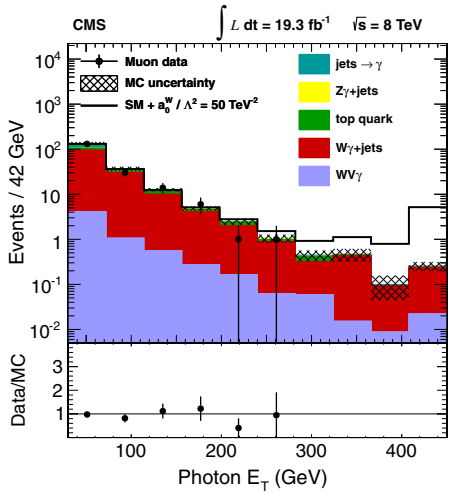

FIG. 24. Photon p_{T} spectrum in $WV\gamma$ candidate events in the $\ell\nu jj\gamma$ final state at 8 TeV and potential impact of aQGCs. From Chatrchyan *et al.*, 2014e.

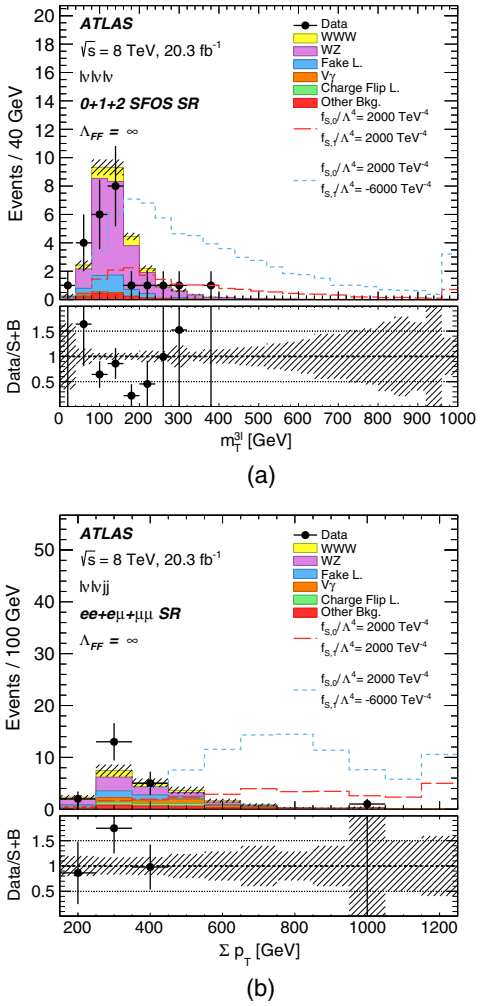

FIG. 25. $W^{\pm}W^{\pm}W^{\mp}$ candidate events at 8 TeV: (a) spectrum of the trilepton transverse mass in the $\ell^{\pm}\nu\ell^{\pm}\nu\ell^{\mp}\nu$ final state and (b) sum of scalar p_{T} for all selected objects (leptons, jets, MET) distribution in the $\ell^{\pm}\nu\ell^{\pm}\nu jj$ final state. The potential impact of aQGCs is shown as well. From Aaboud *et al.*, 2016i.

ATLAS studied both of these signatures at 8 TeV using a data sample with an integrated luminosity of 20 fb^{-1} (Aaboud *et al.*, 2016i). To optimize signal sensitivity, the selection criteria are adjusted according to the number of same-flavor opposite sign (SFOS) lepton pairs present in the leptonic final state and according to the same-sign lepton flavor combination in the semileptonic final state. The latter is a "spin-off" from the $W^{\pm}W^{\pm}jj$ analysis described in Sec. VII.C, where the dijet invariant mass and rapidity separation cuts have been modified to select W boson decays instead.

The data are described well by the signal and background model for both final states as illustrated in Fig. 25 and the combined signal significance is $\approx 1\sigma$. Given the current statistical limitation to establish the signal cross section, upper limits on $W^{\pm}W^{\pm}W^{\mp}$ production are placed based on the observed data yields in good agreement with predictions from theory.

Possible aQGC contributions are constrained using the spectrum of the trilepton transverse mass in the $\ell^{\pm}\nu\ell^{\pm}\nu\ell^{\mp}\nu$ final state and the sum of scalar p_{T} for all selected objects (leptons, jets, MET) in the $\ell^{\pm}\nu\ell^{\pm}\nu jj$ final state, where data extend to 1 TeV. Dimension-8 operators with couplings $f_{S0,1}$ are probed.

VI. VECTOR BOSON FUSION

VBF ($VV \to V$) is an exclusive process wherein a constituent of each proton emits a boson which then both fuse together to form a single boson. The proton emission leads to remnant jets near to the initial beam directions. That topology is exploited in attempting to isolate the specific process. The emitted virtual vector boson can be a photon, W boson, or Z boson.

Typically the rapidity difference of the forward or backward "tag" jets is large as is the dijet mass. These facts are used to enhance the VBF process. Nevertheless, the final states are also available to other processes whose amplitudes interfere with the VBF process, making a completely clean separation impossible, even at a conceptual level.

The study of VBF events also constrains aTGC contributions in a way complementary to diboson production, since in the VBF process the two bosons radiated by the protons exhibit spacelike four-momentum transfer and not timelike four-momentum as is the case in diboson production (Baur and Zeppenfeld, 1993). The sensitivity of such limits can be competitive with that from diboson production (Éboli and Gonzalez-Garcia, 2004).

A. *Wjj* production

The largest cross-section VBF process studied at the LHC is the production of a W boson in association with two jets. The leptonic decay of the W boson is used in the examination of the lepton (e, μ) plus MET plus two jet final state.

CMS studied this signature at 8 TeV using a data sample with integrated luminosity of 19 fb^{-1} (Khachatryan *et al.*, 2016h). As seen in Fig. 26(a), the EW processes can be large in carefully selected regions of phase space. Normalizing the dominant background arising from W boson plus jets production via the strong interaction with a boosted decision tree

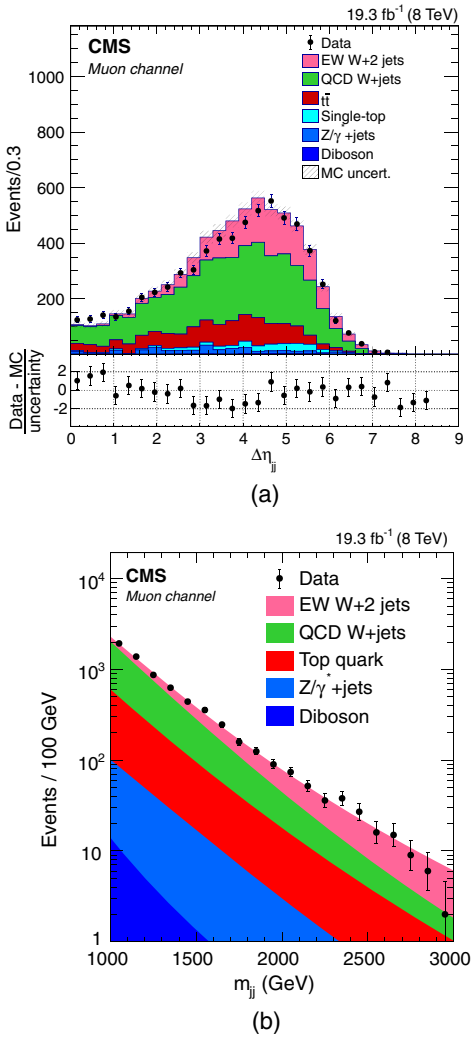

FIG. 26. VBF-W candidate events in the $\ell\nu jj$ final state at 8 TeV. (a) Pseudorapidity difference of the tag jets. (b) Dijet mass spectrum of the tag jets. From Khachatryan *et al.*, 2016h.

(BDT) technique, the dijet mass tail above 1 TeV is examined as shown in Fig. 26(b). At large masses, greater than about 2 TeV, the EW processes dominate the data sample. The largest background, QCD W plus jets production, falls with mass more rapidly than the EW signal. The fiducial electroweak production cross section of a W boson in association with two jets is extracted and found to be consistent with the SM prediction.

The SM $WW\gamma$ and WWZ TGCs contribute to this process, but the aTGC limits are presently not competitive with the limits coming from inclusive VV production. The VBF-W production study shows that the EW process is well modeled and can be enhanced in selected regions of phase space.

B. *Zjj* production

Electroweak production of a Z boson in association with two jets includes VBF Z boson production via the WWZ TGC and has been studied in the final state with a same-flavor, oppositely charged lepton pair (electrons or muons) and two jets.

CMS has performed measurements (Chatrchyan *et al.*, 2013e; Khachatryan *et al.*, 2015a) at both 7 and 8 TeV using data samples with integrated luminosities of 5 and 20 fb^{-1}, respectively. In the 8 TeV analysis a BDT technique is used. As seen in Fig. 27(a), a BDT variable selection can be used to choose a region of phase space dominated by the EW process. The two major processes at high BDT values are EW and Drell-Yan (DY). Since the fit is normalized, the two processes are anticorrelated, as shown in Fig. 27(b). The magnitude of the EW cross section is found to be in agreement with theoretical NLO QCD predictions.

ATLAS studied the $\ell\ell jj$ final state in 20 fb^{-1} of 8 TeV data (Aad *et al.*, 2014f) and used a fit of the dijet invariant mass distribution with electroweak signal and QCD background templates to extract the electroweak production cross section in a fiducial region that enhances the signal contribution. The extracted signal is established with more than 5σ significance and the production rate is found to be in agreement with NLO

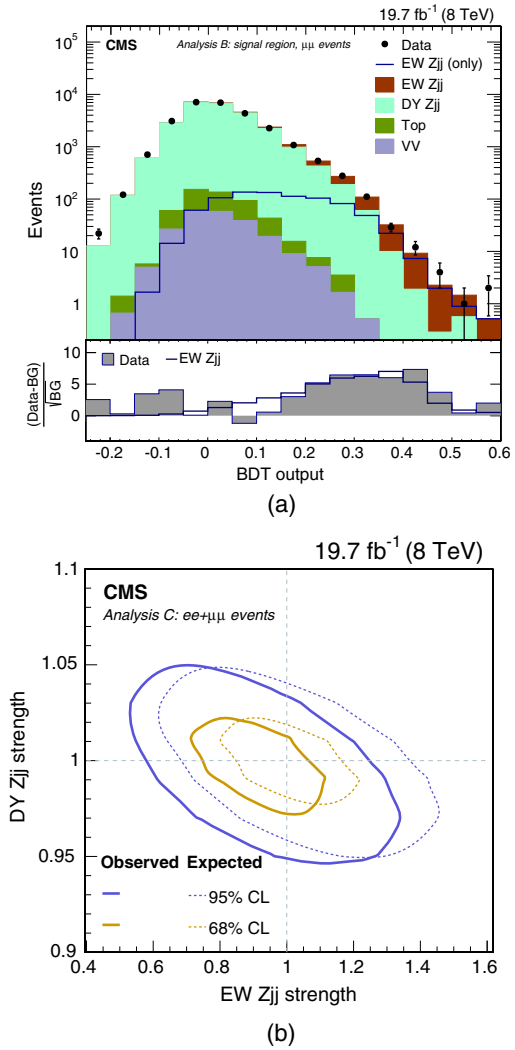

FIG. 27. (a) BDT output and Monte Carlo expectations for VBF-Z candidate events in the $\ell\ell jj$ final state at 8 TeV. From Khachatryan *et al.*, 2015a. (b) Expected and observed 68% and 95% C.L. signal strength contours for EW and DY production of $\ell\ell jj$ at 8 TeV. From Khachatryan *et al.*, 2015a.

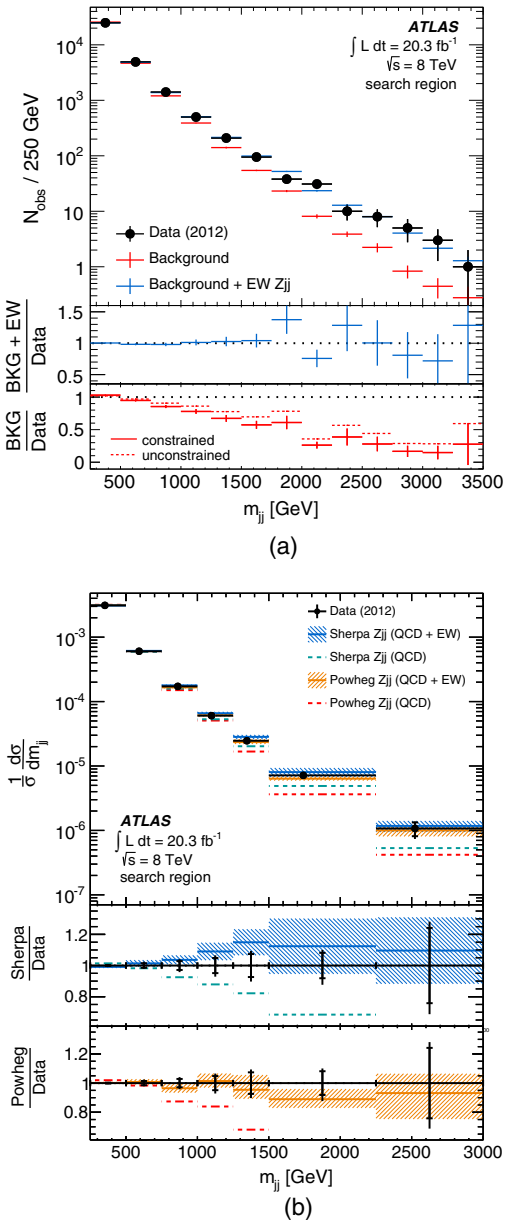

FIG. 28. (a) Dijet invariant mass distribution of VBF-Z candidate events in the $\ell\ell jj$ final state at 8 TeV. From Aad *et al.*, 2014f. (b) Unfolded normalized differential Zjj production cross section as a function of dijet invariant mass. From Aad *et al.*, 2014f.

SM predictions. In addition, cross sections and differential distributions are measured in five fiducial regions with different sensitivity to EW Zjj production, and limits on WWZ aTGCs λ_z and Δg_1^Z are placed based on the observed event yields in the tail of the dijet invariant mass distribution, shown in Fig. 28.

VII. VECTOR BOSON SCATTERING

VBS ($VV \to VV$) is an exclusive process wherein a constituent of each proton emits a boson which then interact with each other causing the emission of two new bosons. As in the case of VBF, the proton emission leads to remnant forward

or backward tag jets near to the initial beam directions with large rapidity difference and dijet mass. The resulting $VVjj$ final state ($V = \gamma, W^{\pm}, Z$) has contributions from both electroweak and QCD mediated processes. The latter can be suppressed by requiring the stated scattering topology. The electroweak processes include quartic boson self-interactions, whose amplitudes interfere with those of the other contributing diagrams, making a completely clean separation impossible.

One main argument for expecting new particles and/or interactions at the TeV scale is the linear divergence of the scattering amplitude for longitudinally polarized weak bosons as the center of mass energy squared increases (Lee, Quigg, and Thacker, 1977), which leads to the violation of unitarity at about 1 TeV. In the framework of the SM, this divergence is canceled through diagrams involving the exchange of a Higgs boson. Even if the recently discovered boson turns out to be the Higgs boson, its role in VBS still needs to be experimentally established to confirm the SM nature of EWSB. A wealth of models with dynamical EWSB in lieu of or in addition to the Higgs mechanism exists, making the measurement of VBS both a fundamental test of the SM and a window to new physics.

A. $W^{\pm}\gamma jj$ production

The largest cross-section VBS process studied at the LHC is the production of a $W\gamma$ boson pair in association with two jets, which includes SM QGC contributions from the $WW\gamma\gamma$ and $WWZ\gamma$ vertices. Purely longitudinal scattering effects cannot be studied in this channel due to the presence of the photon.

CMS performed a search for electroweak $W^{\pm}\gamma jj$ production using leptonic W boson decays in final states with one charged lepton (electron or muon), missing transverse energy, two jets well separated in rapidity and an energetic photon in 8 TeV data with an integrated luminosity of 20 fb^{-1} (Khachatryan *et al.*, 2016b). After preliminary selections the dijet mass of the tag jets is shown in Fig. 29(a). At masses greater than about 1 TeV the electroweak signal process dominates. An upper limit on electroweak $W^{\pm}\gamma jj$ production is placed based on the observed data yields in the tails of the dijet mass distribution, corresponding to about 4.3 times the SM NLO QCD theoretical expectation. The combined electroweak and strong $W^{\pm}\gamma jj$ production is measured in good agreement with theoretical expectations.

The search for aQGCs uses the shape of the p_{T} spectrum of the W boson in events with a tightened selection, including the requirement of a very energetic photon, as shown in Fig. 29(b). The p_{T} values extend to about 0.25 TeV, and constrain dimension-8 operators with couplings $f_{M0,\ldots,7}$ and $f_{T0,\ldots,2,5,\ldots,7}$. The notation for the subscripts indicates which operators are considered, where dots indicate contiguous indices.

B. $W^{\pm}Vjj$ production

The study of the semileptonic WV ($V = W$, Z) VBS process benefits from the large hadronic branching fraction of the W or Z boson compared to the leptonic decays and the ability to fully reconstruct the WW contribution up to a quadratic ambiguity, resulting in improved sensitivity to anomalous event kinematics. Searching for anomalous quartic couplings in the high-mass tail of the WV spectrum is facilitated by the continually improving substructure techniques to analyze boosted monojets arising from the hadronically decaying V boson (see Fig. 5). The $W^{\pm}Vjj$ semileptonic final state includes contributions from the $W^{\pm}W^{\mp}jj$, $W^{\pm}W^{\pm}jj$, and $W^{\pm}Zjj$ VBS processes.

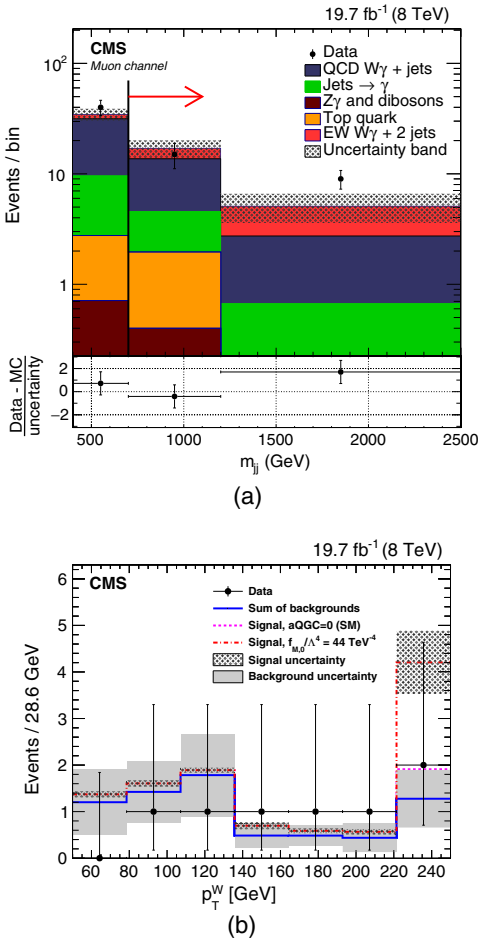

FIG. 29. (a) Dijet mass distribution of the tag jets in the $\mu\nu\gamma jj$ final state at 8 TeV. From Khachatryan *et al.*, 2016b. (b) p_{T} spectrum of the W boson in VBS candidate events in the $\ell\nu\gamma jj$ final state at 8 TeV. The effect of a representative aQGC on the spectrum is also shown. From Khachatryan *et al.*, 2016b.

Building on the semileptonic WV decay signature described in Sec. IV.E with one charged lepton (electron or muon), missing transverse energy, and exactly two jets in the final state, the corresponding VBS processes can be studied by requiring in addition the presence of a tagging jet pair with large invariant mass.

ATLAS (Aaboud *et al.*, 2016h) performed a first search for anomalous couplings in $W^{\pm}Vjj$ semileptonic VBS candidate events at 8 TeV using a data sample with an integrated luminosity of 20 fb^{-1}. While the extraction of the SM signal cross section is not yet possible due to large background contributions from W + jets and $t\bar{t}$ production, the analysis is optimized for aQGC sensitivity in a phase space where the SM contributions are sufficiently suppressed. The hadronic weak

boson decay is reconstructed either via two jets in a "resolved" event category (which is split by lepton charge) or via a large monojet in a "merged" event category.

No excess is observed in the data, and the transverse mass distribution of the WV system in the two resolved and one merged event categories is used to constrain dimension-8 operators with couplings α_4 and α_5. Two of the observed distributions are shown in Fig. 30 with the data extending to about 0.9 TeV in transverse mass. The obtained limits are more stringent than those obtained in the separate analyses of $W^{\pm}W^{\mp}jj$ and $W^{\pm}Zjj$ leptonic final states described in the following two sections. Given the largest sensitivity to aQGCs in the tail of the transverse mass distribution, the merged event category presently improves the expected sensitivity by about 40% compared to the resolved categories alone.

C. $W^{\pm}W^{\pm}jj$ production

The production of same-sign W boson pairs in association with two jets includes the SM QGC contribution from the $WWWW$ vertex and is particularly valuable for the study of VBS processes with massive bosons since the strong production mode does not dominate over the electroweak mode of interest as is the case for the other $VVjj$ ($V = W, Z$) processes. The best signal-to-background ratio is achieved when studying the leptonic W boson decays, giving rise to final states with two leptons of the same sign (e or μ), MET, and two jets.

Both ATLAS (Aad *et al.*, 2014c) and CMS (Khachatryan *et al.*, 2015g) studied this final state in 8 TeV data samples with integrated luminosities of up to 20 fb^{-1}, requiring the two leading (tag) jets to exhibit a large dijet invariant mass and to be well separated in rapidity to enhance the VBS contribution [see Figs. 31(a) and 32]. ATLAS and CMS found evidence for electroweak $W^{\pm}W^{\pm}jj$ production with 3.6σ and 2.0σ significance, respectively, compatible with SM NLO expectations.

To constrain possible aQGC contributions, the measured cross section in the VBS fiducial region (ATLAS) or the dilepton mass shape is used [CMS, see Fig. 31(b)], where the data extend to about 0.5 TeV in dilepton mass. Dimension-8

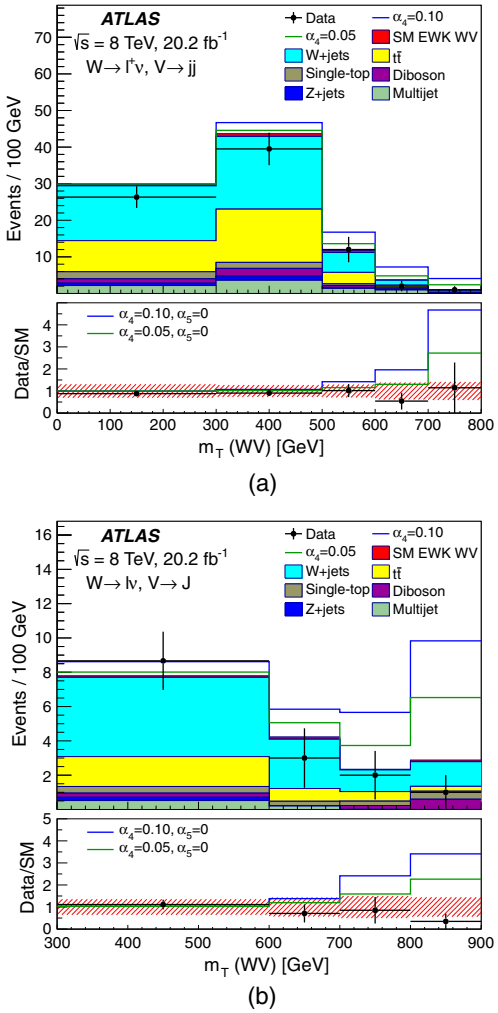

FIG. 30. $W^{\pm}Vjj$ candidate event transverse diboson mass distributions in the $\ell^{\pm}\nu(jj/J)jj$ final state at 8 TeV: (a) resolved ($V \to jj$) category for positively charged leptons and (b) merged ($V \to J$) category. The potential impact of aQGCs is shown as well. From Aaboud *et al.*, 2016h.

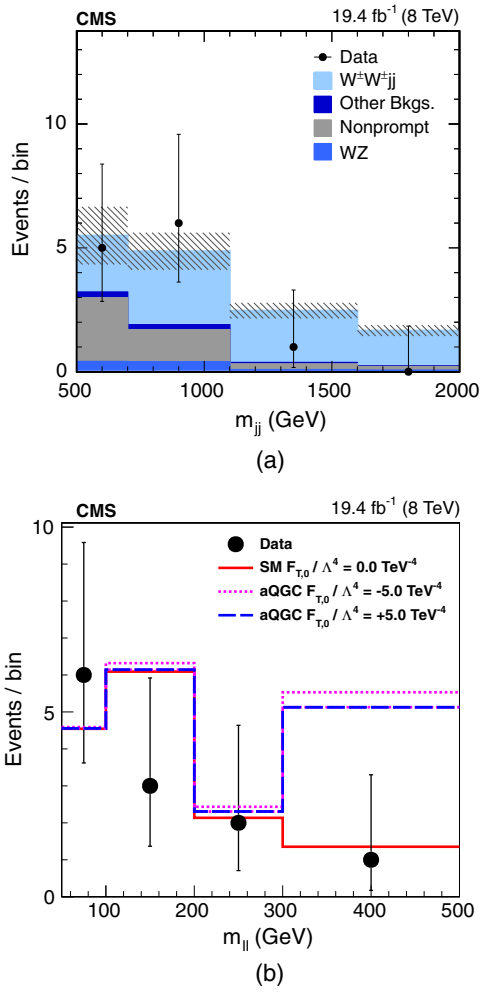

FIG. 31. VBS-$W^{\pm}W^{\pm}$ candidate events in the $\ell^{\pm}\nu\ell^{\pm}\nu jj$ final state at 8 TeV: (a) dijet mass of the tag jets and (b) dilepton mass distribution, where the effect of a representative aQGC on the spectrum is also shown. From Khachatryan *et al.*, 2015g.

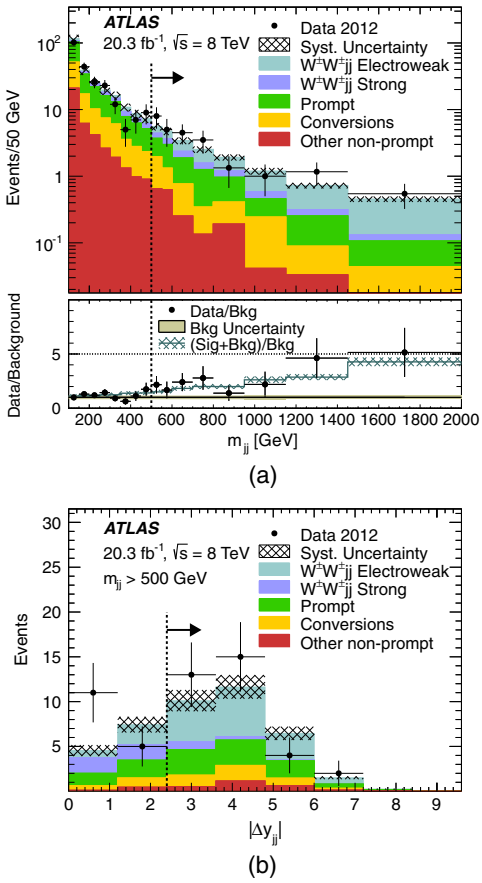

FIG. 32. VBS-$W^{\pm}W^{\pm}$ candidate events in the $\ell^{\pm}\nu\ell^{\pm}\nu jj$ final state at 8 TeV: (a) dijet mass and (b) rapidity separation of the tag jets. The applied selections are indicated by dotted lines. From Aad *et al.*, 2014c.

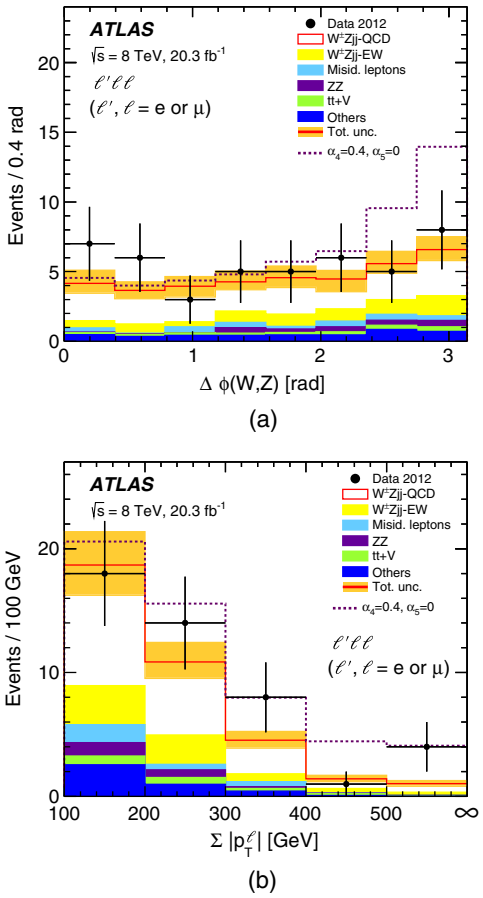

FIG. 33. Electroweak $W^{\pm}Zjj$ candidate event distributions in the $\ell^{\pm}\nu\ell^{\pm}\ell^{\mp}jj$ final state at 8 TeV: (a) the difference in the azimuthal angle between reconstructed W and Z boson directions and (b) the scalar sum of the p_{T} of the three charged leptons. The potential impact of aQGCs is shown as well. From Aad *et al.*, 2016d.

operators with couplings α_4 and α_5 or alternatively $f_{S0,1}$, $f_{M0,1,6,7}$, and $f_{T0,\ldots,2}$ are probed.

ATLAS (Aaboud *et al.*, 2016f) published in addition a detailed writeup of a reanalysis of the same data set, where the sensitivity to anomalous couplings was optimized through an additional cut on the estimated transverse mass of the WW system. As a result, the expected α_4 and α_5 sensitivity is improved by 35% with respect to the previous analysis (Aad *et al.*, 2014c). Upper limits on the cross section in the resulting fiducial volume are provided as well.

D. $W^{\pm}Zjj$ production

The production of $W^{\pm}Z$ boson pairs with two jets includes the SM QGC contribution from the $WZWZ$ and $W\gamma WZ$ vertices. The best signal-to-background ratio is achieved when studying the leptonic boson decay modes involving electrons and muons, resulting in a final state with three charged leptons, MET, and at least two jets.

ATLAS performed a first measurement in this final state at 8 TeV using a data sample with an integrated luminosity of 20 fb^{-1} (Aad *et al.*, 2016d). Requiring a large invariant mass of the two leading tag jets, 95% C.L. limits on electroweak $W^{\pm}Zjj$ production are placed about a factor of 4.8 higher than the SM cross-section expectation at NLO in QCD in the fiducial volume under study, consistent with the expected sensitivity.

Additional selection criteria are applied to the data in order to optimize the expected sensitivity for aQGCs: Both a large difference in azimuthal angle between reconstructed W and Z boson directions and a large scalar sum of the p_{T} of the three charged leptons are required, with the distributions prior to the cuts shown in Fig. 33. The resulting measured fiducial cross section is used to constrain dimension-8 operators with couplings α_4 and α_5 or alternatively $f_{S0,1}$.

E. Exclusive WW production

Exclusive production of a W boson pair $pp \to W^+W^-pp$ proceeds via the emission of photons from the beam protons, which then interact to yield the W boson pair: $\gamma\gamma \to W^+W^-$. In the elastic case, both protons remain intact after the interaction, while in the case of single (double) dissociation one (both) of the protons dissociates. In either case, the proton (remnants) closely follows the original beam direction and hence escape detection, leaving only the W boson decay products in the detector without the additional activity present in inclusive processes. The production of W^+W^- from photon

scattering gives access to the SM QGC from the $WW\gamma\gamma$ vertex. The $WW\gamma\gamma$ coupling is the sole SM QGC contribution to the process since no tag jets indicating beam breakup are allowed which suppresses the $WWWW$, $WWZZ$, and $WWZ\gamma$ processes.

The best signal-to-background ratio is achieved when studying different-flavor leptonic W boson decays, giving rise to a final state with one electron and one muon of opposite charge and MET. ATLAS performed a measurement (Aaboud *et al.*, 2016b) based on the full 20 fb^{-1} of its 8 TeV data set, while CMS utilized both 7 and 8 TeV data samples with integrated luminosities of 5 and 20 fb^{-1}, respectively (Chatrchyan *et al.*, 2013h; Khachatryan *et al.*, 2016g). Exclusive events are selected by requiring no additional charged particles be present at the $e\mu$ vertex and a large p_{T} of the $e\mu$ pair.

ATLAS measured the exclusive W^+W^- cross section in good agreement with SM expectation with a significance of 3.0σ. Figure 34(a) shows the distribution of the difference in azimuthal angle between electron and muon, clearly indicating the need for the signal contribution to describe the observed data. First upper limits on exclusive Higgs boson production in the $H \to WW$ decay mode are provided as well, based on a separately optimized selection.

CMS placed an upper limit on $\gamma\gamma \to W^+W^-$ production in the 7 TeV analysis, corresponding to about 2.6 times the SM theoretical expectation at 95% C.L., while at 8 TeV first evidence for the signal is observed with a significance of 3.2σ. Combining the 7 and 8 TeV data, the signal significance increases to 3.4σ. The $e\mu$ acoplanarity is shown in Fig. 35(a) in the 8 TeV data, indicating consistent yields with respect to signal and background expectations and a dominant VBS contribution.

Both ATLAS and CMS used the shape of the dilepton p_{T} distribution, shown in Figs. 34(b) and 35(b) for the 8 TeV data set, to limit aQGC dimension-6 operators with couplings a_0^W and a_C^W. Corresponding transformed limits on dimension-8 operators with couplings $f_{M0,\ldots,3}$ are provided as well.

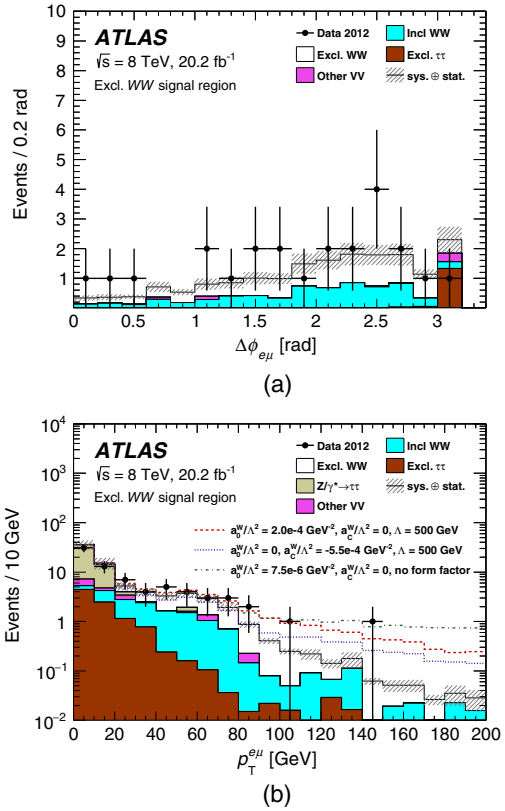

FIG. 34. VBS-$\gamma\gamma \to W^+W^-$ candidate events in the $e^{\pm}\nu\mu^{\mp}\nu$ final state in 8 TeV data: (a) the difference in the azimuthal angle between the electron and muon and (b) dilepton p_{T} distribution before applying the 30 GeV selection cut. The potential impact of aQGCs is shown as well. From Aaboud *et al.*, 2016b.

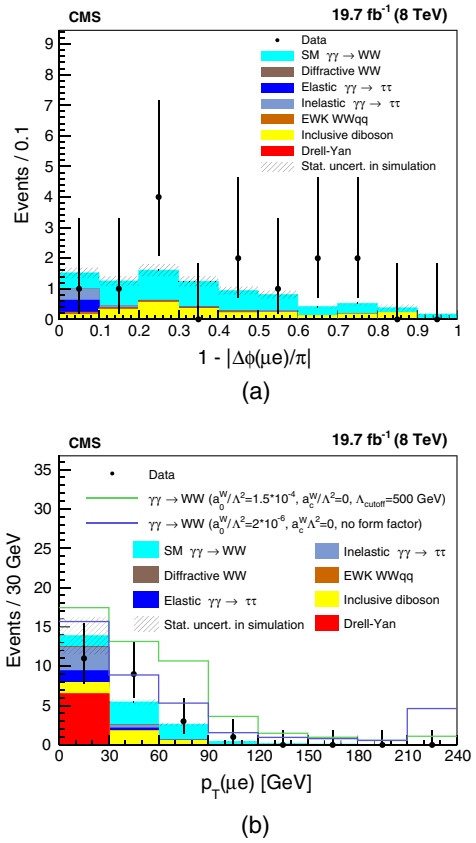

FIG. 35. VBS-$\gamma\gamma \to W^+W^-$ candidate events in the $e^{\pm}\nu\mu^{\mp}\nu$ final state in 8 TeV data: (a) acoplanarity of the $e\mu$ system and (b) dilepton p_{T} distribution before applying the 30 GeV selection cut. The potential impact of aQGCs is shown as well. From Khachatryan *et al.*, 2016g.

VIII. CONSTRAINTS ON ANOMALOUS TRIPLE GAUGE COUPLINGS

The exploration of high-$\hat{s}$ diboson and VBF events leads to limits on possible triple gauge couplings which are differing from or not present in the SM: anomalous triple gauge couplings. Limits on aTGCs have been presented by experiments at LEP, the Tevatron, and the LHC. aTGC limits arise when specific spectra of final state particles are compared to the expectations of the SM with additional aTGC terms in the Lagrangian. The specific spectra used at the LHC were shown in Secs. IV and VI for aTGCs, and Secs. V and VII for aQGCs.

Note that higher-order (NNLO QCD and NLO EW) corrections will significantly impact the SM expectation in the tails of the utilized distributions, and the incorporation of such corrections depends on the timing of the corrections becoming available versus when the analysis was carried out. The various limits made with different diboson and VBF final states are collected here and compared. Typically, one-dimensional (1D) limits are quoted where only one operator is allowed to be nonzero at a time. In a few cases two operators are allowed to float simultaneously, a procedure which illustrates the correlations between the effects of the operators.

In the SM there are $WW\gamma$ and WWZ TGCs. They are studied in WW, WZ, $W\gamma$, VBF-W, and VBF-Z final states. Beyond the SM there are ZZZ, $ZZ\gamma$, $Z\gamma Z$, $Z\gamma\gamma$, and $\gamma\gamma\gamma$ couplings, where limits on the first four are placed by exploring ZZ and $Z\gamma$ final states. In the future, with higher luminosity data taking, the $\gamma\gamma$ final state (Sec. IV.A) can be used to explore the non-SM $\gamma\gamma\gamma$ aTGC.

A. $WW\gamma$ and WWZ limits

WWZ and $WW\gamma$ limits can be formulated with aTGC as was done in other prior experiments at LEP (ALEPH, DELPHI, L3, and OPAL) and the Tevatron (CDF and D0). The five independent C- and P-conserving aTGC parameters that remain after imposing electromagnetic gauge invariance $\Delta g_1^Z (\equiv g_1^Z - 1)$, $\Delta\kappa_Z (\equiv \kappa_Z - 1)$, $\Delta\kappa_\gamma (\equiv \kappa_\gamma - 1)$, λ_Z, and λ_γ are all zero in the SM, and limits on all these parameters have been provided independently by recent LHC publications. In order to be able to compare limits from the LHC, Tevatron, and LEP on equal footing, results from the "LEP scenario" (Altarelli, Sjostrand, and Zwirner, 1996; Gounaris *et al.*, 1996) are used, which are available from all experiments. Motivated by $SU(2) \times U(1)$ symmetry, the LEP scenario assumes $\Delta\kappa_\gamma = (\Delta g_1^Z - \Delta\kappa_Z)/\tan^2\theta_W$, and $\lambda_\gamma = \lambda_Z$, thereby reducing the number of independent parameters to three.

Figure 36 shows a comparison of the most competitive limits derived in the LEP scenario by experiments at the LHC, Tevatron, and LEP. The impact of imposing unitarity constraints on the anomalous couplings via a dipole form factor with a suppression scale Λ_{FF} that dampens the cross-section increase at high $\hat{s}$ for any anomalous coupling α with value α_0 at low energies, $\alpha(\hat{s}) = \alpha_0/(1 + \hat{s}/\Lambda_{\mathrm{FF}}^2)^2$, is shown as well. The LHC limits using WW and WZ final states for constraining $WW\gamma$ and WWZ couplings are already more stringent than the combined D0 or LEP limits. Presently, the higher energy and higher statistics data at 8 TeV give the strongest LHC limits. Increased luminosity and center of mass energy in run II and beyond will further reduce the LHC limits.

The two-dimensional limits shown in Fig. 37 illustrate the anticorrelation of the $\Delta\kappa^V$ and λ^V parameters when no constraints are assumed on the five aTGC parameters. Typically, only the 1D limits are shown since the correlations are usually small.

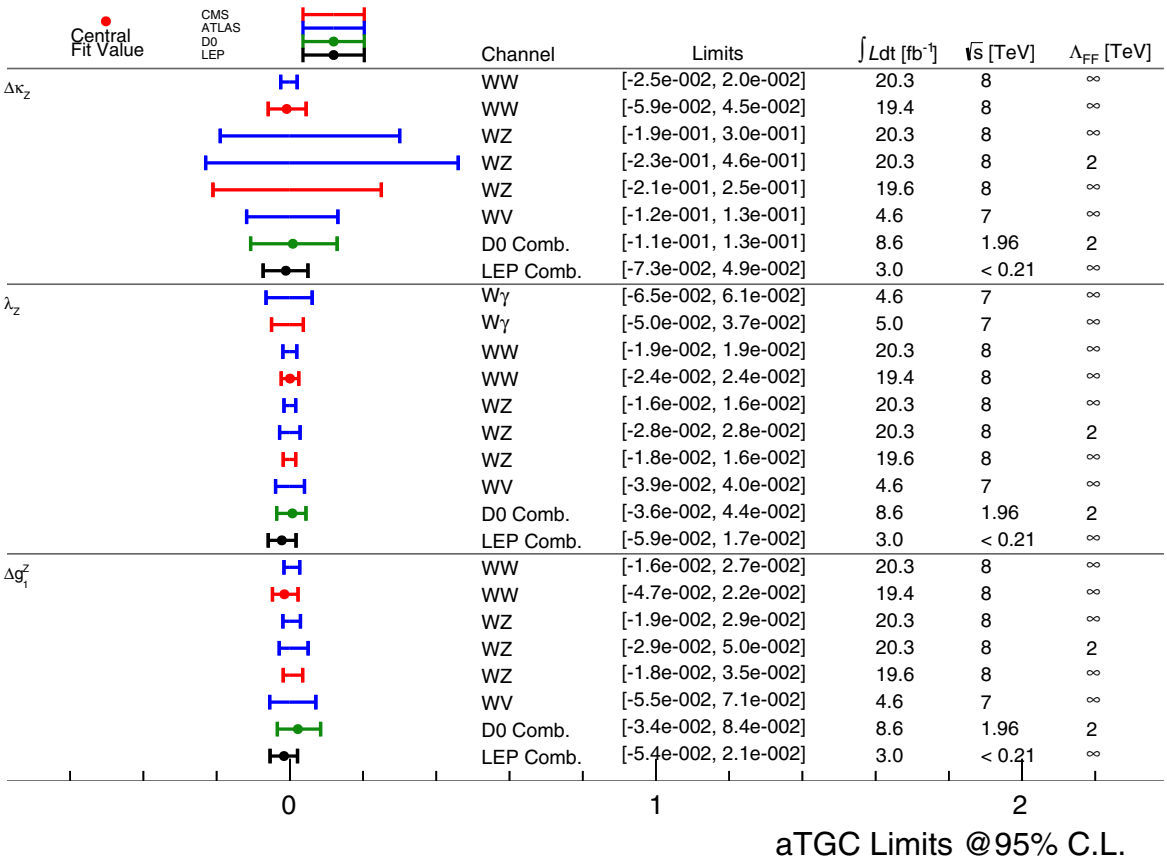

FIG. 36. Comparison of the most competitive aTGC limits in the LEP scenario for the LHC analyses presented in this review as well as the combination of limits by the D0 (Abazov *et al.*, 2012) and LEP (Schael *et al.*, 2013) experiments.

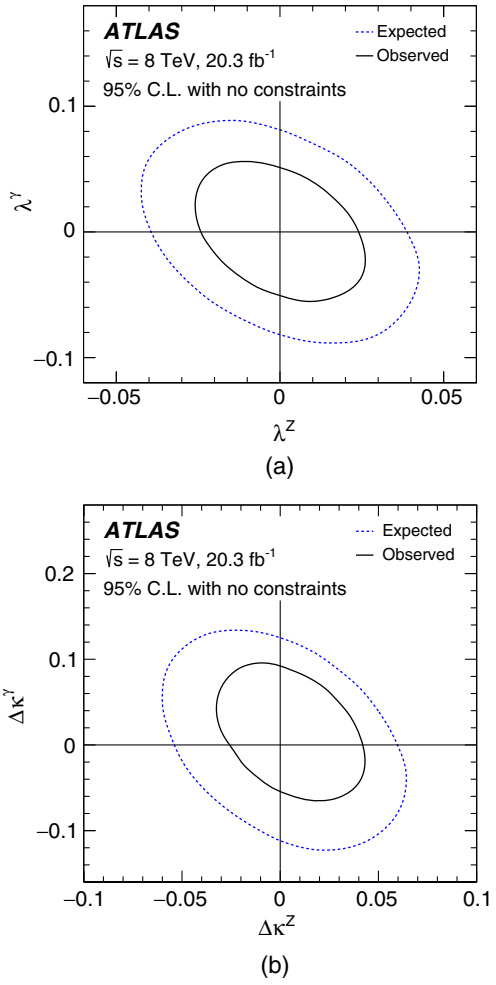

FIG. 37. Expected and observed 95% C.L. contours for aTGC limits derived from 8 TeV fully leptonic WW candidate events, illustrating the anticorrelations between (a) λ^V and (b) $\Delta\kappa^V$ parameters when no constraints between aTGCs are assumed. The aTGCs not shown are set to zero. From Aad *et al.*, 2016g.

More recently, the EFT formulation of possible aTGC in terms of dimension-6 operators for triple boson couplings has come into use. A marked difference with respect to the anomalous Lagrangian vertex couplings is that the EFT-based anomalous couplings are not valid to arbitrary energy scales, but instead are valid only below the scale Λ where new physics sets in. Using the same assumptions as in the LEP scenario and applying no unitarization, the aTGC parameters can be directly translated into EFT coefficients c_W, c_{WWW}, and c_B (Degrande *et al.*, 2013c).

Since these dimension-6 operators are not expected to lead to unitarity violation in diboson production at the LHC center of mass energies (Degrande *et al.*, 2013c), the same must hold true for their aTGC counterparts. The reason that, for example, the ATLAS WW analysis (Aad *et al.*, 2016g) nevertheless gives aTGC unitarization bounds is that the used unitarity considerations in Aihara *et al.* (1996) are valid for arbitrary center of mass energies.

Figure 38 shows a comparison of the best aTGC limits, arising from WW and WZ analyses in leptonic final states by ATLAS and CMS using the full 8 TeV data sets and converted

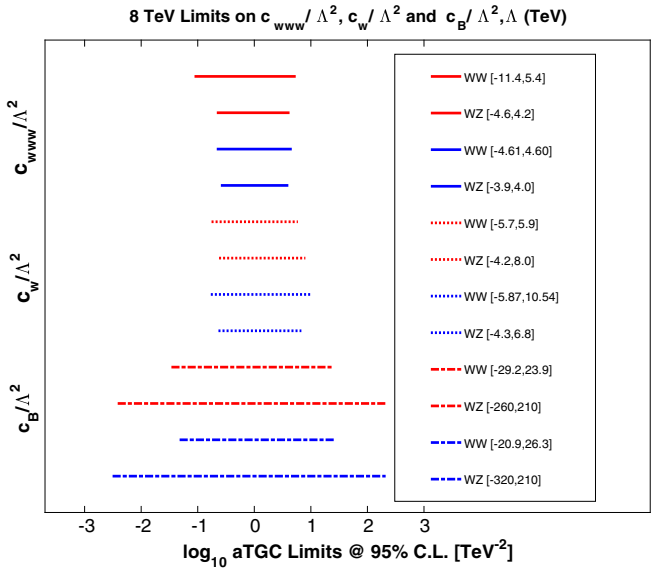

FIG. 38. Comparison of the most competitive aTGC EFT limits based on the 8 TeV WW and WZ analyses in leptonic final states by ATLAS (blue) and CMS (red), using the full available data sets.

to the EFT formalism. Figure 39 illustrates the weak correlations between these EFT parameters.

B. $Z\gamma\gamma$ and $ZZ\gamma$ limits

Limits on the $Z\gamma\gamma$ and $ZZ\gamma$ couplings are usually given using the CP-conserving parameters h_3^V and h_4^V since there is no interference with the CP-violating couplings associated with the h_1^V and h_2^V parameters and the corresponding cross sections and sensitivities are very similar (Baur and Berger, 1993). Figure 40 shows a comparison of the most competitive limits, set by ATLAS and CMS. The combined limits by LEP (Schael *et al.*, 2013) as well as the best Tevatron limits by CDF (Aaltonen *et al.*, 2011) on h_3^V and h_4^V are not competitive with

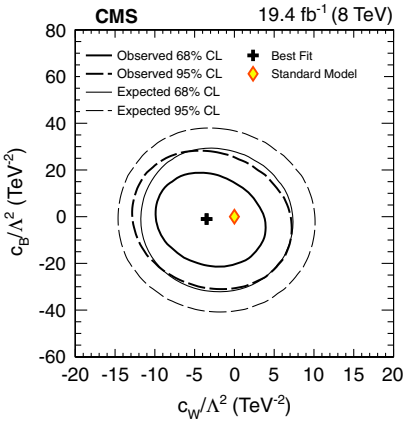

FIG. 39. Expected and observed 68% and 95% C.L. contours for aTGC limits in the EFT formulation derived from 8 TeV fully leptonic WW candidate events illustrating the weak correlations between these EFT parameters, with c_{WWW} set to zero. From Khachatryan *et al.*, 2016d.

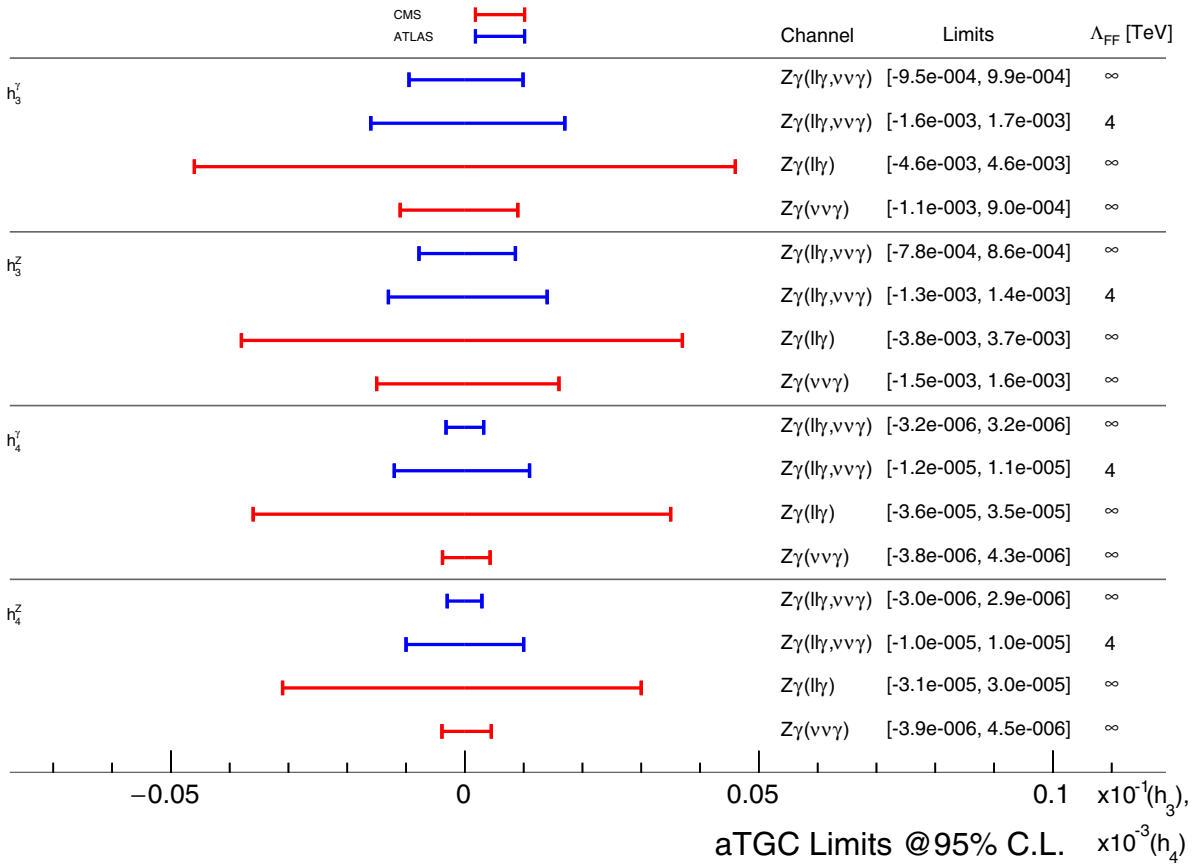

FIG. 40. Comparison of the most competitive $Z\gamma\gamma$ and $Z\gamma Z$ limits, set by the LHC analyses presented in this review. All limits are based on the full 8 TeV, ≈20 fb^{-1} data sets.

those achieved at the LHC. The impact of imposing unitarity constraints on the anomalous couplings via a form factor with a suppression scale Λ_{FF}, $\alpha(\hat{s}) = \alpha_0/(1+\hat{s}/\Lambda_{\mathrm{FF}}^2)^n$, is shown as well. The form factor exponent n is equal to the index i of the parameter h_i^V under study (Baur and Berger, 1993), in contrast with the dipole form factor $n = 2$ assumed in Sec. VIII.A. This illustrates the model dependence inherent in the form factor approach. In general, the parameter Λ_{FF} is chosen differently for different processes and the choice of the exponent n can also vary in the absence of a definitive prediction.

C. $ZZ\gamma$ and ZZZ limits

Turning to ZZ final states, the limits on anomalous triple gauge couplings are expressed in terms of two CP-violating (f_4^V) and two CP-conserving (f_5^V) parameters, all of which are zero in the SM. The limits on f_i^V are negatively correlated for a given i as illustrated in Fig. 41 which is based on 7 TeV ZZ candidate events in the 4ℓ decay mode.

One-dimensional limits for the f_i^V parameters derived from ZZ final states are shown in Fig. 42. The $2\ell 2\nu$ decay mode gives the most stringent limits due to increased branching fraction and detector acceptance. The 8 TeV data give significantly stronger limits on the f_i^V parameters, due to larger statistics and an extended reach in Z boson transverse momentum. The combined limits by LEP (Schael *et al.*, 2013) as well as the best Tevatron limits by D0 (Abazov *et al.*, 2008) are not competitive with those achieved at the LHC. The impact of imposing unitarity constraints on the anomalous couplings via a form factor $\alpha(\hat{s}) = \alpha_0/(1+\hat{s}/\Lambda_{\mathrm{FF}}^2)^3$ is shown as well. In this specific case the exponent $n = 3$ is chosen. Studying the sensitivity at 8 TeV, ATLAS (Aaboud *et al.*,

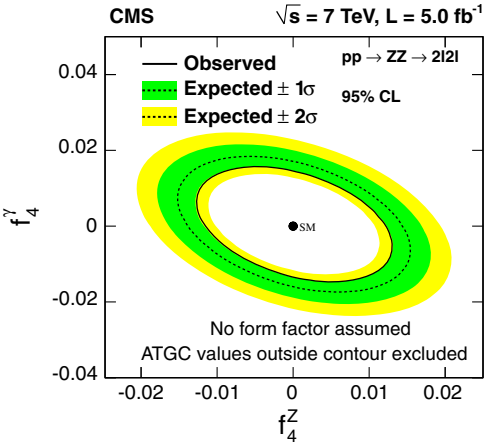

FIG. 41. Expected and observed 95% C.L. contours for aTGC limits derived from 7 TeV ZZ candidate events in the 4ℓ decay mode for the f_4^γ vs f_4^Z parameters. aTGCs not shown are set to zero. From Chatrchyan *et al.*, 2013g.

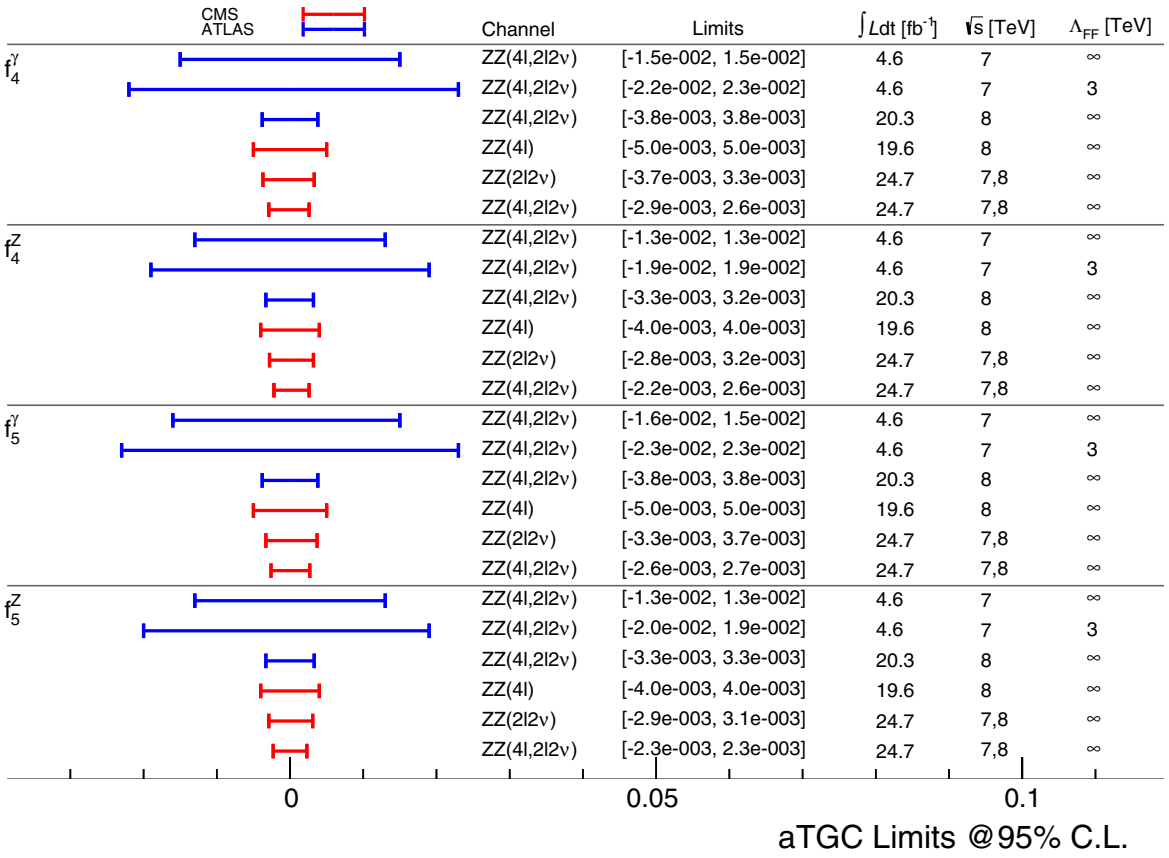

FIG. 42. Comparison of the most competitive $ZZ\gamma$ and ZZZ limits, set by the LHC analyses presented in this review.

2016e) found that a unitarization with a dipole form factor is no longer needed as the aTGC limits more and more approach the SM expectation (Gounaris, Layssac, and Renard, 2000).

ATLAS and CMS also performed a first combination of aTGC limits based on their 7 TeV ZZ analyses (Aad *et al.*, 2016h). With a negligible impact due to systematic uncertainties, the combination improves the aTGC sensitivity by about 20% compared to the sensitivity of each experiment. While the resulting limits are not competitive with the 8 TeV results presented, this is an important first step toward future combined LHC limits on anomalous couplings.

IX. CONSTRAINTS ON ANOMALOUS QUARTIC GAUGE COUPLINGS

In the SM there are $WWWW$, $WWZZ$, $WWZ\gamma$, and $WW\gamma\gamma$ couplings. Beyond the SM there are possible $ZZZZ$, $ZZZ\gamma$, $ZZ\gamma\gamma$, $Z\gamma\gamma\gamma$, and $\gamma\gamma\gamma\gamma$ couplings as listed in Table IV. In run I ATLAS and CMS have only begun to investigate a few of these possible couplings, with much more data planned in run II and beyond.

The aQGC limits follow from the examination of the production of inclusive triple gauge bosons, VBS dibosons, and exclusive dibosons. The limits are generally taken to be limits on the coefficients of dimension-8 operators (Éboli, Gonzalez-Garcia, and Mizukoshi, 2006) f, although with assumptions (Chatrchyan *et al.*, 2014e) some of these are related to an equivalent set a of dimension-6 operators (Belanger and Boudjema, 1992; Éboli, Gonzalez-Garcia, and Novaes, 1994; Stirling and Werthenbach, 2000), commonly used in Tevatron and LEP analyses. Table IV lists the 18 different dimension-8 operators and which quartic vertex they affect. Note that these operators do not include TGCs.

The LEP L3 and OPAL experiments have set their best aQGC limits by combining $W^+W^-\gamma, \nu\bar{\nu}\gamma\gamma$ (Achard *et al.*, 2002) and $W^+W^-\gamma, \nu\bar{\nu}\gamma\gamma$, and $q\bar{q}\gamma\gamma$ (Abbiendi *et al.*, 2004) analyses,

TABLE IV. Dimension-8 operators and the quartic vertices they affect. The first four columns show the only QGC vertices which exist in the SM. From Degrande *et al.*, 2013b.

	$WWWW$	$WWZZ$	$WW\gamma Z$	$WW\gamma\gamma$	$ZZZZ$	$ZZZ\gamma$	$ZZ\gamma\gamma$	$Z\gamma\gamma\gamma$	$\gamma\gamma\gamma\gamma$
$\mathcal{O}_{S,0}, \mathcal{O}_{S,1}$	✓	✓			✓				
$\mathcal{O}_{M,0}, \mathcal{O}_{M,1}, \mathcal{O}_{M,6}, \mathcal{O}_{M,7}$	✓	✓	✓	✓	✓	✓	✓		
$\mathcal{O}_{M,2}, \mathcal{O}_{M,3}, \mathcal{O}_{M,4}, \mathcal{O}_{M,5}$		✓	✓	✓	✓	✓	✓		
$\mathcal{O}_{T,0}, \mathcal{O}_{T,1}, \mathcal{O}_{T,2}$	✓	✓	✓	✓	✓	✓	✓	✓	✓
$\mathcal{O}_{T,5}, \mathcal{O}_{T,6}, \mathcal{O}_{T,7}$		✓	✓	✓	✓	✓	✓	✓	✓
$\mathcal{O}_{T,8}, \mathcal{O}_{T,9}$					✓	✓	✓	✓	✓

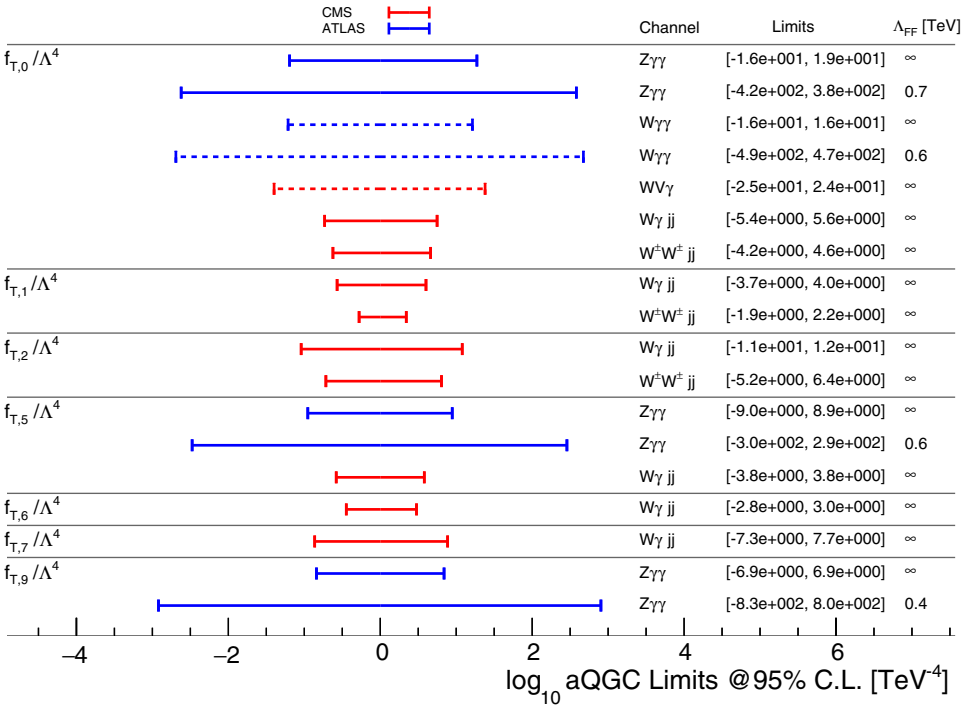

FIG. 43. Comparison of the most competitive limits involving $f_{T,i}$ coefficients, set by the LHC analyses presented in this review. All limits are based on the full 8 TeV, ≈20 fb^{-1} data sets.

respectively. These limits are surpassed by Tevatron's D0 experiment using the exclusive VBS process $\gamma\gamma \to WW$ (Abazov *et al.*, 2013). Since the early LHC results are already considerably more restrictive than the LEP and Tevatron limits, they are not shown in the following comparisons.

The $W\gamma\gamma$ data are affected only by the SM $WW\gamma\gamma$ coupling, while $WV\gamma$ and VBS $W\gamma jj$ data have contributions owing to $WW\gamma\gamma$ and $WWZ\gamma$ couplings. The VBS $WZjj$ data are affected by the SM $WWZZ$ and $WWZ\gamma$ couplings. The WWW and same-sign WW VBS data select only the SM $WWWW$ coupling while the exclusive $\gamma\gamma \to WW$ data select only the SM $WW\gamma\gamma$ coupling. Finally, the VBS $WVjj$ data are affected by all SM quartic couplings.

The one-dimensional limits on the EFT coefficients $f_{T,i}$ for dimension-8 operators containing just the field strength tensors are shown in Fig. 43. The VBS diboson channels yield similar limits, which are better than the triple boson production limits.

The ATLAS $W\gamma\gamma$ and $Z\gamma\gamma$ results are derived with VBFNLO MC samples, which use a different convention for the dimension-8 operators than the corresponding CMS results derived with MADGRAPH5_AMCNLO MC samples. To be able to compare the results with CMS, the ATLAS results were converted using the redefinition of operator coefficients outlined in Degrande *et al.* (2013b).

The impact of imposing unitarity constraints on the anomalous couplings via a dipole form factor with a suppression scale Λ_{FF} is shown as well. Note that the impact of unitarization is much larger than in the case of the aTGCs. Limits without unitarization hence clearly probe a regime where unitarity is violated at the scales probed and are more a benchmark than physically meaningful.

The analogous plots of limits for the $f_{M,i}$ coefficients for "mixed" dimension-8 operators containing covariant derivatives and the field strength tensors are shown in Fig. 44. Again, the VBS diboson channels are all comparable and yield the tightest limits although generally the same-sign WW limits are the most stringent. Where the exclusive process $\gamma\gamma \to WW$ is used to set a limit it is the most stringent, because the signal is so clean that it dominates the final selected data. The sensitivity of ATLAS and CMS to anomalous couplings is generally very similar. Limits on $f_{M,2}$ and $f_{M,3}$ were not included in the summary when they are trivially related to $f_{M,0}$ and $f_{M,1}$ by a factor of 2 under the assumption of a vanishing anomalous $WWZ\gamma$ coupling (Khachatryan *et al.*, 2016g). The ATLAS $W\gamma\gamma$ and $Z\gamma\gamma$ results are again converted to the convention employed by CMS, using the relations given in Degrande *et al.* (2013b). The $WV\gamma$ and $\gamma\gamma \to WW$ results are based on the dimension-6 operators with coefficients $a^W_{0,C}$ which are then converted to dimension-8 operators with coefficients $f_{M,0}$ and $f_{M,1}$. The conversion conventions employed by ATLAS (Degrande *et al.*, 2013b) and CMS (Belanger *et al.*, 2000) differ because CMS implemented their own Lagrangians in MADGRAPH5_AMCNLO for $WV\gamma$ and $\gamma\gamma \to WW$. To enable comparisons, the results from these two analyses and the ATLAS $\gamma\gamma \to WW$ analysis are derived from their $a^W_{0,C}$ results using the conversion in Degrande *et al.* (2013b) to give results following the standard MADGRAPH5_AMCNLO convention.

The impact of imposing unitarity constraints on the anomalous couplings via a dipole form factor with a suppression scale Λ_{FF} is shown as well. Again, unitarization can change some of the limits by orders of magnitude for these dimension-8 operators, indicating that such limits without

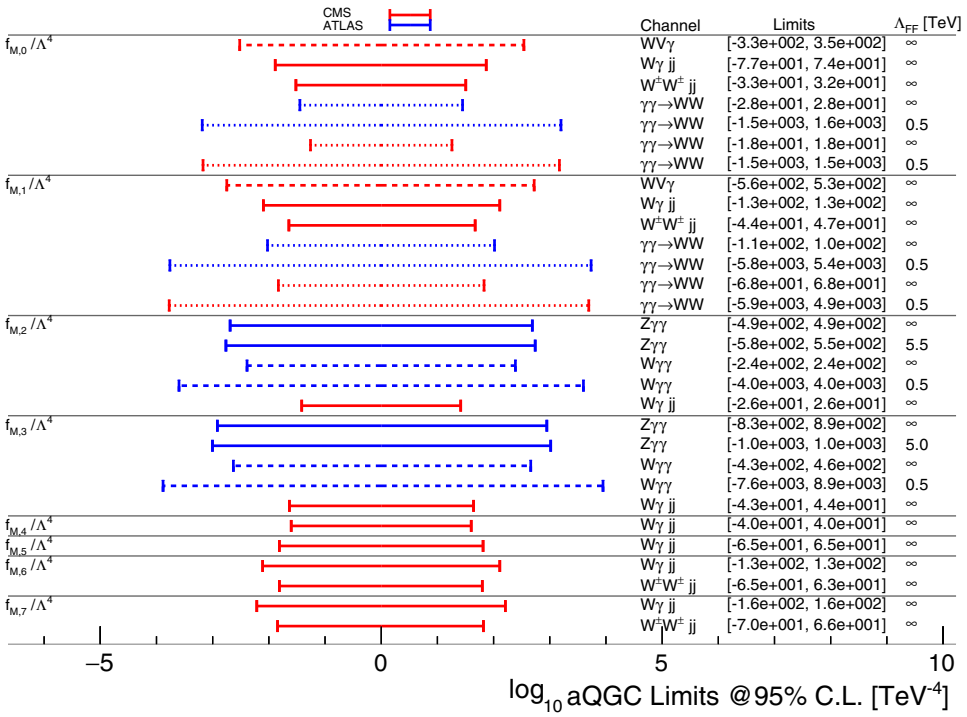

FIG. 44. Comparison of the most competitive limits involving $f_{M,i}$ coefficients, set by the LHC analyses presented in this review. All limits are based on the full 8 TeV, ≈20 fb^{-1} data sets, except for the $\gamma\gamma \to WW$ analysis by CMS, using in addition the full ≈5 fb^{-1} of the 7 TeV data set.

unitarization are driven by unphysical parameter regions where unitarity is violated.

Limits on the $f_{S,i}$ coefficients whose operators affect the scattering of longitudinal vector bosons have been placed by the CMS same-sign WW and ATLAS WWW analyses and are summarized in Fig. 45, illustrating the impact of applying unitarization with a form factor exponent $n = 1$.

The $W^{\pm}Vjj$, $W^{\pm}W^{\pm}jj$, and $W^{\pm}Zjj$ results by ATLAS are not included in the above summary plots since they set limits on the parameters $\alpha_{4,5}$ in an electroweak chiral Lagrangian model (Appelquist and Bernard, 1980; Longhitano, 1980, 1981; Appelquist and Wu, 1993) with K-matrix unitarization (Alboteanu, Kilian, and Reuter, 2008; Kilian *et al.*, 2015) applied. While vertex-dependent conversions to $f_{S,0}$ and $f_{S,1}$ exist (Degrande *et al.*, 2013b), for the $W^{\pm}Vjj$ analysis multiple vertices contribute. Consequently, the resulting limits are summarized separately in Fig. 46.

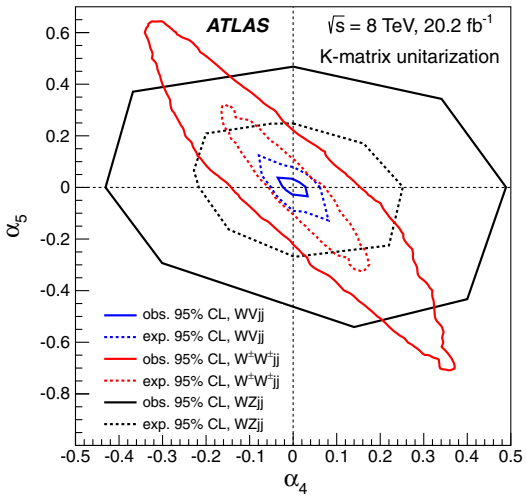

FIG. 45. Expected and observed 95% C.L. contours for aQGC limits in the α_4 and α_5 plane derived from 8 TeV $W^{\pm}Vjj$, $W^{\pm}W^{\pm}jj$, and $W^{\pm}Zjj$ results by ATLAS. From Aaboud *et al.*, 2016h.

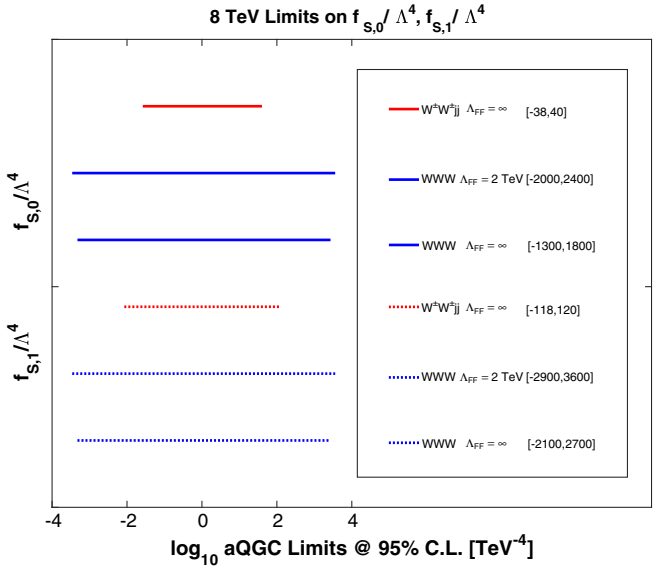

FIG. 46. Comparison of the available limits involving $f_{S,i}$ coefficients, set by the LHC analyses presented in this review. All limits are based on the full 8 TeV, ≈20 fb^{-1} data sets.

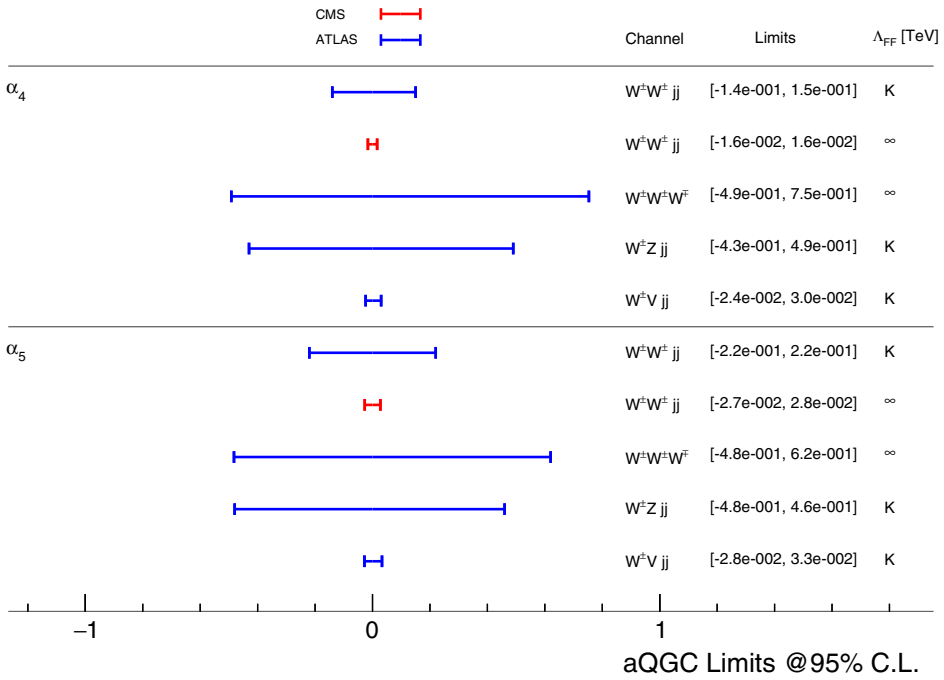

FIG. 47. Comparison of the available limits involving $\alpha_{4,5}$ coefficients, set by the LHC analyses presented in this review. All limits are based on the full 8 TeV, ≈20 fb^{-1} data sets. A "K" in the Λ_{FF} column indicates that K-matrix unitarization was applied.

The introduction of an additional dimension-8 operator $\mathcal{O}_{S,2}$ (Éboli and Gonzalez-Garcia, 2016) enables the vertex-independent conversion to the parameters $\alpha_{4,5}$ when considering quartic gauge boson vertices only, through the study of a linear combination of $\mathcal{O}_{S,2}$ and $\mathcal{O}_{S,0}$ (Rauch, 2016). This would be highly desirable for future studies and note that these resulting conversions are also applicable after K-matrix unitarization (Sekulla *et al.*, 2016).

In order to be able to compare the analyses on equal footing, we use the conversion for the $WWWW$ vertex for the CMS same-sign WW and ATLAS WWW analyses, omitting the results unitarized with a form factor as the applicability of the conversion is then questionable. The resulting comparison is given in Fig. 47, with the relative sensitivities to be taken with a grain of salt when no unitarization is applied.

Note that the $W^\pm Vjj$ analysis is the first semileptonic VBS analysis and exhibits a high sensitivity to anomalous couplings due to the larger branching fraction as well as probing the three distinct processes $W^\pm W^\mp jj$, $W^\pm W^\pm jj$, and $W^\pm Zjj$. It yields the most stringent unitarized limits thus far of $-0.024 < \alpha_4 < 0.030$ and $-0.028 < \alpha_5 < 0.033$ at 95% C.L., corresponding to a new physics scale above ≈1.4 TeV when assuming $\alpha_i = v^2/\Lambda^2$ (Reuter, Kilian, and Sekulla, 2013), where v is the Higgs vacuum expectation value ($v \approx 246$ GeV).

X. SENSITIVITY PROSPECTS AT THE HL-LHC

Both the updated European Strategy for Particle Physics (Council, CERN, 2013) and the Particle Physics Project Prioritization Panel (P5) report (Ritz *et al.*, 2014) outlining a ten-year strategic plan for HEP in the U.S. emphasize the use of the full LHC potential through a high-luminosity upgrade (HL-LHC) as top priority for the field. An important ingredient for the physics case is the detailed studies of multiboson interactions which enable the test of the EWSB mechanism as well as the search for extensions beyond the SM.

The Physics Briefing Book (Aleksan *et al.*, 2013) for the European Strategy for Particle Physics points out that studies of longitudinal VBS to explore the EWSB mechanism in detail will not be possible without the HL-LHC data set. As an example for the enhanced sensitivity achievable with the HL-LHC to unveil new phenomena, a study by ATLAS (Aad *et al.*, 2012l) using simplified detector performance parametrizations is shown, where a new physics VBS ZZ resonance could be discovered only using the HL-LHC data set.

For the Snowmass community study preceding the P5 formation, both ATLAS (Aad *et al.*, 2013g) and CMS (Chatrchyan, 2013i) provided contributions which outline the physics program as well as sensitivity improvements at the HL-LHC. With the enhanced data set, diboson differential cross-section measurements in the high-$\hat{s}$ tails of distributions will be possible as well as detailed studies of VBF, VBS, and triboson production, from establishing the signals to measuring differential cross sections with high precision. The discovery reach for new higher-dimensional operators studied in $W^\pm W^\pm$, WZ, and ZZ VBS processes and $Z\gamma\gamma$ is at least doubled in the HL-LHC data set (Aad *et al.*, 2013h). The proceedings of the Snowmass community study (Bardeen *et al.*, 2013) also quantified the dimension-8 operator sensitivity increase due to the HL-LHC to be a factor of 2 to 3 over the LHC, based on independent studies (Baak *et al.*, 2013; Degrande *et al.*, 2013a) of $W^\pm W^\pm$, WZ, and ZZ VBS processes and WWW and $Z\gamma\gamma$ triboson production.

Both ATLAS and CMS are preparing major detector upgrades for the HL-LHC and used VBS interactions as a

benchmark for the anticipated performance (Aad *et al.*, 2015a; Khachatryan *et al.*, 2015h). Extended tracking systems will enable improved lepton identification also in the forward detector regions as well as crucial suppression of pileup jet contributions to the tagging jet signature.

Measuring the polarization fractions in VBS is a crucial experimental test of the predicted unitarization of the longitudinal VBS cross section by the SM Higgs boson. CMS (Khachatryan *et al.*, 2015h) evaluated the expected sensitivity to measure the longitudinal fraction in $W^{\pm}W^{\pm}$ scattering using a two-dimensional template fit of the $\Delta\Phi$ between the two tagging jets and the p_{T} of the leading lepton and expect a significance of $\approx 2.4\sigma$ in the HL-LHC data set as illustrated in Fig. 48(a). Combining this with a corresponding WZ VBS analysis, the longitudinal VBS significance increases to 2.75σ.

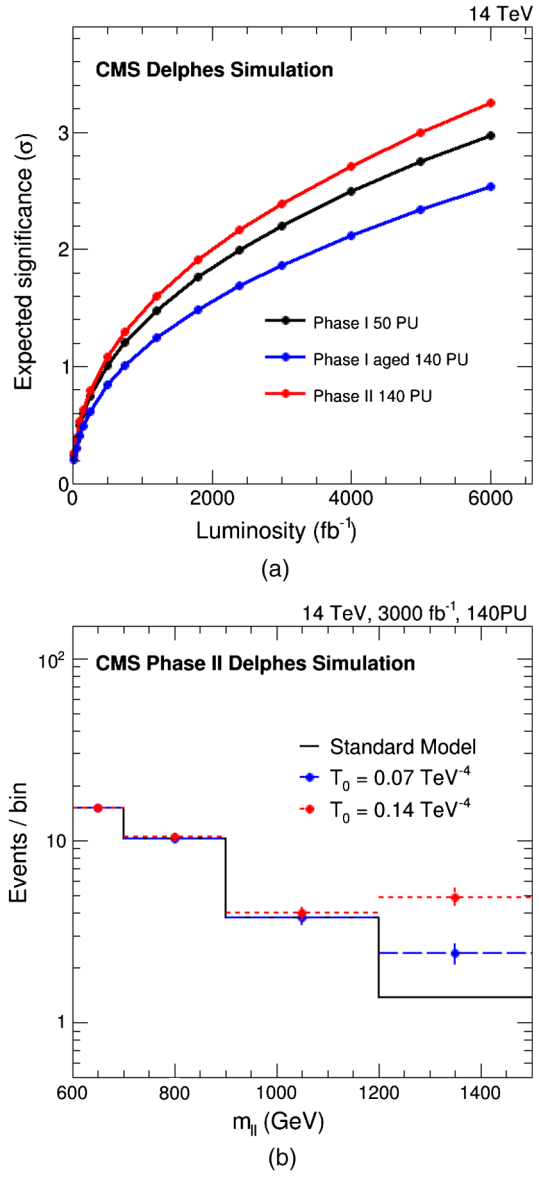

FIG. 48. Expected CMS performance for $W^{\pm}W^{\pm}$ VBS measurements at the HL-LHC: (a) significance of measuring the longitudinal $W^{\pm}W^{\pm}$ VBS cross section as a function of integrated luminosity and (b) dilepton mass distribution, where the effect of aQGCs on the spectrum is also From Khachatryan *et al.*, 2015h.

Note that a significant increase in sensitivity should still be possible using a deep machine learning technique instead of a "simple" variable fit, as demonstrated for the $W^{\pm}W^{\pm}$ VBS case in Searcy *et al.* (2016).

The HL-LHC data set will also greatly enhance the sensitivity to anomalous couplings. Figure 48(b) shows the expected dilepton mass distribution in $W^{\pm}W^{\pm}$ VBS candidate events with 3000 fb^{-1}, where the data extend to about 1.5 TeV. This is a factor of 3 higher than accessible in run I and will improve the aQGC limits by about a factor of 50 for the aQGC example shown.

The search for new physics contributions in multiboson interactions either indirectly through anomalous couplings or directly through resonance searches will greatly benefit from the increased exploitation of final states with hadronically decaying W/Z bosons. To probe the high-mass tail of the VV spectrum, this means the identification of merged dijets into boosted monojets (the hadronically decaying V boson) will be of crucial importance (Khachatryan *et al.*, 2014b; Aad *et al.*, 2016a), in particular, at the HL-LHC (see Fig. 5).

With the advent of the first analyses in the Higgs sector employing the EFT approach (Aad *et al.*, 2016b) rather than the κ framework (Andersen *et al.*, 2013) which allows the modification of Higgs couplings without affecting its kinematics, combined constraints from the Higgs and multiboson analyses will be possible. Such analyses will properly reflect the interconnectedness of multiboson and Higgs interactions in EFTs and yield improved constraints, as demonstrated by external global fits (Corbett *et al.*, 2013; Pomarol and Riva, 2014; Ellis, Sanz, and You, 2015; Falkowski and Riva, 2015; Butter *et al.*, 2016).

To benefit from the tremendous progress in the theoretical predictions it is important to perform measurements of carefully chosen observables that can be studied with high precision and exhibit small theoretical uncertainties. Ratios of diboson production rates have been proposed (Frye *et al.*, 2016) that could enable precision tests of the theoretical predictions, potentially to the level of being sensitive to electroweak corrections.

XI. CONCLUSIONS

The LHC has enabled studies of multiboson interactions at an unprecedented level. Previously unobserved SM processes including vector boson fusion, triboson production, and vector boson scattering were established or at least observed with first evidence. In particular, processes involving quartic gauge boson couplings were probed for the first time, allowing the test of uncharted territory in the SM. The SM signal is modeled in most analyses with MC generators implementing NLO QCD calculations. Higher-order corrections at NNLO QCD and NLO EW generally tend to improve the agreement with the data. Such corrections are sizable (and of opposite sign), in particular, in the high-energy tails of distributions and need to be incorporated where available to set more accurate anomalous coupling limits.

The data taken at the LHC through 2012 yielded many limits on aTGCs and aQGCs which have confirmed the SM gauge couplings at the level of accuracy which was accessible

given the integrated luminosity and the LHC energy. The limits for aTGCs arise largely from inclusive diboson production properties at high diboson mass. The aQGC limits are determined from the inclusive production of three bosons and from the exclusive VBS production of boson pairs, also at high triboson and diboson masses. These limits are presently the most stringent, exceeding those found at LEP and the Tevatron both in the numerical limits themselves and in the breadth of the processes explored in the search for anomalous behavior.

Limits on aQGCs prove to be very sensitive to the application of a unitarization procedure due to the higher dimensionality (eight) of the operators involved, indicating that limits without unitarization are driven by unphysical parameter regions where unitarity is violated. On the other hand, introducing any unitarization turns the EFT ansatz into a specific model, defeating the original purpose of model independence. Limits on aTGCs in an EFT framework can also suffer from inconsistencies if a generic power counting implies that the scale of new physics is parametrically below the mass scale probed by the LHC. Both the aQGC and aTGC EFT issues stem from using the EFT in a region that is not self-consistent. Eventually when the LHC has obtained sufficient precision, and if no deviation from the SM is found, EFTs will be able to be generically used to set precision bounds. However, as emphasized in Sec. II this is not the case as of yet. One way to avoid these issues is to provide upper limits on fiducial cross sections as an alternative to EFT interpretations or unfolded differential cross-section distributions in sensitive variables that can be confronted with any new physics model of interest.

The LHC experiments have already gone well beyond previous limits on triple gauge couplings and have advanced into limits on quartic gauge couplings by using the new energy frontier opened up by the LHC. The LHC has since run at enhanced energy going from 8 TeV in 2012 to 13 TeV starting in 2015. The luminosity has also risen substantially. Thus, the limits given in this review will be improved upon in the near future. In the more distant future the high-luminosity LHC will yet again substantially improve on the aTGC and aQGC limits. These data will serve to explore the mutual couplings of the gauge bosons and ascertain if the SM is the correct description of those non-Abelian couplings.

ACKNOWLEDGMENTS

We thank CERN and the LHC Accelerator team for making this fantastic machine a reality and for operating it so well. In addition, we thank the ATLAS and CMS Collaborations in general, and, in particular, the electroweak and standard model working group members, past and present, for their help and cooperation in advising and encouraging us and for providing experimental details of the results quoted in this review. We also gratefully acknowledge the tremendous effort and progress on the theoretical side, enabling the predictions and MC tools utilized in the measurements presented in this review and those forthcoming. Finally we thank Matt Herndon and Harikrishnan Ramani for useful comments on the draft. The work of M.-A. P. was supported by the DOE Contract No. DE-SC0012704. The work of P. M. was supported in part by the NSF CAREER Awards No. NSF-PHY-1056833 and No. NSF-PHY-1620628.

REFERENCES

Aaboud, Morad, *et al.* (ATLAS Collaboration), 2016a, "Electron efficiency measurements with the ATLAS detector using 2012 LHC proton-proton collision data," arXiv:1612.01456.

Aaboud, Morad, *et al.* (ATLAS Collaboration), 2016b, "Measurement of exclusive $\gamma\gamma \to W^+W^-$ production and search for exclusive Higgs boson production in pp collisions at $\sqrt{s} = 8$ TeV using the ATLAS detector," Phys. Rev. D **94**, 032011.

Aaboud, Morad, *et al.* (ATLAS Collaboration), 2016c, "Measurement of the photon identification efficiencies with the ATLAS detector using LHC Run-1 data," Eur. Phys. J. C **76**, 666.

Aaboud, Morad, *et al.* (ATLAS Collaboration), 2016d, "Measurement of the $W^{\pm}Z$ boson pair-production cross section in pp collisions at $\sqrt{s} = 13$ TeV with the ATLAS Detector," Phys. Lett. B **762**, 1–22.

Aaboud, Morad, *et al.* (ATLAS Collaboration), 2016e, "Measurement of the ZZ production cross section in pp collisions at $\sqrt{s} = 8$ TeV using the $ZZ \to \ell^-\ell^+\ell'^-\ell'^+$ and $ZZ \to \ell^-\ell^+\nu\bar{\nu}$ channels with the ATLAS detector," arXiv:1610.07585.

Aaboud, Morad, *et al.* (ATLAS Collaboration), 2016f, "Measurement of $W^{\pm}W^{\pm}$ vector-boson scattering and limits on anomalous quartic gauge couplings with the ATLAS detector," arXiv:1611.02428.

Aaboud, Morad, *et al.* (ATLAS Collaboration), 2016g, "Measurement of W^+W^- production in association with one jet in proton–proton collisions at $\sqrt{s} = 8$ TeV with the ATLAS detector," Phys. Lett. B **763**, 114–133.

Aaboud, Morad, *et al.* (ATLAS Collaboration), 2016h, "Search for anomalous electroweak production of WW/WZ in association with a high-mass dijet system in pp collisions at $\sqrt{s} = 8$ TeV with the ATLAS detector," arXiv:1609.05122.

Aaboud, Morad, *et al.* (ATLAS Collaboration), 2016i, "Search for triboson $W^{\pm}W^{\pm}W^{\mp}$ production in pp collisions at $\sqrt{s} = 8$ TeV with the ATLAS detector," arXiv:1610.05088.

Aad, Georges, *et al.* (ATLAS Collaboration), 2008, "The ATLAS Experiment at the CERN Large Hadron Collider," J. Instrum. **3**, S08003.

Aad, Georges, *et al.* (ATLAS Collaboration), 2011a, "Measurement of the W^+W^- cross section in $\sqrt{s} = 7$ TeV pp collisions with ATLAS," Phys. Rev. Lett. **107**, 041802.

Aad, Georges, *et al.* (ATLAS Collaboration), 2011b, "Measurement of $W\gamma$ and $Z\gamma$ production in proton-proton collisions at $\sqrt{s} = 7$ TeV with the ATLAS Detector," J. High Energy Phys. 09, 072.

Aad, Georges, *et al.* (ATLAS Collaboration), 2011c, "Expected photon performance in the ATLAS experiment," Report No. ATL-PHYS-PUB-2011-007.

Aad, Georges, *et al.* (ATLAS Collaboration), 2012a, "Measurement of the inclusive $W^{\pm}$ and Z/gamma cross sections in the electron and muon decay channels in pp collisions at $\sqrt{s} = 7$ TeV with the ATLAS detector," Phys. Rev. D **85**, 072004.

Aad, Georges, *et al.* (ATLAS Collaboration), 2012b, "Measurement of the isolated di-photon cross-section in pp collisions at $\sqrt{s} = 7$ TeV with the ATLAS detector," Phys. Rev. D **85**, 012003.

Aad, Georges, *et al.* (ATLAS Collaboration), 2012c, "Measurement of the $W^{\pm}Z$ production cross section and limits on anomalous triple gauge couplings in proton-proton collisions at $\sqrt{s} = 7$ TeV with the ATLAS detector," Phys. Lett. B **709**, 341–357.

Aad, Georges, *et al.* (ATLAS Collaboration), 2012d, "Measurement of the W^+W^- cross section in $\sqrt{s} = 7$ TeV pp collisions with the ATLAS detector and limits on anomalous gauge couplings," Phys. Lett. B **712**, 289–308.

Aad, Georges, *et al.* (ATLAS Collaboration), 2012e, "Measurement of the ZZ production cross section and limits on anomalous neutral triple gauge couplings in proton-proton collisions at $\sqrt{s} = 7$ TeV with the ATLAS detector," Phys. Rev. Lett. **108**, 041804.

Aad, Georges, *et al.* (ATLAS Collaboration), 2012f, "Measurement of $W\gamma$ and $Z\gamma$ production cross sections in pp collisions at $\sqrt{s} =$ 7 TeV and limits on anomalous triple gauge couplings with the ATLAS detector," Phys. Lett. B **717**, 49–69.

Aad, Georges, *et al.* (ATLAS Collaboration), 2012g, "Measurement of $W^{\pm}Z$ production in proton-proton collisions at $\sqrt{s} = 7$ TeV with the ATLAS detector," Eur. Phys. J. C **72**, 2173.

Aad, Georges, *et al.* (ATLAS Collaboration), 2012h, "Observation of a new particle in the search for the Standard Model Higgs boson with the ATLAS detector at the LHC," Phys. Lett. B **716**, 1–29.

Aad, Georges, *et al.* (ATLAS Collaboration), 2012i, "Performance of Missing Transverse Momentum Reconstruction in Proton-Proton Collisions at 7 TeV with ATLAS," Eur. Phys. J. C **72**, 1844.

Aad, Georges, *et al.* (ATLAS Collaboration), 2012j, "Performance of the ATLAS Trigger System in 2010," Eur. Phys. J. C **72**, 1849.

Aad, Georges, *et al.* (ATLAS Collaboration), 2012k, "Search for supersymmetry in final states with jets, missing transverse momentum and one isolated lepton in $\sqrt{s} = 7$ TeV pp collisions using 1 fb^{-1} of ATLAS data," Phys. Rev. D **85**, 012006; **87**, 099903(E) (2013).

Aad, Georges, *et al.* (ATLAS Collaboration), 2012l, "Studies of Vector Boson Scattering with an Upgraded ATLAS Detector at a High-Luminosity LHC," Technical Report No. ATL-PHYS-PUB-2012-005 (CERN, Geneva).

Aad, Georges, *et al.* (ATLAS Collaboration), 2012m, "Measurements of the photon identification efficiency with the ATLAS detector using 4.9 fb^{-1} of pp collision data collected in 2011," Report No. ATLAS-CONF-2012-123.

Aad, Georges, *et al.* (ATLAS Collaboration), 2012n, "Performance of the ATLAS Electron and Photon Trigger in pp Collisions at $\sqrt{s} = 7$ TeV in 2011," Report No. ATLAS-CONF-2012-048.

Aad, Georges, *et al.* (ATLAS Collaboration), 2013a, "Jet energy measurement with the ATLAS detector in proton-proton collisions at $\sqrt{s} = 7$ TeV," Eur. Phys. J. C **73**, 2304.

Aad, Georges, *et al.* (ATLAS Collaboration), 2013b, "Jet energy resolution in proton-proton collisions at $\sqrt{s} = 7$ TeV recorded in 2010 with the ATLAS detector," Eur. Phys. J. C **73**, 2306.

Aad, Georges, *et al.* (ATLAS Collaboration), 2013c, "Measurement of W^+W^- production in pp collisions at $\sqrt{s} = 7$ TeV with the ATLAS detector and limits on anomalous WWZ and $WW\gamma$ couplings," Phys. Rev. D **87**, 112001; **88**, 079906(E) (2013).

Aad, Georges, *et al.* (ATLAS Collaboration), 2013d, "Measurements of $W\gamma$ and $Z\gamma$ production in pp collisions at $\sqrt{s} = 7$ TeV with the ATLAS detector at the LHC," Phys. Rev. D **87**, 112003; **91**, 119901(E) (2015).

Aad, Georges, *et al.* (ATLAS Collaboration), 2013e, "Measurement of isolated-photon pair production in pp collisions at $\sqrt{s} = 7$ TeV with the ATLAS detector," J. High Energy Phys. 01, 086.

Aad, Georges, *et al.* (ATLAS Collaboration), 2013f, "Measurement of ZZ production in pp collisions at $\sqrt{s} = 7$ TeV and limits on anomalous ZZZ and $ZZ\gamma$ couplings with the ATLAS detector," J. High Energy Phys. 03, 128.

Aad, Georges, *et al.* (ATLAS Collaboration), 2013g, "Physics at a High-Luminosity LHC with ATLAS," in *Proceedings, Community Summer Study 2013: Snowmass on the Mississippi (CSS2013)*, arXiv:1307.7292.

Aad, Georges, *et al.* (ATLAS Collaboration), 2013h, "Studies of Vector Boson Scattering And Triboson Production with an Upgraded ATLAS Detector at a High-Luminosity LHC," Technical Report No. ATL-PHYS-PUB-2013-006 (CERN, Geneva).

Aad, Georges, *et al.* (ATLAS Collaboration), 2013i, "Performance of Missing Transverse Momentum Reconstruction in ATLAS studied in Proton–Proton Collisions recorded in 2012 at $\sqrt{s} = 8$ TeV," Report No. ATLAS-CONF-2013-082.

Aad, Georges, *et al.* (ATLAS Collaboration), 2014a, "Electron and photon energy calibration with the ATLAS detector using LHC Run 1 data," Eur. Phys. J. C **74**, 3071.

Aad, Georges, *et al.* (ATLAS Collaboration), 2014b, "Electron reconstruction and identification efficiency measurements with the ATLAS detector using the 2011 LHC proton-proton collision data," Eur. Phys. J. C **74**, 2941.

Aad, Georges, *et al.* (ATLAS Collaboration), 2014c, "Evidence for Electroweak Production of $W^{\pm}W^{\pm}jj$ in pp Collisions at $\sqrt{s} =$ 8 TeV with the ATLAS Detector," Phys. Rev. Lett. **113**, 141803.

Aad, Georges, *et al.* (ATLAS Collaboration), 2014d, "Measurement of the muon reconstruction performance of the ATLAS detector using 2011 and 2012 LHC proton-proton collision data," Eur. Phys. J. C **74**, 3130.

Aad, Georges, *et al.* (ATLAS Collaboration), 2014e, "Muon reconstruction efficiency and momentum resolution of the ATLAS experiment in proton-proton collisions at $\sqrt{s} = 7$ TeV in 2010," Eur. Phys. J. C **74**, 3034.

Aad, Georges, *et al.* (ATLAS Collaboration), 2014f, "Measurement of the electroweak production of dijets in association with a Z-boson and distributions sensitive to vector boson fusion in proton-proton collisions at $\sqrt{s} = 8$ TeV using the ATLAS detector," J. High Energy Phys. 04, 031.

Aad, Georges, *et al.* (ATLAS Collaboration), 2014g, "Pile-up Correction in Missing Transverse Momentum Reconstruction in the ATLAS Experiment in Proton–Proton Collisions at $\sqrt{s} = 8$ TeV," Report No. ATLAS-CONF-2014-019.

Aad, Georges, *et al.* (ATLAS Collaboration), 2015a, "ATLAS Phase-II Upgrade Scoping Document," Technical Report No. CERN-LHCC-2015-020, LHCC-G-166 (CERN, Geneva).

Aad, Georges, *et al.* (ATLAS Collaboration), 2015b, "Evidence of $W\gamma\gamma$ Production in pp Collisions at $\sqrt{s} = 8$ TeV and Limits on Anomalous Quartic Gauge Couplings with the ATLAS Detector," Phys. Rev. Lett. **115**, 031802.

Aad, Georges, *et al.* (ATLAS Collaboration), 2015c, "Jet energy measurement and its systematic uncertainty in proton-proton collisions at $\sqrt{s} = 7$ TeV with the ATLAS detector," Eur. Phys. J. C **75**, 17.

Aad, Georges, *et al.* (ATLAS Collaboration), 2015d, "Performance of the ATLAS muon trigger in pp collisions at $\sqrt{s} = 8$ TeV," Eur. Phys. J. C **75**, 120.

Aad, Georges, *et al.* (ATLAS Collaboration), 2015e, "Measurement of the $WW + WZ$ cross section and limits on anomalous triple gauge couplings using final states with one lepton, missing transverse momentum, and two jets with the ATLAS detector at $\sqrt{s} = 7$ TeV," J. High Energy Phys. 01, 049.

Aad, Georges, *et al.* (ATLAS Collaboration), 2015f, "Monte Carlo Calibration and Combination of In-situ Measurements of Jet Energy Scale, Jet Energy Resolution and Jet Mass in ATLAS," Report No. ATLAS-CONF-2015-037.

Aad, Georges, *et al.* (ATLAS Collaboration), 2016a, "Combination of searches for WW, WZ, and ZZ resonances in pp collisions

at $\sqrt{s} = 8$ TeV with the ATLAS detector," Phys. Lett. B **755**, 285–305.

Aad, Georges, *et al.* (ATLAS Collaboration), 2016b, "Constraints on non-Standard Model Higgs boson interactions in an effective Lagrangian using differential cross sections measured in the $H \to \gamma\gamma$ decay channel at $\sqrt{s} = 8$ TeV with the ATLAS detector," Phys. Lett. B **753**, 69–85.

Aad, Georges, *et al.* (ATLAS Collaboration), 2016c, "Identification of boosted, hadronically decaying W bosons and comparisons with ATLAS data taken at $\sqrt{s} = 8$ TeV," Eur. Phys. J. C **76**, 154.

Aad, Georges, *et al.* (ATLAS Collaboration), 2016d, "Measurements of $W^{\pm}Z$ production cross sections in pp collisions at $\sqrt{s} = 8$ TeV with the ATLAS detector and limits on anomalous gauge boson self-couplings," Phys. Rev. D **93**, 092004.

Aad, Georges, *et al.* (ATLAS Collaboration), 2016e, "Measurements of $Z\gamma$ and $Z\gamma\gamma$ production in pp collisions at $\sqrt{s} = 8$ TeV with the ATLAS detector," Phys. Rev. D **93**, 112002.

Aad, Georges, *et al.* (ATLAS Collaboration), 2016f, "Performance of algorithms that reconstruct missing transverse momentum in $\sqrt{s} =$ 8 TeV proton-proton collisions in the ATLAS detector," arXiv:1609.09324.

Aad, Georges, *et al.* (ATLAS Collaboration), 2016g, "Measurement of total and differential W^+W^- production cross sections in proton-proton collisions at $\sqrt{s} = 8$ TeV with the ATLAS detector and limits on anomalous triple-gauge-boson couplings," J. High Energy Phys. 09, 029.

Aad, Georges, *et al.* (ATLAS, CMS Collaborations), 2016h, "Combination of results from the ATLAS and CMS experiments on anomalous triple gauge couplings in ZZ production from pp collisions at a centre-of-mass energy of 7 TeV at the LHC," ATLAS-CONF-2016-036, CMS-PAS-SMP-15-001.

Aaltonen, T., *et al.* (CDF Collaboration), 2011, "Limits on Anomalous Trilinear Gauge Couplings in $Z\gamma$ Events from $p\bar{p}$ Collisions at $\sqrt{s} = 1.96$ TeV," Phys. Rev. Lett. **107**, 051802.

Abazov, V. M., *et al.* (D0 Collaboration), 2008, "Search for ZZ and $Z\gamma^*$ production in $p\bar{p}$ collisions at $\sqrt{s} = 1.96$ TeV and limits on anomalous ZZZ and $ZZ\gamma^*$ couplings," Phys. Rev. Lett. **100**, 131801.

Abazov, Victor Mukhamedovich, *et al.* (D0 Collaboration), 2012, "Limits on anomalous trilinear gauge boson couplings from WW, WZ and $W\gamma$ production in $p\bar{p}$ collisions at $\sqrt{s} = 1.96$ TeV," Phys. Lett. B **718**, 451–459.

Abazov, Victor Mukhamedovich, *et al.* (D0 Collaboration), 2013, "Search for anomalous quartic $WW\gamma\gamma$ couplings in dielectron and missing energy final states in $p\bar{p}$ collisions at $\sqrt{s} = 1.96$ TeV," Phys. Rev. D **88**, 012005.

Abbiendi, G., *et al.* (OPAL Collaboration), 2004, "Constraints on anomalous quartic gauge boson couplings from nu anti-nu gamma gamma and q anti-q gamma gamma events at LEP-2," Phys. Rev. D **70**, 032005.

Abdallah, Jalal, *et al.*, 2015, "Simplified Models for Dark Matter Searches at the LHC," Phys. Dark Universe **9–10**, 8–23.

Achard, P., *et al.* (L3 Collaboration), 2002, "Study of the $W^+W^-\gamma$ process and limits on anomalous quartic gauge boson couplings at LEP," Phys. Lett. B **527**, 29–38.

Adam, W., *et al.* (CMS Trigger and Data Acquisition Group), 2006, "The CMS high level trigger," Eur. Phys. J. C **46**, 605–667.

Aihara, H., *et al.*, 1996, Summary of the Working Subgroup on "Anomalous Gauge Boson Interactions of the DPF Long-Range Planning Study," in *Electroweak Symmetry Breaking and New Physics at the TeV Scale*, Advanced Series on Directions in High Energy Physics, edited by T. L. Barklow, S. Dawson, H. E. Haber, and J. L. Siegrist (World Scientific, Singapore).

Alboteanu, Ana, Wolfgang Kilian, and Juergen Reuter, 2008, "Resonances and Unitarity in Weak Boson Scattering at the LHC," J. High Energy Phys. 11, 010.

Aleksan, R., *et al.* (European Strategy for Particle Physics Preparatory Group), 2013, "Physics Briefing Book: Input for the Strategy Group to draft the update of the European Strategy for Particle Physics."

Alioli, Simone, Christian W. Bauer, Calvin Berggren, Frank J. Tackmann, Jonathan R. Walsh, and Saba Zuberi, 2014, "Matching Fully Differential NNLO Calculations and Parton Showers," J. High Energy Phys. 06, 089.

Alioli, Simone, Fabrizio Caola, Gionata Luisoni, and Raul Röntsch, 2016, "ZZ production in gluon fusion at NLO matched to parton-shower," arXiv:1609.09719.

Alioli, Simone, Paolo Nason, Carlo Oleari, and Emanuele Re, 2010, "A general framework for implementing NLO calculations in shower Monte Carlo programs: the POWHEG BOX," J. High Energy Phys. 06, 043.

Altarelli, G., T. Sjostrand, and F. Zwirner, 1996, Eds., "Physics at LEP2," Vol. 1.

Alwall, J., R. Frederix, S. Frixione, V. Hirschi, F. Maltoni, O. Mattelaer, H. S. Shao, T. Stelzer, P. Torrielli, and M. Zaro, 2014, "The automated computation of tree-level and next-to-leading order differential cross sections, and their matching to parton shower simulations," J. High Energy Phys. 07, 079.

Andersen, J. R., *et al.* (LHC Higgs Cross Section Working Group), 2013, "Handbook of LHC Higgs Cross Sections: 3. Higgs Properties," Report No. 10.5170/CERN-2013-004, arXiv:1307.1347.

Andersen, J. R., *et al.*, 2016, "Les Houches 2015: Physics at TeV Colliders Standard Model Working Group Report," in *9th Les Houches Workshop on Physics at TeV Colliders (PhysTeV 2015) Les Houches, France*, arXiv:1605.04692.

Appelquist, Thomas, and Claude W. Bernard, 1980, "Strongly Interacting Higgs Bosons," Phys. Rev. D **22**, 200.

Appelquist, Thomas, and Guo-Hong Wu, 1993, "The Electroweak chiral Lagrangian and new precision measurements," Phys. Rev. D **48**, 3235–3241.

Arkani-Hamed, N., A. G. Cohen, E. Katz, and A. E. Nelson, 2002, "The Littlest Higgs," J. High Energy Phys. 07, 034.

Arkani-Hamed, Nima, Andrew G. Cohen, and Howard Georgi, 2001, "Electroweak symmetry breaking from dimensional deconstruction," Phys. Lett. B **513**, 232–240.

Arnold, K., *et al.*, 2009, "VBFNLO: A Parton level Monte Carlo for processes with electroweak bosons," Comput. Phys. Commun. **180**, 1661–1670.

Arnold, K., *et al.*, 2011, "VBFNLO: A Parton Level Monte Carlo for Processes with Electroweak Bosons—Manual for Version 2.5.0," arXiv:1107.4038.

Arzt, C., M. B. Einhorn, and J. Wudka, 1995, "Patterns of deviation from the standard model," Nucl. Phys. B **433**, 41–66.

Baak, M., *et al.*, 2013, "Working Group Report: Precision Study of Electroweak Interactions," in *Proceedings, Community Summer Study 2013: Snowmass on the Mississippi (CSS2013)*, arXiv:1310.6708.

Baglio, J., *et al.*, 2014, "Release Note—VBFNLO 2.7.0," arXiv:1404.3940.

Bardeen, M., *et al.*, 2013, *Proceedings, Community Summer Study 2013: Snowmass on the Mississippi (CSS2013).*

Baur, U., and Edmond L. Berger, 1993, "Probing the weak boson sector in $Z\gamma$ production at hadron colliders," Phys. Rev. D **47**, 4889–4904.

Baur, U., Tao Han, N. Kauer, R. Sobey, and D. Zeppenfeld, 1997, "$W\gamma\gamma$ production at the Fermilab Tevatron collider: Gauge invariance and radiation amplitude zero," Phys. Rev. D **56**, 140–150.

Baur, U., and D. Zeppenfeld, 1993, "Measuring three vector boson couplings in $qq \to qqW$ at the SSC," in *Workshop on Physics at Current Accelerators and the Supercollider*, pp. 0327–334, arXiv:hep-ph/9309227.

Beaudette, Florian (CMS Collaboration), 2013, "The CMS Particle Flow Algorithm," in *Proceedings, International Conference on Calorimetry for the High Energy Frontier (CHEF 2013)*, pp. 295–304, arXiv:1401.8155.

Belanger, G., and F. Boudjema, 1992, "$\gamma\gamma \to W^+W^-$ and $\gamma\gamma \to ZZ$ as tests of novel quartic couplings," Phys. Lett. B **288**, 210–220.

Belanger, G., F. Boudjema, Y. Kurihara, D. Perret-Gallix, and A. Semenov, 2000, "Bosonic quartic couplings at LEP-2," Eur. Phys. J. C **13**, 283–293.

Biedermann, B., A. Denner, S. Dittmaier, L. Hofer, and B. Jäger, 2016, "Electroweak corrections to $pp \to \mu^+\mu^-e^+e^- + X$ at the LHC: a Higgs background study," Phys. Rev. Lett. **116**, 161803.

Biedermann, Benedikt, Marina Billoni, Ansgar Denner, Stefan Dittmaier, Lars Hofer, Barbara Jäger, and Lukas Salfelder, 2016, "Next-to-leading-order electroweak corrections to $pp \to W^+W^- \to 4$ leptons at the LHC," J. High Energy Phys. 06, 065.

Biedermann, Benedikt, Ansgar Denner, and Mathieu Pellen, 2016, "Large electroweak corrections to vector-boson scattering at the Large Hadron Collider," arXiv:1611.02951.

Boughezal, Radja, John M. Campbell, R. Keith Ellis, Christfried Focke, Walter Giele, Xiaohui Liu, Frank Petriello, and Ciaran Williams, 2017, "Color Singlet Production at NNLO in MCFM," Eur. Phys. J. C **77**, 7.

Buchmuller, W., and D. Wyler, 1986, "Effective Lagrangian Analysis of New Interactions and Flavor Conservation," Nucl. Phys. B **268**, 621–653.

Buttar, C., *et al.*, 2006, "Les Houches physics at TeV colliders 2005, standard model and Higgs working group: Summary report," in *Physics at TeV colliders. Proceedings, Workshop, Les Houches*, arXiv:hep-ph/0604120.

Butter, Anja, Oscar J. P. Éboli, J. Gonzalez-Fraile, M. C. Gonzalez-Garcia, Tilman Plehn, and Michael Rauch, 2016, "The Gauge-Higgs Legacy of the LHC Run I," J. High Energy Phys. 07, 152.

Campanario, F., M. Kerner, L. D. Ninh, M. Rauch, R. Roth, and D. Zeppenfeld, 2015, "NLO corrections to processes with electroweak bosons at hadron colliders," Nucl. Part. Phys. Proc. **261–262**, 268–307.

Campbell, John M., and R. Keith Ellis, 1999, "An Update on vector boson pair production at hadron colliders," Phys. Rev. D **60**, 113006.

Campbell, John M., R. Keith Ellis, and Walter T. Giele, 2015, "A Multi-Threaded Version of MCFM," Eur. Phys. J. C **75**, 246.

Campbell, John M., R. Keith Ellis, Ye Li, and Ciaran Williams, 2016, "Predictions for diphoton production at the LHC through NNLO in QCD," J. High Energy Phys. 07, 148.

Campbell, John M., R. Keith Ellis, and Ciaran Williams, 2011a, "Gluon-Gluon Contributions to W_+W_- Production and Higgs Interference Effects," J. High Energy Phys. 10, 005.

Campbell, John M., R. Keith Ellis, and Ciaran Williams, 2011b, "Vector boson pair production at the LHC," J. High Energy Phys. 07, 018.

Caola, Fabrizio, Kirill Melnikov, Raoul Röntsch, and Lorenzo Tancredi, 2015, "QCD corrections to ZZ production in gluon fusion at the LHC," Phys. Rev. D **92**, 094028.

Caola, Fabrizio, Kirill Melnikov, Raoul Röntsch, and Lorenzo Tancredi, 2016, "QCD corrections to W^+W^- production through gluon fusion," Phys. Lett. B **754**, 275–280.

Cascioli, F., T. Gehrmann, M. Grazzini, S. Kallweit, P. Maierhöfer, A. von Manteuffel, S. Pozzorini, D. Rathlev, L. Tancredi, and E. Weihs, 2014, "ZZ production at hadron colliders in NNLO QCD," Phys. Lett. B **735**, 311–313.

Chanowitz, Michael S., and Mary K. Gaillard, 1985, "The TeV Physics of Strongly Interacting W's and Z's," Nucl. Phys. B **261**, 379–431.

Chatrchyan, Serguei, *et al.* (CMS Collaboration), 2008, "The CMS experiment at the CERN LHC," J. Instrum. **3**, S08004.

Chatrchyan, Serguei, *et al.* (CMS Collaboration), 2010, "Performance of the CMS Level-1 Trigger during Commissioning with Cosmic Ray Muons," J. Instrum. **5**, T03002.

Chatrchyan, Serguei, *et al.* (CMS Collaboration), 2011a, "Determination of Jet Energy Calibration and Transverse Momentum Resolution in CMS," J. Instrum. **6**, P11002.

Chatrchyan, Serguei, *et al.* (CMS Collaboration), 2011b, "Measurement of W^+W^- production and search for the Higgs boson in pp collisions at $\sqrt{s} = 7$ TeV," Phys. Lett. B **699**, 25–47.

Chatrchyan, Serguei, *et al.* (CMS Collaboration), 2011c, "Measurement of $W\gamma$ and $Z\gamma$ production in pp collisions at $\sqrt{s} = 7$ TeV," Phys. Lett. B **701**, 535–555.

Chatrchyan, Serguei, *et al.* (CMS Collaboration), 2012a, "Measurement of the Production Cross Section for Pairs of Isolated Photons in pp collisions at $\sqrt{s} = 7$ TeV," J. High Energy Phys. 01, 133.

Chatrchyan, Serguei, *et al.* (CMS Collaboration), 2012b, "Observation of a new boson at a mass of 125 GeV with the CMS experiment at the LHC," Phys. Lett. B **716**, 30–61.

Chatrchyan, Serguei, *et al.* (CMS Collaboration), 2013a, "Measurement of the sum of WW and $W^\pm Z$ production with $W +$ dijet events in pp collisions at $\sqrt{s} = 7$ TeV," Eur. Phys. J. C **73**, 2283.

Chatrchyan, Serguei, *et al.* (CMS Collaboration), 2013b, "Measurement of the W^+W^- Cross section in pp Collisions at $\sqrt{s} = 7$ TeV and Limits on Anomalous $WW\gamma$ and WWZ couplings," Eur. Phys. J. C **73**, 2610.

Chatrchyan, Serguei, *et al.* (CMS Collaboration), 2013c, "Measurement of W_+W_- and ZZ production cross sections in pp collisions at $\sqrt{s} = 8$ TeV," Phys. Lett. B **721**, 190–211.

Chatrchyan, Serguei, *et al.* (CMS Collaboration), 2013d, "The performance of the CMS muon detector in proton-proton collisions at $\sqrt{s} = 7$ TeV at the LHC," J. Instrum. **8**, P11002.

Chatrchyan, Serguei, *et al.* (CMS Collaboration), 2013e, "Measurement of the hadronic activity in events with a Z and two jets and extraction of the cross section for the electroweak production of a Z with two jets in pp collisions at $\sqrt{s} = 7$ TeV," J. High Energy Phys. 10, 062.

Chatrchyan, Serguei, *et al.* (CMS Collaboration), 2013f, "Measurement of the production cross section for $Z\gamma \to \nu\bar{\nu}\gamma$ in pp collisions at $\sqrt{s} = 7$ TeV and limits on $ZZ\gamma$ and $Z\gamma\gamma$ triple gauge boson couplings," J. High Energy Phys. 10, 164.

Chatrchyan, Serguei, *et al.* (CMS Collaboration), 2013g, "Measurement of the ZZ production cross section and search for anomalous couplings in 2 l2l' final states in pp collisions at $\sqrt{s} = 7$ TeV," J. High Energy Phys. 01 063.

Chatrchyan, Serguei, *et al.* (CMS Collaboration), 2013h, "Study of exclusive two-photon production of W^+W^- in pp collisions at $\sqrt{s} = 7$ TeV and constraints on anomalous quartic gauge couplings," J. High Energy Phys. 07, 116.

Chatrchyan, Serguei, *et al.* (CMS Collaboration), 2013i, "Projected Performance of an Upgraded CMS Detector at the LHC and HL-LHC: Contribution to the Snowmass Process," in *Proceedings of the Community Summer Study 2013: Snowmass on the Mississippi (CSS2013)*, arXiv:1307.7135.

Chatrchyan, Serguei, *et al.* (CMS Collaboration), 2014a, "Measurement of differential cross sections for the production of a pair of

isolated photons in pp collisions at $\sqrt{s} = 7$ TeV," Eur. Phys. J. C **74**, 3129.

Chatrchyan, Serguei, *et al.* (CMS Collaboration), 2014b, "Measurement of inclusive W and Z boson production cross sections in pp collisions at $\sqrt{s} = 8$ TeV," Phys. Rev. Lett. **112**, 191802.

Chatrchyan, Serguei, *et al.* (CMS Collaboration), 2014c, "Measurement of the $W\gamma$ and $Z\gamma$ inclusive cross sections in pp collisions at $\sqrt{s} = 7$ TeV and limits on anomalous triple gauge boson couplings," Phys. Rev. D **89**, 092005.

Chatrchyan, Serguei, *et al.* (CMS Collaboration), 2014d, "Measurement of WZ and ZZ production in pp collisions at $\sqrt{s} = 8$ TeV in final states with b-tagged jets," Eur. Phys. J. C **74**, 2973.

Chatrchyan, Serguei, *et al.* (CMS Collaboration), 2014e, "Search for $WW\gamma$ and $WZ\gamma$ production and constraints on anomalous quartic gauge couplings in pp collisions at $\sqrt{s} = 8$ TeV," Phys. Rev. D **90**, 032008.

Contino, Roberto, 2016, "How Best to Use LHC Results and EFT to Probe Physics Above the Scale of the LHC," in *SEARCH 2016* (Oxford University, New York).

Corbett, Tyler, O. J. P. Éboli, J. Gonzalez-Fraile, and M. C. Gonzalez-Garcia, 2013, "Determining Triple Gauge Boson Couplings from Higgs Data," Phys. Rev. Lett. **111**, 011801.

Cornwall, John M., David N. Levin, and George Tiktopoulos, 1973, "Uniqueness of spontaneously broken gauge theories," Phys. Rev. Lett. **30**, 1268–1270; **31**, 572(E) (1973).

Cornwall, John M., David N. Levin, and George Tiktopoulos, 1974, "Derivation of Gauge Invariance from High-Energy Unitarity Bounds on the s Matrix," Phys. Rev. D **10**, 1145; **11**, 972(E) (1975).

Council, CERN, 2013, "The European Strategy for Particle Physics Update 2013. 16th Session of European Strategy Council."

Csaki, Csaba, Christophe Grojean, Hitoshi Murayama, Luigi Pilo, and John Terning, 2004a, "Gauge theories on an interval: Unitarity without a Higgs," Phys. Rev. D **69**, 055006.

Csaki, Csaba, Christophe Grojean, Luigi Pilo, and John Terning, 2004b, "Towards a realistic model of Higgsless electroweak symmetry breaking," Phys. Rev. Lett. **92**, 101802.

Curtin, David, Prerit Jaiswal, and Patrick Meade, 2013, "Charginos Hiding In Plain Sight," Phys. Rev. D **87**, 031701.

Curtin, David, Prerit Jaiswal, Patrick Meade, and Pin-Ju Tien, **2013**, "Casting Light on BSM Physics with SM Standard Candles," J. High Energy Phys. 08, 068.

Curtin, David, Patrick Meade, and Pin-Ju Tien, 2014, "Natural SUSY in Plain Sight," Phys. Rev. D **90**, 115012.

Czakon, Michal, Alexander Mitov, Michele Papucci, Joshua T. Ruderman, and Andreas Weiler, 2014, "Closing the stop gap," Phys. Rev. Lett. **113**, 201803.

Dawson, S., P. Jaiswal, Ye Li, H. Ramani, and Mao Zeng, 2016, "Resummation of Jet Veto Logarithms at partial $N^3LL + NNLO$ for W^+W^- Production at the LHC," Phys. Rev. D **94**, 114014.

Dawson, S., Ian M. Lewis, and Mao Zeng, 2013, "Threshold resummed and approximate next-to-next-to-leading order results for W^+W^- pair production at the LHC," Phys. Rev. D **88**, 054028.

Degrande, C., *et al.*, 2013a, "Studies of Vector Boson Scattering And Triboson Production with DELPHES Parametrized Fast Simulation for Snowmass 2013," in *Proceedings, Community Summer Study 2013: Snowmass on the Mississippi (CSS2013)*, arXiv:1309.7452.

Degrande, Celine, Oscar Éboli, Bastian Feigl, Barbara Jäger, Wolfgang Kilian, Olivier Mattelaer, Michael Rauch, Jürgen Reuter, Marco Sekulla, and Doreen Wackeroth, 2013b, "Monte Carlo tools for studies of non-standard electroweak gauge boson interactions in multi-boson processes: A Snowmass White Paper," in *Proceedings, Community Summer Study 2013: Snowmass on the Mississippi (CSS2013)*, arXiv:1309.7890.

Degrande, Celine, Nicolas Greiner, Wolfgang Kilian, Olivier Mattelaer, Harrison Mebane, Tim Stelzer, Scott Willenbrock, and Cen Zhang, 2013c, "Effective Field Theory: A Modern Approach to Anomalous Couplings," Ann. Phys. (Amsterdam) **335**, 21–32.

Denner, Ansgar, Stefan Dittmaier, Markus Hecht, and Christian Pasold, 2015, "NLO QCD and electroweak corrections to $W + \gamma$ production with leptonic W-boson decays," J. High Energy Phys. 04, 018.

Denner, Ansgar, Stefan Dittmaier, Markus Hecht, and Christian Pasold, 2016, "NLO QCD and electroweak corrections to $Z + \gamma$ production with leptonic Z-boson decays," J. High Energy Phys. 02, 057.

Dicus, D. A., and V. S. Mathur, 1973, "Upper bounds on the values of masses in unified gauge theories," Phys. Rev. D **7**, 3111–3114.

Éboli, O. J. P., and M. C. Gonzalez-Garcia, 2004, "Probing trilinear gauge boson interactions via single electroweak gauge boson production at the CERN LHC," Phys. Rev. D **70**, 074011.

Éboli, O. J. P., and M. C. Gonzalez-Garcia, 2016, "Classifying the bosonic quartic couplings," Phys. Rev. D **93**, 093013.

Éboli, O. J. P., M. C. Gonzalez-Garcia, and J. K. Mizukoshi, 2006, "$pp \to jje^{\pm}\mu^{\pm}\nu\nu$ and $jje^{\pm}\mu^{\mp}\nu\nu$ at $\mathcal{O}(\alpha_{\rm em}^6)$ and $\mathcal{O}(\alpha_{\rm em}^4\alpha_s^2)$ for the Study of the Quartic Electroweak Gauge Boson Vertex at LHC," Phys. Rev. D **74**, 073005.

Éboli, Oscar J. P., M. C. Gonzalez-Garcia, and S. F. Novaes, 1994, "Quartic anomalous couplings in e gamma colliders," Nucl. Phys. B **411**, 381–396.

Ellis, John, Veronica Sanz, and Tevong You, 2015, "The Effective Standard Model after LHC Run I," J. High Energy Phys. 03, 157.

Evans, Lyndon, and Philip Bryant, 2008, "LHC Machine," J. Instrum. **3**, S08001.

Falkowski, Adam, and Francesco Riva, 2015, "Model-independent precision constraints on dimension-6 operators," J. High Energy Phys. 02, 039.

Farhi, Edward, and Leonard Susskind, 1981, "Technicolor," Phys. Rep. **74**, 277.

Fox, Patrick J., Roni Harnik, Joachim Kopp, and Yuhsin Tsai, 2012, "Missing Energy Signatures of Dark Matter at the LHC," Phys. Rev. D **85**, 056011.

Frixione, Stefano, Paolo Nason, and Carlo Oleari, 2007, "Matching NLO QCD computations with Parton Shower simulations: the POWHEG method," J. High Energy Phys. 11, 070.

Frye, Christopher, Marat Freytsis, Jakub Scholtz, and Matthew J. Strassler, 2016, "Precision Diboson Observables for the LHC," J. High Energy Phys. 03, 171.

Gaemers, K. J. F., and G. J. Gounaris, 1979, "Polarization Amplitudes for $e^+e^- \to W^+W^-$ and $e^+e^- \to ZZ$," Z. Phys. C **1**, 259.

Gehrmann, T., M. Grazzini, S. Kallweit, P. Maierhöfer, A. von Manteuffel, S. Pozzorini, D. Rathlev, and L. Tancredi, 2014, "W^+W^- Production at Hadron Colliders in Next to Next to Leading Order QCD," Phys. Rev. Lett. **113**, 212001.

Georgi, Howard, and David B. Kaplan, 1984, "Composite Higgs and Custodial SU(2)," Phys. Lett. B **145**, 216–220.

Giudice, G. F., C. Grojean, A. Pomarol, and R. Rattazzi, 2007, "The Strongly-Interacting Light Higgs," J. High Energy Phys. 06, 045.

Gleisberg, T., Stefan. Höche, F. Krauss, M. Schönherr, S. Schumann, F. Siegert, and J. Winter, 2009, "Event generation with SHERPA 1.1," J. High Energy Phys. 02, 007.

Gleisberg, Tanju, and Stefan Höche, 2008, "Comix, a new matrix element generator," J. High Energy Phys. 12, 039.

Gounaris, G., *et al.*, 1996, "Triple gauge boson couplings," in *AGS / RHIC Users Annual Meeting*, pp. 525–576, hep-ph/9601233.

Gounaris, G. J., J. Layssac, and F. M. Renard, 2000, "New and standard physics contributions to anomalous Z and gamma self-couplings," Phys. Rev. D **62**, 073013.

Grazzini, Massimiliano, Stefan Kallweit, Stefano Pozzorini, Dirk Rathlev, and Marius Wiesemann, 2016, "W^+W^- production at the LHC: fiducial cross sections and distributions in NNLO QCD," J. High Energy Phys. 08, 140.

Grazzini, Massimiliano, Stefan Kallweit, and Dirk Rathlev, 2015a, "$W\gamma$ and $Z\gamma$ production at the LHC in NNLO QCD," J. High Energy Phys. 07, 085.

Grazzini, Massimiliano, Stefan Kallweit, and Dirk Rathlev, 2015b, "ZZ production at the LHC: fiducial cross sections and distributions in NNLO QCD," Phys. Lett. B **750**, 407–410.

Grazzini, Massimiliano, Stefan Kallweit, Dirk Rathlev, and Marius Wiesemann, 2016, "$W^{\pm}Z$ production at hadron colliders in NNLO QCD," Phys. Lett. B **761**, 179–183.

Grazzini, Massimiliano, Stefan Kallweit, Dirk Rathlev, and Marius Wiesemann, 2015, "Transverse-momentum resummation for vector-boson pair production at NNLL + NNLO," J. High Energy Phys. 08, 154.

Grzadkowski, B., M. Iskrzynski, M. Misiak, and J. Rosiek, 2010, "Dimension-Six Terms in the Standard Model Lagrangian," J. High Energy Phys. 10, 085.

Hagiwara, Kaoru, R. D. Peccei, D. Zeppenfeld, and K. Hikasa, 1987, "Probing the Weak Boson Sector in $e^+e^- \to W^+W^-$," Nucl. Phys. B **282**, 253–307.

Henning, Brian, Xiaochuan Lu, Tom Melia, and Hitoshi Murayama, 2015, "2, 84, 30, 993, 560, 15456, 11962, 261485, ...: Higher dimension operators in the SM EFT," arXiv:1512.03433.

Höche, Stefan, Frank Krauss, Steffen Schumann, and Frank Siegert, 2009, "QCD matrix elements and truncated showers," J. High Energy Phys. 05, 053.

Jaiswal, Prerit, Karoline Kopp, and Takemichi Okui, 2013, "Higgs Production Amidst the LHC Detector," Phys. Rev. D **87**, 115017.

Jaiswal, Prerit, Patrick Meade, and Harikrishnan Ramani, 2016, "Precision diboson measurements and the interplay of pT and jet-veto resummations," Phys. Rev. D **93**, 093007.

Jaiswal, Prerit, and Takemichi Okui, 2014, "Explanation of the WW excess at the LHC by jet-veto resummation," Phys. Rev. D **90**, 073009.

Kaplan, David B., and Howard Georgi, 1984, "$SU(2) \times U(1)$ Breaking by Vacuum Misalignment," Phys. Lett. B **136**, 183–186.

Khachatryan, Vardan, *et al.* (CMS Collaboration), 2014a, "Identification techniques for highly boosted W bosons that decay into hadrons," J. High Energy Phys. 12, 017.

Khachatryan, Vardan, *et al.* (CMS Collaboration), 2014b, "Search for massive resonances decaying into pairs of boosted bosons in semi-leptonic final states at $\sqrt{s} = 8$ TeV," J. High Energy Phys. 08, 174.

Khachatryan, Vardan, *et al.* (CMS Collaboration), 2015a, "Measurement of electroweak production of two jets in association with a Z boson in proton-proton collisions at $\sqrt{s} = 8$ TeV," Eur. Phys. J. C **75**, 66.

Khachatryan, Vardan, *et al.* (CMS Collaboration), 2015b, "Measurement of the $pp \to ZZ$ production cross section and constraints on anomalous triple gauge couplings in four-lepton final states at $\sqrt{s} = 8$ TeV," Phys. Lett. B **740**, 250–272.

Khachatryan, Vardan, *et al.* (CMS Collaboration), 2015c, "Measurements of the Z Z production cross sections in the $2l2\nu$ channel in proton-proton collisions at $\sqrt{s} = 7$ and 8 TeV and combined constraints on triple gauge couplings," Eur. Phys. J. C **75**, 511.

Khachatryan, Vardan, *et al.* (CMS Collaboration), 2015d, "Performance of Electron Reconstruction and Selection with the CMS Detector in Proton-Proton Collisions at $\sqrt{s} = 8$ TeV," J. Instrum. **10**, P06005.

Khachatryan, Vardan, *et al.* (CMS Collaboration), 2015e, "Performance of Photon Reconstruction and Identification with the CMS Detector in Proton-Proton Collisions at $\sqrt{s} = 8$ TeV," J. Instrum. **10**, P08010.

Khachatryan, Vardan, *et al.* (CMS Collaboration), 2015f, "Performance of the CMS missing transverse momentum reconstruction in pp data at $\sqrt{s} = 8$ TeV," J. Instrum. **10**, P02006.

Khachatryan, Vardan, *et al.* (CMS Collaboration), 2015g, "Study of vector boson scattering and search for new physics in events with two same-sign leptons and two jets," Phys. Rev. Lett. **114**, 051801.

Khachatryan, Vardan, *et al.* (CMS Collaboration), 2015h, "Technical Proposal for the Phase-II Upgrade of the CMS Detector," Technical Report No. CERN-LHCC-2015-010. LHCC-P-008 (CERN, Geneva).

Khachatryan, Vardan, *et al.* (CMS Collaboration), 2015i, "Measurement of the $Z\gamma$ Production Cross Section in pp Collisions at 8 TeV and Search for Anomalous Triple Gauge Boson Couplings," J. High Energy Phys. 04, 164.

Khachatryan, Vardan, *et al.* (CMS Collaboration), 2016a, "Jet energy scale and resolution in the CMS experiment in pp collisions at 8 TeV," arXiv:1607.03663.

Khachatryan, Vardan, *et al.* (CMS Collaboration), 2016b, "Measurement of electroweak-induced production of $W\gamma$ with two jets in pp collisions at $\sqrt{s} = 8$ TeV and constraints on anomalous quartic gauge couplings," arXiv:1612.09256.

Khachatryan, Vardan, *et al.* (CMS Collaboration), 2016c, "Measurement of the $Z\gamma \to \nu\bar{\nu}\gamma$ production cross section in pp collisions at $\sqrt{s} = 8$ TeV and limits on anomalous $ZZ\gamma$ and $Z\gamma\gamma$ trilinear gauge boson couplings," Phys. Lett. B **760**, 448–468.

Khachatryan, Vardan, *et al.* (CMS Collaboration), 2016d, "Measurement of the W^+W^- cross section in pp collisions at $\sqrt{s} =$ 8 TeV and limits on anomalous gauge couplings," Eur. Phys. J. C **76**, 401.

Khachatryan, Vardan, *et al.* (CMS Collaboration), 2016e, "Measurement of the WZ production cross section in pp collisions at $\sqrt{s} = 7$ and 8 TeV and search for anomalous triple gauge couplings at $\sqrt{s} = 8$ TeV," arXiv:1609.05721.

Khachatryan, Vardan, *et al.* (CMS Collaboration), 2016f, "The CMS trigger system," arXiv:1609.02366.

Khachatryan, Vardan, *et al.* (CMS Collaboration), 2016g, "Evidence for exclusive $\gamma\gamma \to W^+W^-$ production and constraints on anomalous quartic gauge couplings in pp collisions at $\sqrt{s} = 7$ and 8 TeV," J. High Energy Phys. 08, 119.

Khachatryan, Vardan, *et al.* (CMS Collaboration), 2016h, "Measurement of electroweak production of a W boson and two forward jets in proton-proton collisions at $\sqrt{s} = 8$ TeV," J. High Energy Phys. 11, 147.

Kilian, Wolfgang, Thorsten Ohl, Jürgen Reuter, and Marco Sekulla, 2015, "High-Energy Vector Boson Scattering after the Higgs Discovery," Phys. Rev. D **91**, 096007.

Kotwal, Ashutosh V., Heidi Schellman, and Jadranka Sekaric, 2015, "Review of Physics Results from the Tevatron: Electroweak Physics," Int. J. Mod. Phys. A **30**, 1541004.

Lampl, W., S. Laplace, D. Lelas, P. Loch, H. Ma, S. Menke, S. Rajagopalan, D. Rousseau, S. Snyder, and G. Unal, 2008, "Calorimeter clustering algorithms: Description and performance," ATL-LARG-PUB-2008-002.

Lazopoulos, Achilleas, Kirill Melnikov, and Frank Petriello, 2007, "QCD corrections to tri-boson production," Phys. Rev. D **76**, 014001.

Lee, Benjamin W., C. Quigg, and H. B. Thacker, 1977, "The Strength of Weak Interactions at Very High-Energies and the Higgs Boson Mass," Phys. Rev. Lett. **38**, 883–885.

Lehman, Landon, and Adam Martin, 2016, "Low-derivative operators of the Standard Model effective field theory via Hilbert series methods," J. High Energy Phys. 02, 081.

Liu, Da, Alex Pomarol, Riccardo Rattazzi, and Francesco Riva, 2016, "Patterns of Strong Coupling for LHC Searches," J. High Energy Phys. 11, 141.

Llewellyn Smith, C. H., 1973, "High-Energy Behavior and Gauge Symmetry," Phys. Lett. B **46**, 233–236.

Longhitano, Anthony C., 1980, "Heavy Higgs Bosons in the Weinberg-Salam Model," Phys. Rev. D **22**, 1166.

Longhitano, Anthony C., 1981, "Low-Energy Impact of a Heavy Higgs Boson Sector," Nucl. Phys. B **188**, 118–154.

Mangano, Michelangelo L., Mauro Moretti, Fulvio Piccinini, Roberto Pittau, and Antonio D. Polosa, 2003, "ALPGEN, a generator for hard multiparton processes in hadronic collisions," J. High Energy Phys. 07, 001.

Meade, Patrick, Harikrishnan Ramani, and Mao Zeng, 2014, "Transverse momentum resummation effects in W^+W^- measurements," Phys. Rev. D **90**, 114006.

Melia, Tom, Paolo Nason, Raoul Rontsch, and Giulia Zanderighi, 2011, "W_+W_-, WZ and ZZ production in the POWHEG BOX," J. High Energy Phys. 11, 078.

Nason, Paolo, 2004, "A New method for combining NLO QCD with shower Monte Carlo algorithms," J. High Energy Phys. 11, 040.

Nason, Paolo, and Giulia Zanderighi, 2014, "W^+W^-, WZ and ZZ production in the POWHEG-BOX-V2," Eur. Phys. J. C **74**, 2702.

Peskin, Michael E., and Tatsu Takeuchi, 1992, "Estimation of oblique electroweak corrections," Phys. Rev. D **46**, 381–409.

Pomarol, Alex, and Francesco Riva, 2014, "Towards the Ultimate SM Fit to Close in on Higgs Physics," J. High Energy Phys. 01, 151.

Rauch, Michael, 2016, "Vector-Boson Fusion and Vector-Boson Scattering," arXiv:1610.08420.

Reuter, J., Wolfgang Kilian, and Marco Sekulla, 2013, "Simplified Models for New Physics in Vector Boson Scattering—Input for Snowmass 2013," arXiv:1307.8170.

Ritz, Steve, *et al.* (HEPAP Subcommittee), 2014, "Building for Discovery: Strategic Plan for U.S. Particle Physics in the Global Context."

Rolbiecki, Krzysztof, and Kazuki Sakurai, 2013, "Light stops emerging in WW cross section measurements?" J. High Energy Phys. 09, 004.

Schael, S., *et al.* (DELPHI, OPAL, LEP Electroweak, ALEPH, L3 Collaborations), 2013, "Electroweak Measurements in Electron-Positron Collisions at W-Boson-Pair Energies at LEP," Phys. Rep. **532**, 119–244.

Schumann, Steffen, and Frank Krauss, 2008, "A Parton shower algorithm based on Catani-Seymour dipole factorisation," J. High Energy Phys. 03, 038.

Searcy, Jacob, Lillian Huang, Marc-André Pleier, and Junjie Zhu, 2016, "Determination of the WW polarization fractions in $pp \to W^{\pm}W^{\pm}jj$ using a deep machine learning technique," Phys. Rev. D **93**, 094033.

Sekulla, Marco, Wolfgang Kilian, Thorsten Ohl, and Jürgen Reuter, 2016, "Effective Field Theory and Unitarity in Vector Boson Scattering," in *4th Large Hadron Collider Physics Conference (LHCP 2016)*, arXiv:1610.04131.

Skiba, Witold, 2011, "Effective Field Theory and Precision Electroweak Measurements," in *Physics of the large and the small, TASI 09, proceedings of the Theoretical Advanced Study Institute in Elementary Particle Physics*, pp. 5–70, arXiv:1006.2142.

Stirling, W. James, and Anja Werthenbach, 2000, "Anomalous quartic couplings in $W^+W^-\gamma$, $Z^0Z^0\gamma$ and $Z^0\gamma\gamma$ production at present and future e^+e^- colliders," Eur. Phys. J. C **14**, 103–110.

Susskind, Leonard, 1979, "Dynamics of Spontaneous Symmetry Breaking in the Weinberg-Salam Theory," Phys. Rev. D **20**, 2619–2625.

Wang, Yan, Chong Sheng Li, Ze Long Liu, Ding Yu. Shao, and Hai Tao Li, 2013, "Transverse-Momentum Resummation for Gauge Boson Pair Production at the Hadron Collider," Phys. Rev. D **88**, 114017.

Weinberg, Steven, 1976, "Implications of Dynamical Symmetry Breaking," Phys. Rev. D **13**, 974–996.

Wiesemann, Marius, Massimiliano Grazzini, Stefan Kallweit, and Dirk Rathlev, 2016, "MATRIX: A fully-differential NNLO(+NNLL) process library," *Proc. Sci.*, LL2016 072.

Yong-Bai, Shen, Zhang Ren-You, Ma Wen-Gan, Li Xiao-Zhou, and Guo Lei, 2016, "NLO QCD + EW corrections to WWW production with leptonic decays at the LHC," arXiv:1605.00554.

Yong-Bai, Shen, Zhang Ren-You, Ma Wen-Gan, Li Xiao-Zhou, Zhang Yu, and Guo Lei, **2015**, "NLO QCD + NLO EW corrections to WZZ productions with leptonic decays at the LHC," J. High Energy Phys. 10, 186.